Fondo Sociale Europeo - FSE
Programma Operativo Nazionale 2000/06
"Ricerca, Sviluppo tecnologico ed Alta Formazione nelle regioni dell'Obiettivo 1" - Misura 1.1 (F.S.E)

Università degli Studi della Calabria

Dottorato di Ricerca in Ingegneria Chimica e dei Materiali

Tesi

Studio teorico di membrane biocompatibili per applicazioni farmaceutiche

Settore Scientifico Disciplinare CHIM07 – Fondamenti chimici delle tecnologie

Supervisori

Dott. ssa Elena TOCCI

Dott. Efrem CURCIO

Candidato

Patrizia Cairo

Ciclo XXII

Il Coordinatore del Corso di Dottorato

Ch.mo Prof. Raffaele MOLINARI

A.A. 2008 – 2009

To someone who has been always present

CONTENTS

Chapter IV

Theoretical methods

PART II: Results

Chapter V

β-cyclodextrin interactions with three drugs used in inflammatory pathologies: an experimental and theoretical study

Chapter VI

Modeling of drug release from polymer cyclodextrin system

Chapter VII

Molecular recognition of naringin by olymeric membranes entrapping ß-cyclodextrins: a theoretical study

Chapter VIII

Computational evaluation of monomers and polymers for molecular imprinting of 5-fluorouracil for use as drug delivery systems

INTRODUZIONE

L'ingegneria chimica deve oggi soddisfare nuovi e stringenti requisiti di mercato per prodotti di elevata qualità aventi proprietà altamente specifiche. L'ingegneria chimica e di processo si occupa mediante comprensione e sviluppo di procedure sistematiche del *design* di sistemi di processo chimico, petrolchimico, farmaceutico, alimentare, cosmetico, ecc., andando da processi continui e di gruppo dell'ordine del nano- e microsistema alla scala industriale, tutti entro il concetto di catena.

In questo contesto si rende necessaria l'implementazione di metodi computazionali di modellazione e simulazione, a livello multiscala (dalle molecole alla scala di produzione) e secondo un approccio multidisciplinare. Il *design* di un prodotto è da intendersi come la traslazione della struttura molecolare al mondo macroscopico, e l'applicazione dei principi della modellistica molecolare rappresenta un'area nuova e promettente per l'ingeneria chimica.

Un tale approccio è di grande utilità dal punto di vista dell'ottimizzazione della farmacoterapia dei tumori ed antiinfiammatoria: l'interesse crescente nei confronti di nuovi sistemi terapeutici ha portato alla realizzazione di sistemi definiti *Drug Delivery Systems* (DDS). Le forme di rilascio controllato rigenerano i vecchi farmaci riducendo i loro difetti e migliorandone le proprietà. Questa è un'alternativa allo sviluppo di nuovi farmaci che è estremamente costoso.

Nella maggior parte dei casi, i farmaci per raggiungere la loro efficacia terapeutica devono essere presenti in circolo per periodi di tempo sufficientemente lunghi. Con l'impiego delle formulazioni tradizionali questo può essere ottenuto solo mediante somministrazioni ripetute, mantenendo in questo modo la concentrazione ematica del farmaco all'interno della finestra terapeutica. Una soluzione a questo problema è l'impiego di sistemi di rilascio controllato del farmaco. Tali formulazioni sono in grado di alterare l'assorbimento del farmaco e la conseguente concentrazione ematica modificando il rilascio del principio attivo. Questo riduce le fluttuazioni della concentrazione ematica del farmaco con conseguente riduzione degli effetti secondari e aumento della *compliance* del paziente.

La progettazione di questo tipo di formulazioni richiede lo sviluppo costante di biomateriali con elevate prestazioni in accordo allo scopo terapeutico e alle proprietà farmacologiche del principio attivo. Le abilità di promuovere l'assorbimento, il direzionamento su specifici siti bersaglio e il rilascio controllato del farmaco sono proprietà desiderabili in tali forme di dosaggio. Da un punto di vista della sicurezza di tali sistemi importante è la biocompatibilità di tali materiali.

Oggigiorno le attività di ricerca nel campo dei DDS puntano all'ingegnerizzazione del *design* architettonico a livello molecolare di biomateriali. In quest'ottica le simulazioni permettono in maniera veloce ed

economica la comprensione a livello molecolare della struttura e delle proprietà fisiche e chimiche dei materiali, coadiuvando la progettazione di nuovi materiali.

Questo lavoro di tesi si basa sull'area della chimica *host-guest* con l'investigazione di *carriers* ciclodestrinici supportati su membrane polimeriche e polimeri molecolarmente *imprinted*. Viene proposto un uso combinato di polimeri e/o strutture supramolecolari per rilasciare farmaci impiegati nel morbo di Crhon e nella terapia antitumorale.

In questo modo, lo scopo del lavoro è studiare le interazioni specifiche tra farmaco e *carriers* del farmaco che sono alla base del riconoscimento molecolare per un *design* razionale di DDS, mediante le metodologie computazionali di meccanica molecolare, dinamica molecolare e *docking* delle interazioni tra farmaco e *carrier* del farmaco, valutando anche i meccanismi che sono alla base del rilascio.

Le ciclodestrine agiscono come carrier del farmaco permettendone il rilascio al sito bersaglio in quantità adeguate, sia precisamente che efficacemente. I vantaggi che derivano dal loro uso sono numerosi: esse facilitano l'assorbimento dei farmaci inclusi migliorando l'*uptake* cellulare, aumentano la biodisponibilità orale consentendo una riduzione dei dosaggi impiegati, e, ancora, solubilizzano e stabilizzano i farmaci. Tutto questo avviene senza l'uso di solventi organici, di tensioattivi o in condizioni di pH estreme, che comportano in generale, irritazioni ed effetti collaterali. D'altronde l'inserimento del farmaco nella ciclodestrina previene sia il diretto contatto del principio attivo con le membrane biologiche sia l'entrata del farmaco in tessuti non *target*, riducendone in tal modo gli effetti secondari.

La tecnica dell'*imprinting* molecolare ha enormi potenziali nella creazione di sistemi di rilascio controllato del farmaco. Tale tecnica coinvolge la formazione di un complesso di pre-polimerizzazione tra la molecola stampo e i gruppi funzionali di monomeri con struttura chimica specifica designati per interagire con la molecola stampo attraverso interazioni covalenti, non covalenti o di coordinazione. Dopo la formazione del complesso di pre-polimerizzazione, la reazione di polimerizzazione avviene in presenza di agenti cross-linking e di appropriato solvente che controllano la morfologia del polimero. A seguito della rimozione della molecola stampo, il prodotto finale è una matrice etero polimerica con specifici elementi di riconoscimento selettivo per la molecola stampo. Nella progettazione di nuovi sistemi di rilascio la tecnica dell'*imprinting* molecolare rappresenta una metodologia nuova per poter raggiungere sistemi di rilascio controllato e/o sostenuto nel tempo.
In particolare l'intera tesi è suddivisa come segue:

Capitolo I: *Biomateriali per rilascio controllato.* Questo capitolo è un'introduzione generale sulle proprietà dei polimeri usati in applicazioni biomedicali, con particolare attenzione per i polimeri usati nei sistemi di rilascio

controllato. Saranno descritti anche i principali meccanismi di rilascio controllato e i *carriers* farmaceutici.

Capitolo II: *Le ciclodestrine.* In questo capitolo saranno descritte le caratteristiche delle ciclodestrine e la formazione dei relativi complessi di inclusione, con particolare attenzione alla termodinamica di complessazione. Saranno illustrate le applicazioni farmaceutiche di queste sostanze e le principali tecniche teoriche impiegate per studiare i complessi ciclodestrinici.

Capitolo III: *Polimeri molecolarmente imprinted.* Questo capitolo è un'introduzione generale sulla tecnica dell'*imprinting* molecolare. Saranno introdotte le applicazioni di tali polimeri nei sistemi di rilascio del farmaco ed anche le simulazioni computazionali applicate a questo tipo di materiali.

Capitolo IV: *Metodi teorici.* In questo capitolo saranno introdotti i principi delle tecniche di modellistica molecolare usate in questo lavoro.

Capitolo V: *Interazioni tra β-ciclodestrina e tre farmaci usati in malattie infiammatorie: studio teorico e sperimentale.* In questo capitolo saranno caratterizzate le interazioni tra la β-ciclodestrina e tre farmaci antinfiammatori non steroidei, mediante metodi teorici e sperimentali.

Capitolo VI: *Simulazione del rilascio di farmaci da un sistema di polimero-ciclodestrina.* In questo capitolo sarà descritta la dinamica molecolare del sistema polimerico formato dall'aggiunta del complesso β-ciclodestrina/farmaco sulla superficie di una membrana di PEEK-WC, descrivendo il rilascio del farmaco complessato in una soluzione acquosa.

Capitolo VII: *Riconoscimento molecolare di naringina da parte di una membrana polimerica contenente β-ciclodestrina: studio teorico.* In questo capitolo saranno date informazioni sulla geometria e l'energia di complessazione della naringina con un derivato della β-ciclodestrina, inoltre sarà descritta la complessazione della naringina su membrane di PEEK-WC contenente la β-ciclodestrina modificata.

Capitolo VIII: *Valutazione computazionale di monomeri e polimeri per l'imprinting molecolare del 5-fluorouracile per l'utilizzo come sistema di rilascio del farmaco.* In questo capitolo sarà trattata la descrizione quantitativa e qualitativa del processo di *imprinting* del 5-fluorouracile con tecniche di modellistica molecolare. Sarà inoltre valutata la diffusione del farmaco in una tale matrice polimerica.

Sommario: In questa parte finale saranno riassunte le conclusioni più importanti dei precedenti capitoli.

INTRODUCTION

Nowadays, chemical engeneering has to satisfy market requirements for specific end-use properties of the products manufacactured. The chemical and process engeneering is concerned with understanding and developing systematic procedures for the design and optimal operation of chemical, petrochemical, pharmaceutical, food, cosmetics, etc., process systems, ranging from nano- and microsystems to industrial-scale continuos and batch processes, all within the concept of the chemical supply chain.

In such a frame, the implementation of computational modelling and simulation at multiscale (from molecules to production scale) and multidisciplinary level is necessary. Product design is the traslation of molecular structure into macroscopic world, and application of the principles of molecular modelling represents a new and promising area of investigation for chemical engeneering.

Such an approach is of great utility from the viewpoint of the optimization of the (in use) pharmacoterapy of cancer and inflammatory diseases: a growing interest for new therapeutic systems brought to the realization of systems called Drug Delivery Systems (DDS). Controlled release dosage forms revitalize old drugs by reducing pharmaceutical shortcomings and improving biopharmaceutical properties of the drugs. This is an alternative to the development of new drugs which is extremely costly.

Drugs, in the majority of cases, are toxic at high doses however, they must be present in the circulation for a time sufficient to reach therapeutically useful results. This is a commonly achieved by repeated drug administrations, which give rise to peak and valley drug concentration. A solution to these problems comes from the controlled release technology. Controlled release formulations attempt to alter drug adsorption and subsequent drug concentration in blood by modifying the drug release from the device. This lead to reduced fluctuations in the plasma drug concentration, sustained drug effects with fewer side effects, and increased patient compliance.

To design advanced dosage forms, suitable carrier materials are used to overcome the undesirable properties of drug molecules. Hence various kinds of high-performance biomaterials are being constantly developed. From the viewpoint of the optimization of pharmacotherapy, drug release should be controlled in accordance with the therapeutic purpose and pharmacological properties of active substances.

The desirable attributes of drug carriers in drug delivery system are the multi-functional properties such as controlled- release, targeting, and absorption enhancing abilities. From the safety viewpoint, bioadaptability is an important necessity, and high quality, cost-performance, etc. are required for drug carriers,

because an appropriate drug release from the dosage forms is of critical importance realizing their therapeutic efficacy.

The today research activities in the field of drug delivery carriers, the major emphasis has being focused toward engeneering of architectural design of biomaterilas on a molecular level. In this optics, molecular simulation techniques are playing an increasingly important role in the designing and development of materials for various industrial applications. These simulations are likely to benefit the study of materials by increasing our understanding of their chemical and physical properties at a molecular level and by assisting us in the design of new materials and predicting their properties. Simulations are usually considerably cheaper and faster than experiments. Molecular simulations also offer a unique perspective on the molecular level processes controlling structural, physical, optical, chemical, mechanical, and transport properties.

Our study focus on the area of host-guest chemistry by analysing membranes containing cyclodextrins and membranes based on molecular imprinting technique. For the first time a combined use of polymer and/or supramolecular structure have been used to release drugs used in Crhon's disease and in the anticancer therapy.

Thus, our aim is to study the specific interactions between drugs and drug carriers that are the basis of molecular recognition for a rational design of DDS by using combined molecular dynamics, molecular mechanics, and docking computational techniques.

Cyclodextrins are a group of structurally related cyclic oligosaccharides that are formed by enzymatic degradation of starch. Cyclodextrins have a hydrophilic external surface and a hydrophobic internal cavity that enables the complexation of lipophilic 'guest' drug molecules. The complexation affects many of the physicochemical properties of the drug without affecting their intrinsic lipophilicity or pharmacological properties. Cyclodextrins are widely used in the pharmaceutical field because they enhance the solubility in aqueous solvent, the stability, the bioavailability of drug molecules and reduce the toxic effects of drugs. Often the cyclodextrin's formulation improves the selective transfer and/or reduces side effects. Cyclodextrins act as drug carriers delivering the necessary amount to the targeted site for a necessary time period, both efficiently and precisely.

The molecular imprinting technology has an enormous potential for creating satisfactory drug dosage forms. Molecular imprinting involves forming a pre-polymerization complex between the template molecule and functional monomers or functional oligomers (or polymers) with specific chemical structures designed to interact with the template either by covalent, non-covalent chemistry (self-assembly) or both. Once the pre-polymerization complex is formed, the polymerization reaction occurs in the presence of a cross-linking monomer and an

appropriate solvent, which controls the overall polymer morphology and macroporous structure. Once the template is removed, the product is a heteropolymer matrix with specific recognition elements for the template molecule. Despite the already developed interesting applications of molecularly imprinted polymers, the incorporation of the molecular imprinting approach for the development of drug delivery systems is just at its incipient stage. Nevertheless, it can be foreseen that, in the next few years, significant progress will occur in this field, taking advantage of the improvements of this technology in other areas.
In particular the entire thesis will be divided as follows:

Chapter I: *Biomaterials for controlled release*. This chapter is a general overview about the properties of polymers used in biomedical applications, with particular attention for the polymers used in controlled release systems. The main mechanisms of controlled release, as also the pharmaceutical carriers, are also described.
Chapter II: *Cyclodextrins*. In this chapter, structural features of cyclodextrins and the formation of inclusion complexes will be described, focusing the attention on the thermodynamics of complexation. Pharmaceutical applications will be also introduced and the main theoretical technique commonly used to study cyclodextrinic complexes will be illustrated.
Chapter III: *Molecularly imprinted polymers*. This chapter is a general overview about the molecular imprinting technique. The applications of molecularly imprinted polymers in the drug delivery will be also introduced. The use of computational simulations applied to these materials will be shown.
Chapter IV: *Theoretical methods*. In this chapter fundamentals of molecular modelling techniques used in this work will be introduced.
Chapter V: *β-cyclodextrin interactions with three drugs used in inflammatory pathologies: an experimental and theoretical study*. The characterization of the interactions between the β-cyclodextrin and three nonsteroid anti-inflammatory drug molecules with a wide range of actions, with both experimental and theoretical methods will be described in this chapter.
Chapter VI: *Modelling of drug release from polymer cyclodextrin system.* The molecular dynamics on the polymeric system formed by adding on the surface of PEEK-WC membrane the β-cyclodextrin/drug complex will be described, showing the release of included drug in a water solution.
Chapter VII: *Molecular recognition of naringin by polymeric membranes entrapping β-cyclodextrins: a theoretical study.* Informations on the geometry and the energy of complexation of a β-cyclodextrin derivative with naringin will be illustrated in this chapter, moreover the complexation of naringin on the PEEK-WC membrane surface containing the β-cyclodextrin derivative will be also described.

Chapter VIII: *Computational evaluation of monomers and polymers for molecular imprinting of 5-fluorouracil for use as drug delivery systems*. The quantitative/qualitative description of the imprinting process and of the recognition mechanisms of 5-fluorouracil will be treated with molecular modelling techniques. The drug diffusion in a such material will be also described.

Summary: In this final part, the most important conclusions of the previous chapters will be summarized.

PART I

General introduction

FIRST CHAPTER

BIOMATERIALS FOR CONTROLLED RELEASE

1.1 Introduction

Currently used biomaterials can be divided into two categories: biological and synthetic. The biological materials are composed of polypeptides, polysaccharides, nucleic acids, polyesters, hydroxyapatites, or their composites. Remarkable advantages of biological materials over synthetics are their excellent physiological activities such as selective cell adhesion (e.g. collagen and fibrin), similar mechanical properties to natural tissues (e.g. animal heart valves and blood vessels), and biodegradability (e.g. gelatine and chitin). However, similar to synthetics, biological materials have several deficiencies including risk of viral infection, antigenicity, unstable material supply, and deterioration which accompanies long-term implantation.

Application of biological materials in medicine has a longer history than synthetic biomaterials but the demand for biological biomaterials has recently decreased because they have unavoidable deficiencies. Certainly, between synthetic materials, polymers have an important role in medical applications.

1.2 Biomedical application of functional polymers

Of the many materials used in pharmaceutical formulations, polymers play the most important roles.

Polymers have found applications in such diverse biomedical fields as tissue engineering, implantation of medical devices and artificial organs, prostheses, ophthalmology, dentistry, bone repair and many other medical fields. An important application of polymers undoubtedly resides in the development of sophisticated controlled drug delivery systems enable to control release of drugs into the body.

Polymeric materials have also extensively been used for biosensors, in testing devices and for bio-regulation. Polymeric material suitable for a biomedical application must be ‘biocompatible’, at least on its surface. Strictly speaking, many polymeric systems used for implantation of medical devices into the body are considered to be ‘biocompatible’, though after implantation they become isolated from the tissues of the body by collagenous encapsulation. They are, therefore, actually rejected by the body. However, they do not induce any harmful effects, thanks to encapsulation of the biofilm generated on the surface.

Interactions with the body are thus hindered. Functional groups, properly located on a polymer as well as its structure, are usually responsible for its

biocompatibility and/or biodegradability and may impart on it either therapeutic or/and toxic characteristics. For example, carboxylic groups induce therapeutic activity of many drugs.

As indicated above, an implanted polymeric material may be considered to be 'biocompatible', if its insertion into the body does not provoke an adverse reaction. A thrombus is formed very fast when polymers contact blood cells. Materials with non-thrombogenic blood-compatible surfaces must, therefore, be used in contact with the blood stream. Truly biocompatible polymers, used for medical purposes should be able to recognize and cooperate in harmony with bio-assemblies and living cells without any non-specific interactions. Biological molecules and synthetic ligands, designed to fit cell surface receptors, which are able to induce specific healing pathways should be immobilized on the surface to induce such effects. Biocompatible polymers used in biomedical applications must often be also biodegradable, and harmful products should not be generated as a result of their biodegradation. Biodegradable may be of synthetic or natural origin. Non-toxic alcohols, acids and other low molecular products, easily eliminated by the body, are formed as a result of hydrolysis 'in vivo' of such biocompatible polymers. High molecular weight polymers with hydrolytically unstable crosslinks may be may be bioeroded as a result of the release of their crosslinked chains. Finally, water insoluble polymers may be converted into water soluble as a result of ionization, protonation, or hydrolysis of side chains. Such conversion does not significantly affect molecular weight, but may be responsible for bioerosion in topical applications. Several useful biocompatible polymers of microbial origin are being produced from natural sources by fermentation processes. They are non-toxic and truly biodegradable. Biodegradation is usually catalyzed by enzymes and it may involve both hydrolysis and oxidation. Aliphatic chains are more flexible than aromatic ones and can more easily fit into active sites of enzymes. Hence, they are usually easier to biodegrade. Crystallinity hinders polymer degradation. Irregularities in chain morphology prevent crystallization and favour degradation.

Biological fouling of surfaces, due to adsorption of proteins and/or adhesion of cells, which may be highly undesirable in some cases, may be prevented by grafting onto surface such polymers as poly(N-isopropyl acrylamide) and its derivatives, or by deposition of a thin layer of poly(ethylene oxide) or its derivatives.

1.3 Polymers used in controlled release systems

One of most important applications of polymers in modern pharmaceutics is the development of new, advanced drug delivery systems.

Drugs, in the majority of cases, are toxic at high doses, however, they must be present in the circulation for a time sufficient to reach therapeutically useful

results. This is a commonly achieved by repeated drug administrations, which give rise to peak and valley drug concentration. Such a method of administration has two disadvantages: on the one hand the low compliance by the patient and, on the other, the risk of reaching toxic levels. A solution to these problems comes from the controlled release technology. Controlled release formulations attempt to alter drug adsorption and subsequent drug concentration in blood by modifying the drug release from the device. This lead to reduced fluctuations in the plasma drug concentration, sustained drug effects with less side effects, and increased patient compliance. Controlled release products consist of the active agent and the polymer matrix or membrane that regulates its release.

Advances in controlled release technology in recent years have been possible as a result of advances in polymer science which allow fabrication of polymers with tailor-made specifications, such as molecular size, charge density, hydrophobicity, specific functional groups, biocompatibility, and degradability. Controlled release dosage forms revitalize old drugs by reducing pharmaceutical shortcomings and improving biopharmaceutical properties of the drugs. This is an alternative to the development of new drugs which is extremely costly. They providing control over the drug delivery can be the most important factor at times when traditional oral or injectable drug formulations cannot be used. These include situations requiring the slow release of water-soluble drugs, the fast release of low-solubility drugs, drug delivery to specific sites, delivery of two or more agents with the same formulation, and systems based on carriers that can dissolve or degrade and be readily eliminated.

To design advanced dosage forms, suitable carrier materials are used to overcome the undesirable properties of drug molecules. Hence various kinds of high-performance biomaterials are being constantly developed. From the viewpoint of the optimization of pharmacotherapy, drug release should be controlled in accordance with the therapeutic purpose and pharmacological properties of active substances. There has been a growing interest in developing the rate- or time-controlled type in oral preparations, because an appropriate drug release from the dosage forms is of critical importance realizing their therapeutic efficacy. In recent years, controller drug delivery formulations have become much more sophisticated, with the ability to do more than simply extend the effective release period for a particular drug, such as respond to changes in the biological environment and deliver, or cease to deliver, drugs based on these changes. In addition, materials have been developed that should lead to targeted delivery systems, in which a particular formulation can be directed to the specific cell, tissue, or site where the drug it contains is to be delivered.

The plasma drug levels-time profiles can be mainly classified into two categories: rate-controlled type and time-controlled type (delayed release type) (figure 1.1). The rate-controlled type is further classified into three types, that is, immediate release, prolonged release, and modified release types. Moreover to control the moment at which delivery should begin the two following approaches

have been developed: i) activation-modulated drug delivery: the release is activated by some physical, chemical or biochemical processes; ii) feedback-regulated drug delivery: the rate of drug release is regulated by the concentration of a triggering agent, such as a biochemical substance.

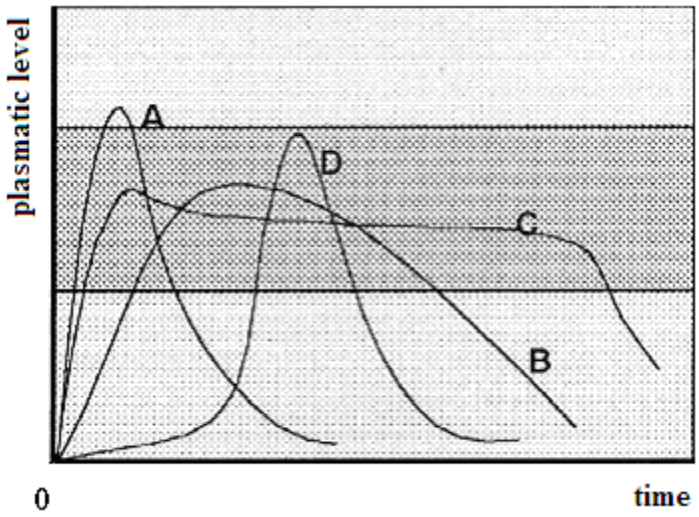

Figure 1.1 *Typical drug release profiles following oral administration: A) immediate release; B) prolonged release; C) modified release; D) delayed release.*

The release of drugs, absorbed or encapsulated by polymers, involves their slow and controllable diffusion from/or through polymeric matrix materials. Drugs, covalently attached to biodegradable polymers or dispersed in the polymeric matrix of such macromolecules, may be released by erosion/degradation of the polymer. Both mechanisms may sustain the release of therapeutic agent by some systems. Therapeutic molecules, complexed by polymers, may be released from gels by diffusion. In others, the release mechanism may simply involve desorption of the adsorbed active agent. Targeting can be attained by attaching biomolecules, capable to recognize specific cells, to the surface of nanoparticles containing a therapeutic agent. In the absence of such recognition sites on their surface, less specific targeting can be achieved by using relatively large particles or macromolecules as vehicles of drug delivery. Such particles or macromolecules accumulate preferentially in tumor cells, which are more permeable than healthy ones.

The term ‘prodrug’ has been coined as designation of a therapeutic agent chemically bound to an another molecule, which becomes active upon its release. Such release may be triggered by cell enzymes or by enzymes in the cell vicinity. Local delivery may also be quite effective. It is achieved by insertion of biodegradable implants near locations to be treated, or by introduction of catheters containing capsules either filled or coated with the slowly released drugs.

Biodegradable implants and nanoparticles with appropriate drugs dispersed evenly in the polymeric matrix (monolithic dispersion) as well as nanoparticles with a therapeutic agent adsorbed at the surface or loaded into the core, have been formulated for such applications.

The ideal drug delivery system should be inert, biocompatible, mechanically strong, comfortable for the patient, capable of achieving high drug loading, safe from accidental release, simple to administer and remove, and easy to fabricate and sterilize.

Their applications are numerous, from drug protective coating for oral administration, to drug carrier at target site (nanoparticles, transdermal systems, etc.).

1.4 Controlled-release mechanisms

The mechanisms of controlled drug delivery (figure 1.2) can be classified into the following five mechanisms: (1) diffusion; (2) dissolution; (3) osmosis; (4) ion-exchange; and (5) polymeric prodrug.

Although any therapeutic system may employ more than one mechanism, there is a predominant mechanism for each delivery system. In all cases, polymers function as a principal component which controls the transport of drug molecules and the way this process is utilized in the device determines the primary mechanism for each drug delivery system.

1.4.1 Diffusion-controlled systems

In general, two types of diffusion-controlled systems have been used: reservoir and monolithic systems. In reservoir systems, the drug is encapsulated by a polymeric membrane through which the drug is released by diffusion. Polymer films used in the diffusion-controlled reservoir system are commonly known as solution-diffusion membranes. The polymer membrane can be either nonporous or microporous. Drug release through nonporous membranes is governed mainly by the diffusion through the polymer chains. Thus, the drug release rate through the solution-diffusion membrane can be easily controlled by selecting a polymer showing desirable drug solubility and diffusivity in the polymer matrix. Rubbery polymers have potentially higher release rates than conventional glassy or semicrystalline polymers because of their high internal free volume (i.e. space between molecules).

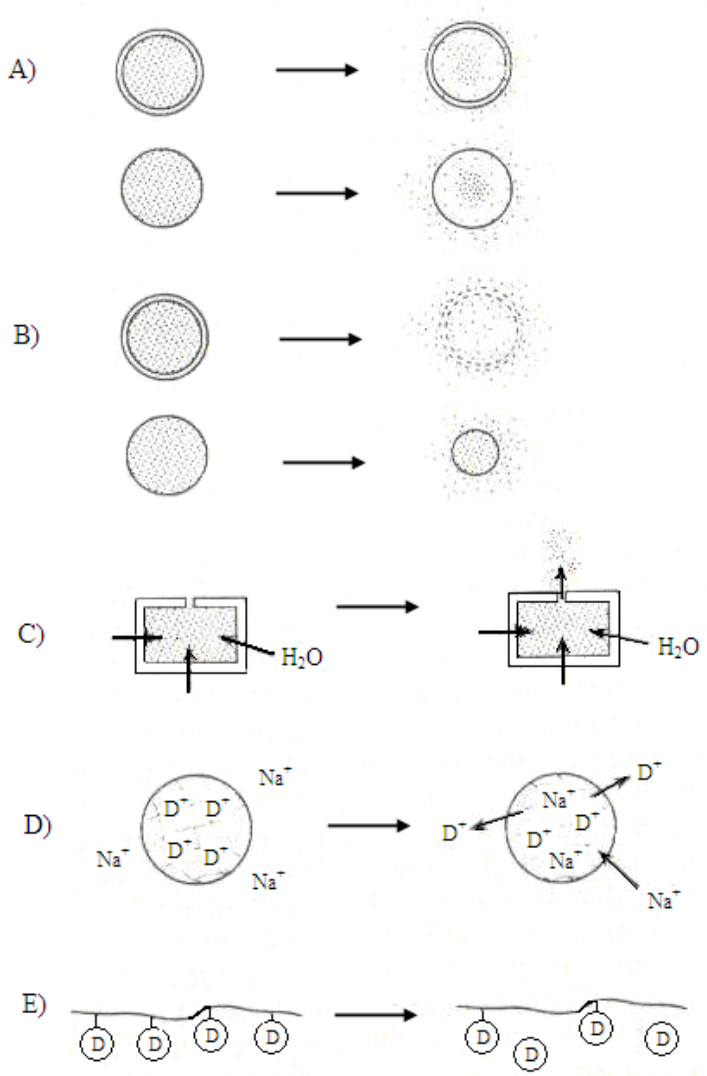

Figure 1.2 *Mechanisms of controlled release drug delivery. A) dffusion-controlled, B) dissolution-controlled, C) osmotically controlled, D) ion-exchange controlled, E) degradation-controlled (polymeric prodrug) system.*

The drug-release rate for a specific drug is generally increased if the free volume of the barrier is increased. The following equation, which describes diffusion (D) in a polymeric film, illustrates the concept of free volume:

$$D = D_0 e^{k\frac{v_f}{v_d}} \qquad (1.2)$$

where D_0 and k are phenomenological coefficients, v_f is polymer free volume, and v_d is the volume of the drug molecule.

In case of microporous membranes, which have pores ranging in size from 10Å to several hundred mm, the pores are filled with a drug-permeable liquid or

gel medium. Thus, the diffusion of the drug through the medium in the pores will dominate the drug release process. Microporous membranes are useful in the delivery of high molecular weight drugs such as peptide and protein drugs.

In monolithic devices, the drug is dissolved or dispersed homogeneously throughout the water insoluble polymer matrix. The polymer matrix can also be non-porous or microporous. Unlike the reservoir devices, the drug release from the monolithic devices rarely provide zero-order release. Matrix devices do not release drugs at constant rate; instead, the initial release rate is rapidly followed by an exponential decay with time.

1.4.2 Dissolution-controlled systems

Polymers used in the design of dissolution-controlled dosage forms are usually water-soluble, but water-insoluble polymers can be used as long as they absorb significant amount of water and disintegrate the dosage. The dissolution-controlled systems also have both reservoir and matrix dissolution systems. In reservoir systems, the drug core particles are coated with water-soluble polymeric membranes. The solubility of the polymeric membrane, and thus the drug release, depends on the thickness of the membrane and the type of the polymer used. Drug release can be achieved in more controlled fashion by preparing a system with alternating layers of drug and polymeric coats or by preparing a mixture of particles which have different coating characteristics. Matrix dissolution devices are generally prepared by compressing powder mix of drug and a water- soluble or water-swellable polymer. They can also be made by casting and drying of a polymer solution containing a suitable amount of dissolved or dispersed drug.

In a early stage of the dissolution process, the polymer starts swelling as a result of water penetration. During swelling, outer portion of polymer matrix forms a mucilaginous barrier which retards further ingress of water and acts as a rate-controlling layer to drug release. Thus, diffusion of the drug through this barrier also contributes to the drug release rate in addition to the dissolution kinetics of the polymer matrix.

The term “dissolution” generally describes the physical disentanglement of polymer chains in the presence of excess water without involving any chemical changes. The cleavage of polymer chains into smaller fragments by either chemical or biological process and subsequent release into the medium is known as (bio)degradation. Biodegradable delivery systems can be considered as a special case of the dissolution-controlled system since they show the same physical phenomenon. Biodegradable polymers are useful in the development of targetable drug delivery systems to specific cells or organs in the body where the removal of the polymeric systems becomes almost impossible.

1.4.3 Osmotic delivery systems

The osmotic device comprises a core reservoir of drugs, whit or without osmotically active salt, coated with a semi-permeable polymer membrane. The presence of salt or drug molecules creates an osmotic pressure gradient across the membrane and the diffusion of water into the device gradually forces the drug molecules out through an orifice made in the device. The mechanical strength of the semi-permeable membrane should be strong enough to resist the stress building inside the device during the operational lifetime of the device. The drug release rate from the osmotic devices, which is directly related to the rate of external water diffusion, can be controlled by the type, thickness, and area of the semi-permeable polymer membrane.

1.4.4 Ion-exchange systems

The ion-exchange systems are useful in the controlled release of ionic (or ionisable) drugs. Polyelectrolytes are crosslinked to form water-insoluble ion-exchange resins. The drug is bound to the ionic groups by salt formation during absorpition and released after being replaced by appropriately charged ions in the surrounding media. Cationic drugs form complexes with anionic charges in ion-exchange resin. Hydrogen ions and/or other cations such as sodium or potassium ions activate the release of cationic drugs by replacing them from the drug-resin complex. For the delivery of anionic drugs, one can utilise cationic ion-exchange resins with contain basic group such as amino or quaternary ammonium groups. Sometime the ion-exchange resins are additionally coated with a polymer film to regulate the swelling of the resin and to further control the drug release.

1.4.5 Polymeric prodrugs

Many water-soluble polymers possess functional groups to which drug molecules can be covalently attached. Polymer backbone, which itself as no therapeutic effect, serves as a carrier for the drug. The drug molecules are gradually released from the polymer by hydrolytic or enzymatic cleavage. If the cleavage occurs by chemical hydrolysis, the drug release depends on the nature of the covalent bonds and pH of the environment. In the body, this occurs very slowly. If the drugs molecules are released by enzymatic hydrolysis, the release is mainly dependent on the concentration of enzymes. Thus, the exact release profile depends on the in vivo condition not on the delivery system itself. To be a useful drug carrier, a polymer needs to posses certain features. The polymer should remain water-soluble even after drug loading. The molecular weight of the polymer should be large enough to permit glomerular filtration but small enough to reach all cell types. The drug-carrier linkages should be stable in body fluid and

yet degradable once captured by the target cells. The polymeric carrier of course, as to be non-toxic, non-immunogenic, and biocompatible.

1.5 Pharmaceutical carriers

In developing carriers (figure 1.3) one may want to have a combination of various properties/functions, i.e. to construct and use multifunctional pharmaceutical nanocarriers demonstrating the following set of properties: (i) prolonged circulation in the blood; (ii) ability to accumulate – specifically or non-specifically in the required pathological zone, (iii) responsiveness to local stimuli, such as pH and/or temperature changes, resulting, for example, in accelerated drug release; (iv) allow for an effective intracellular drug delivery and further to individual cell organelles, and (v) bear a contrast/reporter moiety allowing for the real-time observation of its accumulation inside the target.

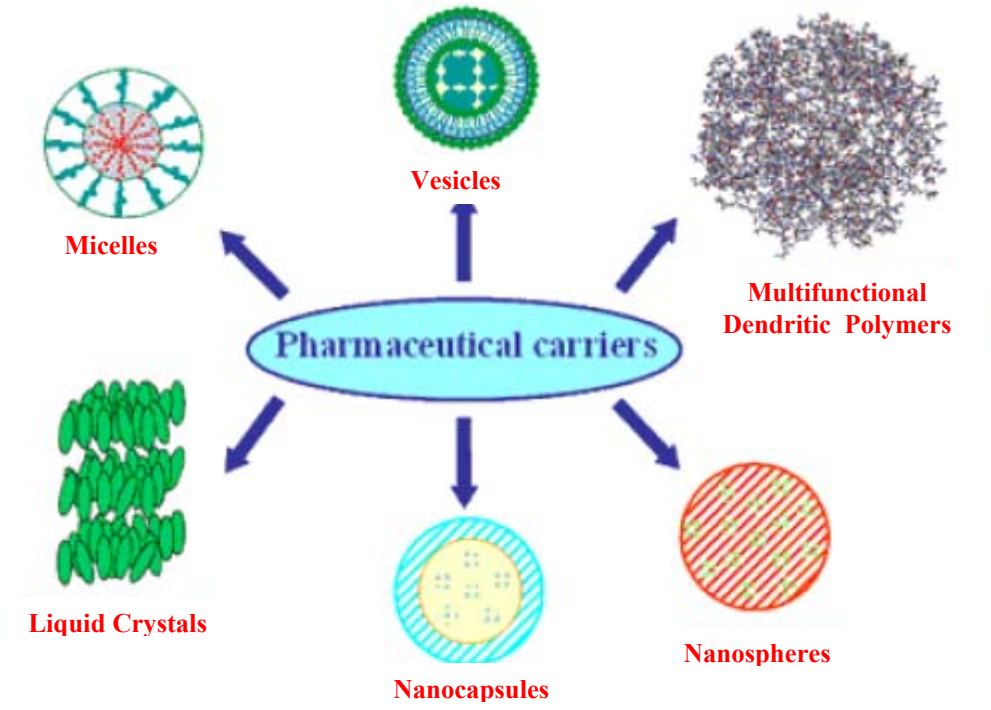

Figure 1.3 *Pharmaceutical carriers.*

Evidently, to prepare such smart multifunctional pharmaceutical nanocarrier, chemical moieties providing certain required individual properties have to be simultaneously assembled on the surface (within the structure) of the same nanoparticle. Moreover, these individual moieties have to function in a certain coordinated way to provide a desired combination of useful properties. However, systems like this still represent a challenge.

Colloidal drug carrier systems such as micellar solutions, vesicle and liquid crystal dispersions, as well as nanoparticle dispersions consisting of small particles of 10-400 nm diameter show great promise as drug delivery systems. When developing these formulations, the goal is to obtain systems with optimized drug loading and release properties, long shelf-life and low toxicity. The incorporated drug participates in the microstructure of the system, and may even influence it due to molecular interactions, especially if the drug possesses amphiphilic and/or mesogenic properties. Micelles formed by self-assembly of amphiphilic block copolymers (5-50 nm) in aqueous solutions are of great interest for drug delivery applications. The drugs can be physically entrapped in the core of block copolymer micelles and transported at concentrations that can exceed their intrinsic water-solubility. Moreover, the hydrophilic blocks can form hydrogen bonds with the aqueous surroundings and form a tight shell around the micellar core. As a result, the contents of the hydrophobic core are effectively protected against hydrolysis and enzymatic degradation. In addition, the corona may prevent recognition by the reticuloendothelial system and therefore preliminary elimination of the micelles from the bloodstream. A final feature that makes amphiphilic block copolymers attractive for drug delivery applications is the fact that their chemical composition, total molecular weight and block length ratios can be easily changed, which allows control of the size and morphology of the micelles. Functionalization of block copolymers with crosslinkable groups can increase the stability of the corresponding micelles and improve their temporal control. Substitution of block copolymer micelles with specific ligands is a very promising strategy to a broader range of sites of activity with a much higher selectivity.

Liposomes are a form of vesicles that consist either of many, few or just one phospholipid bilayers. The polar character of the liposomal core enables polar drug molecules to be encapsulated. Amphiphilic and lipophilic molecules are solubilized within the phospholipid bilayer according to their affinity towards the phospholipids. Participation of non-ionic surfactants instead of phospholipids in the bilayer formation results in niosomes. Channel proteins can be incorporated without loss of their activity within the hydrophobic domain of vesicle membranes, acting as a size-selective filter, only allowing passive diffusion of small solutes such as ions, nutrients and antibiotics. Thus, drugs that are encapsulated in a nanocage-functionalized with channel proteins are effectively protected from premature degradation by proteolytic enzymes. The drug molecule, however, is able to diffuse through the channel, driven by the concentration difference between the interior and the exterior of the nanocage.

Dendrimers are nanometer-sized, highly branched and monodisperse macromolecules with symmetrical architecture. They consist of a central core, branching units and terminal functional groups. The core together with the internal units, determine the environment of the nanocavities and consequently

their solubilizing properties, whereas the external groups the solubility and chemical behaviour of these polymers. Targeting effectiveness is affected by attaching targeting ligands at the external surface of dendrimers, while their stability and protection from the Mononuclear Phagocyte System is being achieved by functionalization of the dendrimers with polyethylene glycol chains.

Liquid Crystals combine the properties of both liquid and solid states. They can be made to form different geometries, with alternative polar and non-polar layers (i.e., a lamellar phase) where aqueous drug solutions can be included.

Nanoparticles (including nanospheres and nanocapsules of size 10-200 nm) are in the solid state and are either amorphous or crystalline. They are able to adsorb and/or encapsulate a drug, thus protecting it against chemical and enzymatic degradation. Nanocapsules are vesicular systems in which the drug is confined to a cavity surrounded by a unique polymer membrane, while nanospheres are matrix systems in which the drug is physically and uniformly dispersed. Nanoparticles as drug carriers can be formed from both biodegradable polymers and non-biodegradable polymers. In recent years, biodegradable polymeric nanoparticles have attracted considerable attention as potential drug delivery devices in view of their applications in the controlled release of drugs, in targeting particular organs/tissues, as carriers of DNA in gene therapy, and in their ability to deliver proteins, peptides and genes through the peroral route.

Hydrogels are three-dimensional, hydrophilic, polymeric networks capable of imbibing large amounts of water or biological fluids. The networks are composed of homopolymers or copolymers, and are insoluble due to the presence of chemical crosslinks (tie-points, junctions), or physical crosslinks, such as entanglements or crystallites. Hydrogels exhibit a thermodynamic compatibility with water, which allows them to swell in aqueous media. They are used to regulate drug release in reservoir-based, controlled release systems or as carriers in swellable and swelling-controlled release devices. On the forefront of controlled drug delivery, hydrogels as in vivo-intelligent and stimuli-sensitive gel systems modulate release in response to pH, temperature, ionic strength, electric field, or specific analyte concentration differences. In these systems, release can be designed to occur within specific areas of the body (e.g., within a certain pH of the digestive tract) or also via specific sites (adhesive or cell receptor specific gels via tethered chains from the hydrogel surface). Hydrogels as drug delivery systems can be very promising materials if combined with the technique of molecular imprinting.

The molecular imprinting technology has an enormous potential for creating satisfactory drug dosage forms. Molecular imprinting involves forming a pre-polymerization complex between the template molecule and functional monomers or functional oligomers (or polymers) with specific chemical structures designed to interact with the template either by covalent, noncovalent chemistry

(self-assembly) or both. Once the pre-polymerization complex is formed, the polymerization reaction occurs in the presence of a cross-linking monomer and an appropriate solvent, which controls the overall polymer morphology and macroporous structure. Once the template is removed, the product is a heteropolymer matrix with specific recognition elements for the template molecule. Examples of molecular imprinted polymers based drug delivery systems involve: (i) rate-programmed drug delivery, where drug diffusion from the system has to follow a specific rate profile, (ii) activation modulated drug delivery, where the release is activated by some physical, chemical or biochemical processes and (iii) feedback-regulated drug delivery, where the rate of drug release is regulated by the concentration of a triggering agent, such as a biochemical substance, the concentration of which is dependent on the drug concentration in the body. Despite the already developed interesting applications of molecularly imprinted polymers (MIPs), the incorporation of the molecular imprinting approach for the development of drug delivery systems is just at its incipient stage. Nevertheless, it can be foreseen that, in the next few years, significant progress will occur in this field, taking advantage of the improvements of this technology in other areas. Among the evolution lines that should contribute more to enhance the applicability of imprinting for drug delivery, the application of predictive tools for a rational design of imprinted systems and the development of molecular imprinting in water may be highlighted.

Conjugation of biological (peptides/proteins) and synthetic polymers is an efficient means to improve control over nanoscale structure formation of synthetic polymeric materials that can be used as drug delivery systems. Conjugation of suitable biocompatible polymers to bioactive peptides or proteins can reduce toxicity, prevent immunogenic or antigenic side reactions, enhance blood circulation times and improve solubility. Modification of synthetic polymers or polymer therapeutics with suitable oligopeptide sequences, on the other hand, can prevent random distribution of drugs throughout a patient's body and allow active targeting. Functionalization of synthetic polymers or polymer surfaces with peptide sequences derived from extracellular matrix proteins is an efficient way to mediate cell adhesion. The ability of cationic peptide sequences to complex and condense DNA and oligonucleotides offers prospects for the development of non-viral vectors for gene-delivery based on synthetic polymeric hybrid materials.

The field of in-situ forming implants has grown exponentially in recent years. Liquid formulations generating a (semi-)solid depot after subcutaneous injection, also designated as implants, are an attractive delivery system for parenteral application because they are less invasive and painful compared to implants. Localized or systemic drug delivery can be achieved for prolonged periods of time, typically ranging from one to several months. Generally, parenteral depot systems could minimize side effects by achieving constant, 'infusion-like' plasma-level time profiles, especially important for proteins with

narrow therapeutic indices. From a manufacturing point of view, in-situ forming depot systems offer the advantage of being relatively simple to manufacture from polymers. Injectable in-situ forming implants are classified into four categories, according to their mechanism of depot formation: (i) thermoplastic pastes, (ii) in-situ cross-linked polymer systems, (iii) in-situ polymer precipitation, and (iv) thermally induced gelling systems.

The ultimate goal in controlled release is the development of a microfabricated device with the ability to store and release multiple chemical substances on demand. Recent advances in microelectro-mechanical systems (MEMS) have provided a unique opportunity to fabricate miniature biomedical devices for a variety of applications ranging from implantable drug delivery systems to lab-on-a-chip devices. The controlled release microchip has the following advantages: (i) multiple chemicals in any form (e.g. solid, liquid or gel) can be stored inside and released from the microchip, (ii) the release of chemicals is initiated by the disintegration of the barrier membrane via the application of an electric potential, (iii) a variety of highly potent drugs can potentially be delivered accurately and in a safe manner, (iv) complex release patterns (e.g. simultaneous constant and pulsatile release) can be achieved, (v) the microchip can be made small enough to make local chemical delivery possible thus achieving high concentrations of drug at the site where it is needed while keeping the systemic concentration of the drug at a low level and (vi) water penetration into the reservoirs is avoided by the barrier membrane and thus the stability of protein-based drugs with limited shelf-life is enhanced.

1.6 Future Opportunities and Challenges

Nanoparticles and nanoformulations have already been applied as drug delivery systems with great success; and nanoparticulate drug delivery systems have still greater potential for many applications, including anti-tumour therapy, gene therapy, AIDS therapy, radiotherapy, in the delivery of proteins, antibiotics, virostatics, vaccines and as vesicles to pass the blood-brain barrier. Nanoparticles provide massive advantages regarding drug targeting, delivery and release and, with their additional potential to combine diagnosis and therapy, emerge as one of the major tools in nanomedicine. The main goals are to improve their stability in the biological environment, to mediate the bio-distribution of active compounds, improve drug loading, targeting, transport, release, and interaction with biological barriers. The cytotoxicity of nanoparticles or their degradation products remains a major problem, and improvements in biocompatibility obviously are a main concern of future research.

There are many technological challenges to be met, in developing the following techniques:

- nano-drug delivery systems that deliver large but highly localized quantities of drugs to specific areas to be released in controlled ways;
- controllable release profiles, especially for sensitive drugs;
- materials for nanoparticles that are biocompatible and biodegradable;
- architectures/structures, such as biomimetic polymers, nanotubes;
- technologies for self-assembly;
- functions (active drug targeting, on-command delivery, intelligent drug release devices/bioresponsive triggered systems, self-regulated delivery systems, systems interacting with the body, smart delivery);
- virus-like systems for intracellular delivery;
- nanoparticles to improve devices such as implantable devices/nanochips for nanoparticle release, or multi reservoir drug delivery-chips;
- nanoparticles for tissue engineering; e.g. for the delivery of cytokines to control cellular growth and differentiation, and stimulate regeneration; or for coating implants with nanoparticles in biodegradable polymer layers for sustained release;
- advanced polymeric carriers for the delivery of therapeutic peptide/proteins (biopharmaceutics);

and also in the development of:

- combined therapy and medical imaging, for example, nanoparticles for diagnosis and manipulation during surgery (e.g. thermotherapy with magnetic particles);
- universal formulation schemes that can be used as intravenous, intramuscular or peroral drugs;
- cell and gene targeting systems;
- user-friendly lab-on-a-chip devices for point-of-care and disease prevention and control at home;
- devices for detecting changes in magnetic or physical properties after specific binding of ligands on paramagnetic nanoparticles that can correlate with the amount of ligand;
- better disease markers in terms of sensitivity and specificity.

References

1. J. Jagur-Grodzinski, *React. Funct. Polym.,* 39 (1999) 99-138.
2. *Controlled Drug Delivery: Challenges and Strategies,* K. Park - Ed. American Chemical Society: Washington, DC, 1997.
3. *Integrated Biomaterials Science,* R. Barbucci - Ed. Kluwer Academic/Plenum Publishers: New York, 2002, CAP. 29.
4. *Polymers of Biological and Biomedical Significance,* S. W. Shalaby, Y. Ikada, R. Langer, J. Williams - Ed. American Chemical Society: Washington, DC, 1994, Symposium series 540, CAP 1, 4.
5. V. P. Torchilin, *Adv. Drug Delivery Rev.,* 58 (2006) 1532-1555.
6. W. N. Charman, H. -K. Chan, B. C. Finnin, S. A. Charman, *Drug Dev. Res.,* 46 (1999) 316-327.
7. Jr J. T. Santini, A. C. Richards, R. Scheidt, M. J. Cima, R. Langer, *Angew. Chem. Int. Ed.,* 39 (2000) 2396-2407.
8. J. Kopecek, *Eu. J. Pharm. Sci.*, 20 (2003) 1-16.
9. V. P. Torchilin, *J. Contr. Rel.*, 73 (2001) 137-172.
10. C. C.Muller-Goymann, *Eur. J. Pharm. and Biopharm.,* 58 (2004) 343-356.
11. R. Haag, *Angew. Chem. Int. Ed.,* 43 (2004) 278-282.
12. Y. Bae, S. Fukushima, A. Harada, K. Kataoka, *Angew. Chem. Int. Ed.,* 42 (2003) 4640-4643.
13. K. S. Soppimath, T. M. Aminabhavi, A. R. Kulkarni, W. E. Rudzinski, *J. Contr. Rel.*, 70 (2001) 1-20.
14. C. B. Packhaeuser, J. Schnieders, C. G. Oster, T. Kissel, *Eur. J. Pharm. and Biopharm.,* 58 (2004) 445-455.
15. S. A. Agnihotri, N. N. Mallikarjuna, T. M. Aminabhavi, *J. Contr. Rel.*, 100 (2004) 5-28.
16. A. Sood, R. Panchagnula, *Chem. Rev.,* 101 (2000) 3275-3303.
17. I. Niculescu-Duvaz, C. J. Springer, *Adv. Drug Delivery Rev.,* 26 (1997) 151-172.
18. T. Manabe, H. Okino, R. Maeyama, K. Mizumoto, E. Nagai, M. Tanaka, T. Matsuda, *J. Contr. Rel.*, 100 (2004) 317-330.
19. B. Ziaie, A. Baldi, M. Lei, Y. Gu, R. A. Siegel, *Adv. Drug Delivery Rev.,* 56 (2004) 145-172.
20. M. E. Byrne, K. Park, N. Peppas, *Adv. Drug Delivery Rev.,* 54 (2002) 149-161.
21. G. W. M. Vandermeulen, H.-A. Klok, *Macromol. Biosci.,* 4 (2003) 383-398.
22. A. Rosler, G. W. M. Vandermeulen, H.-A. Klok, *Adv. Drug Delivery Rev.,* 53 (2001) 95-108.
23. C. Alvarez-Lorenzo, A. Concheiro, *J. Chromatogr. B,* 804 (2004) 231-245.
24. J. K. Vasir, K. Tambwekar, S. Garg, *Int. J. Pharm.,* 255 (2003) 13-32.

25. M. Winterhalter, C. Hilty, S. M. Bezrukov, C. Nardin, W. Meier, D. Fournier, *Talanta*, 55 (2001) 965-971.

SECOND CHAPTER

CYCLODEXTRINS

2.1 History

Cyclodextrins are natural substances deriving from starch by means of enzymatic degradation at the enzyme's expense cycloglycosiltransferasi (CGTase), produced by about 15 bacterial kinds, especially *B. Macerans, B. Circulans, B. Megaterium, B. Sterotermophilus, B. Alkalophilic.*

The first reference to a substance which later proved to be a cyclodextrin, was published by Villiers in1891 [1]. Digesting starch with *Bacillus Amylobacter* (which probably was not a pure culture, but also contained heat-resistant spores of *Bacillus Macerans*), he isolated about 3 g of a crystalline substance from 1000 g starch, and determined its composition to be $(C_6H_{10}O_5)_2 \cdot 3H_2O$. Villiers named this product "cellulosine", because it resembled cellulose with regard to its resistance against acidic hydrolysis and because it did not show reducing properties. Even at that time, he observed that two distinct crystalline "cellulosines" were formed, probably α- and β-cyclodextrin.

Twelve years later, Schardinger, who studied various isolated strains of bacteria that survived the cooking process and which were thought to be responsible for certain cases of food poisoning, published a report that digesting starch with such a microorganism resulted in the formation of small amounts of two different crystalline products. These substances seemed to be identical with the "cellulosines" of Villiers. Schardinger continued to study these crystallized dextrins, with the expectation that they would shed some light on the synthesis and degradation of starch. He named the isolated microbe *Bacillus Macerans* [2].

At beginning of the second period, in the 1930s, Freudenberg and co-workers, came to the conclusion that the crystalline Schardinger dextrins are built from maltose units and contain only α-1,4-glycosidic linkages. They described the first scheme for the isolation of homogeneous and pure fractions, and in 1936 postulated the cyclic structure of these crystalline dextrins [3].

With the beginning of the 1950s, two groups, D. French et al. [4] and F. Cramer *et al.* [5] began to work intensively on the enzymic production of cyclodextrins, on fractionating them to pure components, and on characterizing their true chemical and physical properties. French discovered that there are even larger cyclodextrins, while Cramer's group mainly directed their attention toward the inclusion complex forming properties of the cyclic dextrins.

Numerous publications and patents testify the applicability of cyclodextrins in several scientific fields, their use is widespread on large scale in the industry, because through their ability to form inclusion most important properties of complexed molecules can be modified.

2.2 Structural Features

Cyclodextrins (CDs) comprise a family of three well known industrially produced major, and several rare, minor cyclic oligosaccharides. The three major cyclodextrins are crystalline, homogeneous, non hygroscopic substances, which are torus-like macro-rings built up from glucopyranose units. The α-cyclodextrin comprises six glucopyranose units, β-CD comprises seven such units, and γ-CD comprises eight such units. The most important characteristics of the CDs are summarized in table 2.1.

N° glucopyranose units	6	7	8
Molecular weight	972	1135	1297
Cavity diameter in Å	4.7-5.3	6.0-6.5	7.5-8.3
Cavity volume in $Å^3$	174	262	427
Melting range (°C)	250-255	250-265	240-245
Solubility in water at 25°C (g/100ml)	14.5	1.85	23.2
Water molecules in the cavity	6	11	17

Table 2.1 *Characteristics of α-, β-, and γ-CDs.*

As a consequence of the $^4C_1$ conformation of the glucopyranose units, all secondary hydroxyl groups are situated on one of the two edges of the ring, whereas all the primary ones are placed on the other edge. The ring, in reality, is a cylinder, or better said a conical cylinder, which is frequently characterized as a doughnut or wreath-shaped truncated cone (figure 2.1). The cavity is lined by the hydrogen atoms and the glycosidic oxygen bridges, respectively. The nonbonding electron pairs of the glycosidic oxygen bridges are directed toward the inside of the cavity producing a high electron density there and lending to it some Lewis base characteristics.

The C-2-OH group of one glucopyranoside unit can form a hydrogen bond with the C-3-OH group of the adjacent glucopyranose unit. In the CD molecule, a complete secondary belt is formed by these H bonds, therefore the β-CD is a rather rigid structure. This intramolecular hydrogen bond formation is probably the explanation for the observation that β-CD has the lowest water solubility of all CDs.

The hydrogen-bond belt is incomplete in the α-CD molecule, because one glucopyranose unit is in a distorted position. Consequently, instead of the six possible H-bonds, only four can be established fully. The γ-CD is a noncoplanar, more flexible structure; therefore, it is the more soluble of the three CDs.

On the side where the secondary hydroxyl groups are situated, the diameter of the cavity is larger than on the side with the primary hydroxyls, since free rotation of the latter reduces the effective diameter of the cavity.

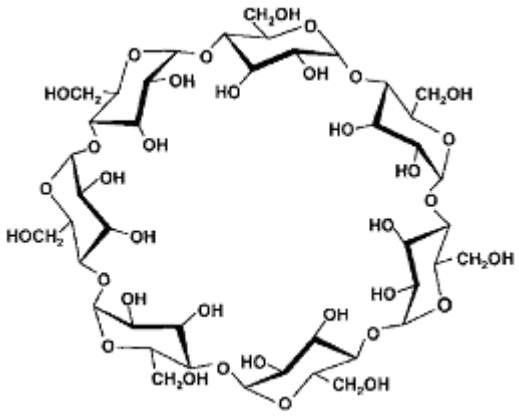

Figure 2.1 *a) Schematic representation of β-CD, b) Structure of glucopyranose unit, c) Truncated conical cylinder form of cavity with -OH primary groups on narrow edge and -OH secondary ones on the wide edge.*

2.3 Formation of inclusion complexes

The most notable feature of cyclodextrins is their ability to form solid inclusion complexes (host-guest complexes) with a very wide range of solid, liquid and gaseous compounds by a molecular complexation. In these complexes, a guest molecule is held within the cavity of the cyclodextrin host molecule. The lipophilic cavity of cyclodextrin molecules provides a microenvironment into which appropriately sized non-polar moieties can enter to form inclusion complexes [6]. The main driving force of complex formation is the release of

enthalpy-rich water molecules from the cavity. Water molecules are displaced by more hydrophobic guest molecules present in the solution to attain an apolar-apolar association and decrease of cyclodextrin ring strain resulting in a more stable lower energy state [7].

One, two, or three cyclodextrin molecules contain one or more entrapped "guest" molecules. Most frequently the host:guest ratio is 1:1. This is the essence of "molecular encapsulation".

The formed inclusion complexes can be isolated as stable crystalline substances. Upon dissolving these complexes, an equilibrium is established between dissociated and associated species, and this is expressed by the complex stability constant K_a. The association of the CD and guest (D) molecules, and the dissociation of the formed CD/guest complex is governed by a thermodynamic equilibrium [7].

$$CD + D \Leftrightarrow CD \cdot D \tag{2.1}$$

$$K_{1:1} = \frac{[CD \cdot D]}{[CD][D]} \tag{2.2}$$

Binding strength depends on how well the 'host-guest' complex fits together and on specific local interactions between surface atoms. Complexes can be formed either in solution or in the crystalline state and water is typically the solvent of choice. Inclusion complexation can be accomplished in a co-solvent system and in the presence of any non-aqueous solvent.

The potential guest list for molecular encapsulation in cyclodextrins is quite varied and includes such compounds as straight or branched chain aliphatics, aldehydes, ketones, alcohols, organic acids, fatty acids, aromatics, gases, and polar compounds such as halogens, oxyacids and amines. Due to the availability of multiple reactive hydroxyl groups, the functionality of cyclodextrins is greatly increased by chemical modification. Through modification, the applications of cyclodextrins are expanded. CDs are modified through substituting various functional compounds on the primary and/or secondary face of the molecule.

The ability of a cyclodextrin to form an inclusion complex with a guest molecule is a function of two key factors. The first is steric and depends on the relative size of the cyclodextrin to the size of the guest molecule or certain key functional groups within the guest. If the guest is the wrong size, it will not fit properly into the cyclodextrin cavity. The second critical factor is the thermodynamic interactions between the different components of the system (cyclodextrin, guest, solvent). For a complex to form there must be a favourable net energetic driving force that pulls the guest into the cyclodextrin. While the height of the cyclodextrin cavity is the same for all three types, the number of glucose units determines the internal diameter of the cavity and its volume. Based

on these dimensions, α-cyclodextrin can typically complex low molecular weight molecules or compounds with aliphatic side chains, β-cyclodextrin will complex aromatics and heterocycles and γ-cyclodextrin can accommodate larger molecules such as macrocycles and steroids.

In general, therefore, there are four energetically favourable interactions that help shift the equilibrium to form the inclusion complex:

- the displacement of polar water molecules from the apolar cyclodextrin cavity;
- the increased number of hydrogen bonds formed as the displaced water returns to the larger pool;
- a reduction of the repulsive interactions between the hydrophobic guest and the aqueous environment;
- an increase in the hydrophobic interactions as the guest inserts itself into the apolar cyclodextrin cavity.

While this initial equilibrium to form the complex is very rapid (often within minutes), the final equilibrium can take much longer to reach. Once inside the cyclodextrin cavity, the guest molecule makes conformational adjustments to take maximum advantage of the weak van der Waals forces that exist.

Complexes can be formed by a variety of techniques that depend on the properties of the active material, the equilibrium kinetics, the other formulation ingredients and processes and the final dosage form desired. However, each of these processes depends on a small amount of water to help drive the thermodynamics. Among the methods used are simple dry mixing, mixing in solutions and suspensions followed by a suitable separation, the preparation of pastes and several thermo-mechanical techniques.

The most important primary consequences of the interaction between a poorly soluble guest and a CD in aqueous solution are as follows [7]:

- the concentration of the guest in the dissolved phase increases significantly, while the concentration of the dissolved CD decreases. This latter point is not always true, however, because ionized guests, or hydrogen-bond establishing compounds may enhance the solubility of the CD;
- the spectral properties of the guest are modified;
- the reactivity of the included molecule is modified. In most cases the reactivity decreases, i.e., the guest is stabilized, but in many cases the CD behaves as an artificial enzyme, accelerating various reactions and modifying the reaction pathway;
- the diffusion and volatility (in case of volatile substances) of the included guest decrease strongly;
- the formerly hydrophobic guest, upon complexation, becomes hydrophilic;

and in the solid state:

- the complexed substance is molecularly dispersed in a carbohydrate matrix, forming a microcrystalline or amorphous powder, even with gaseous guest molecules;
- the complexed substance is effectively protected against any type of reaction, except that with the CD hydroxyls, or reactions catalyzed by them;
- sublimation and volatility are reduced to a very low level;
- the complex is hydrophilic, easily wettable, and rapidly soluble.

Therefore, cyclodextrins are used in food, pharmaceuticals, cosmetics, environment protection, bioconversion, packing and the textile industry [8].

Dissociation of the inclusion complex is a relatively rapid process usually driven by a large increase in the number of water molecules in the surrounding environment. The resulting concentration gradient shifts the equilibrium to the left. In highly dilute and dynamic systems like the body, the guest has difficulty finding another cyclodextrin to reform the complex and is left free in solution.

2.4 Thermodynamics of complexation

The most important contributions to the complexation thermodynamics of cyclodextrins are believed to originate from (a) penetration of the hydrophobic part of the guest molecule into the cyclodextrin cavity and (b) dehydration of the organic guest [9]. Usually the sum of the contributions a and b is considered to be the entity of the hydrophobic effect, although occasionally contribution a is separated from the total effect as a "pure" van der Waals interaction.

The general trends of the thermodynamic quantities for the complexation reactions of natural and modified cyclodextrins are consistent with the hydrophobic nature of the host-guest interactions. Obviously, much higher affinities as defined by $-\Delta G°$ are obtained for neutral compounds compared to those of the corresponding charged species derived from the same original guest molecules. Similarly, the affinity increases with increasing ionic strength or concentration of the salt in aqueous solution.

The thermodynamic data ($\Delta G°$, $\Delta H°$ e $\Delta S°$) present in literature [10] for a very wide variety of homologous aliphatic and aromatic guest compounds were rationalized in terms of position and number of additional methyl or methylene, hydroxyl, and other functional group(s) in aliphatic and/or aromatic guest homologues, as well as the flexibility and the chirality of organic guest molecules. These are the governing factors that determine the thermodynamic quantities of the complexation of cyclodextrins with various organic guests.

In a very general sense, the size-fit concept, which predicts the highest complex stabilities for the best size-matched host-guest pairs, may explain the global trends of the thermodynamic quantities for complexation of natural cyclodextrins. For instance, because the cavity diameter of α-cyclodextrin (ca. 4.9

Å) is much smaller than that of β-cyclodextrin (ca. 6.2 Å) and because van der Waals forces are critically dependent on the distance of separation, one can expect that the forces induced upon complexation of straight-chain guests will be larger (more negative ΔH°) for α-cyclodextrin than for β-cyclodextrin, while the same forces will be larger for the complexation of adamantyl guests with β-cyclodextrin than with α-cyclodextrin.

Certainly, the van der Waals interactions will be highly dependent not only on the size but also on the shape of the guest molecule. When the guest molecule cannot be completely accommodated within the cyclodextrin cavity, steric effects may play a dominant role. One can note that the ΔH and ΔG values become more negative with increasing of the extent in which the guest penetrates into cyclodextrin cavity for all combinations of hosts and guests. The differences in solute-solvent interactions of the free guest prior to inclusion complexation do not contribute measurably to the complexation thermodynamics but only those parts of a guest molecule that experience any changes in their environment upon complexation contribute to the thermodynamic quantities.

It is apparent that additional hydrogen-bond formation does not necessarily lead to an enhanced stability of the complex, as demonstrated by the data for 3-phenylpropionate ($\Delta G° = -12.4$ kJ mol^{-1}) and 3-(2-hydroxyphenyl)propionate ($\Delta G° = -10.9$ kJ mol^{-1}). In this particular case, a weaker complex was obtained with β-cyclodextrin as compared to the parent compound. This destabilization arises as a result of an unfavourable entropy change associated with the substitution of the 2-position of the aromatic ring. It does not depend on the chemical nature of the substituent, only on the position at which the hydroxyl group is introduced. Moreover is necessary remember that the charged and hydrophilic groups of the guests, with the exception of the phenolic hydroxyl group, remain in the bulk solution before and after association with cyclodextrin. Finally even aliphatic hydroxyl groups can form a hydrogen bond to the cyclodextrin's peripheral hydroxyls, although these interactions are not as strong as those formed by phenolic hydroxyl groups. Moreover the stability of hydrogen bonds decrease with the increase of temperature, while the hydrophobic interaction contribution of methylene groups remains unchanged also later on temperature variations.

The introduction of a double bond into the aliphatic chain reduces the flexibility of the molecule. Thus, unsaturated compounds have lower conformational degrees of freedom than the analogous saturated compounds. The increasing flexibility or degrees of freedom in a guest molecule leads to a more favourable complexation entropy, since more of the possible "conformers" can fit properly into the cavity.

No appreciable differences are found in the thermodynamic quantities for the complexation of α- and β-cyclodextrin with the enantiomeric pairs of *sec*-alkanols, norvaline and norleucine, or carbohydrates. Among several enantiomeric

pairs of aromatic guests such as phenylalanine, α-methylbenzylamine, mandelate, phenylfluoroethanol, and amphetamine, only α-methylbenzylamine gives significantly different thermodynamic quantities for its enantiomeric pair upon complexation with α-cyclodextrin. It seems, therefore, quite exceptional to find significant chiral discriminations in the complexation thermodynamics of enantiomeric guests with natural cyclodextrins, probably because most of the guest molecules are included only through nonorientating van der Waals and hydrophobic interactions and are not rigorously fixed either conformationally or rotationally in the cavity [10].

2.5 Pharmaceutical Applications

Cyclodextrins act as a drug delivery system and are potential drug delivery candidates in many applications because of their ability to alter the physical, chemical, and biological properties of guest molecules through the formation of inclusion complexes. Their bioadaptability and multi-functional characteristics make them capable of alleviating the undesirable properties of drug molecules in various routes of administration including oral, rectal, nasal, ocular, transdermal and dermal.

The principal advantages of natural cyclodextrins as drug carriers are the following: (i) well-defined chemical structure, yielding many potential sites for chemical modification or conjugation; (ii) availability of cyclodextrins of different cavity size; (iii) low toxicity and low pharmacological activity; (iv) certain water solubility; (v) protection of included/conjugated drugs from biodegradation.

2.5.1 Enhancement of drug absorption

One of the unique properties of cyclodextrins is their ability to enhance drug delivery through biological membranes. A drug substance has to have a certain level of water solubility to be readily delivered to the cellular membrane, but it needs to be hydrophobic enough to cross the membrane. The cyclodextrin molecules are relatively large (molecular weight ranging from almost 1000 to over 1500 Da), with a hydrated outer surface, and under normal conditions, cyclodextrin molecules will permeate biological membranes with considerable difficulty [11], they act as true carriers by keeping the hydrophobic drug molecules in solution and delivering them to the surface of the biological membrane, e.g. skin, mucosa or the eye cornea, where they partition into the membrane. The relatively lipophilic membrane has a low affinity for the hydrophilic cyclodextrin molecules and therefore, they remain in the aqueous membrane exterior. Cyclodextrins, on the other hand, act as penetration enhancers by disrupting the lipid layers of the biological barrier and thus increase drug availability at the surface of the biological barrier. Moreover, cyclodextrins are

used to improve the stability of substances to increase their resistance to hydrolysis, oxidation, heat, light and metal salts. At the same time, the inclusion of irritating products in cyclodextrins can also protect the gastric mucosa for the oral route, and reduce skin damage for the dermal route. Furthermore, cyclodextrins can be applied to reduce the effects of bitter or irritant tasting and bad smelling drugs [12].

Practical formulations usually contain a large quantity of pharmaceutical excipients, which may compete with the drug for the cyclodextrin cavity. Such competition may also occur with endogenous substances existing at the absorption site. The displacement of the drug from the cyclodextrin cavity by exogenous and endogenous substances at the absorption site is responsible for acceleration of the drug absorption [13]. For instance, the overall process of drug absorption from the solid complex in the presence of the competing agent is shown in figure 2.2, where k_d is the dissolution rate constant, K_c is the stability constant of the complex of the drug with the cyclodextrin, K_i is the stability constant of the complex of the competing agent with the cyclodextrin, and ka is the absorption rate constant of the drug. High dissolution rates and the relative stability of the complexes ($K_i > K_c$) favor a free drug which is readily available for absorption.

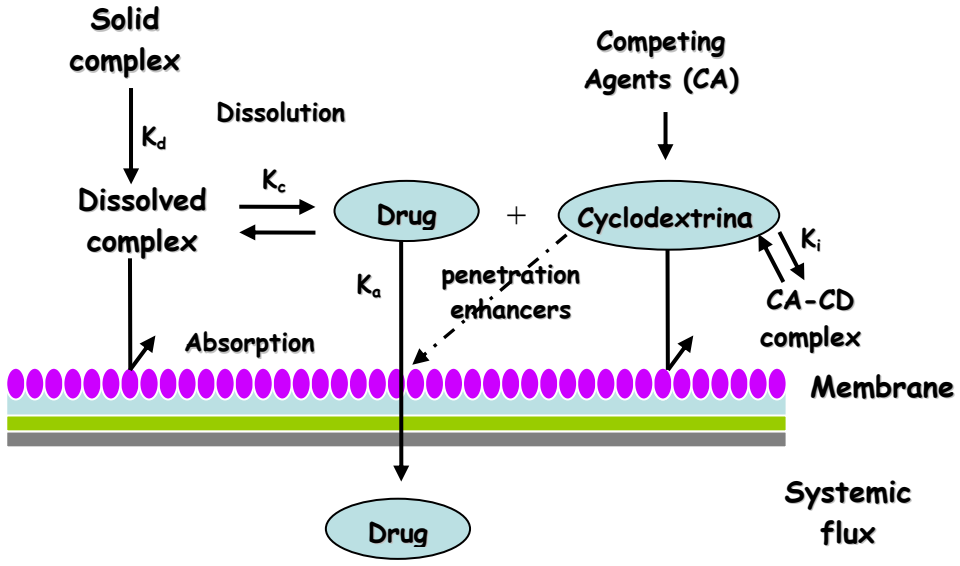

Figure 2.2 *Schematic representation of dissociation of drug-cyclodextrin complex and following systemic absorption of drug across biological membrane.*

Thus, the possible enhancing mechanisms of cyclodextrin on the bioavailability of drugs in various administration routes can be summarized as follows: (i) hydrophilic cyclodextrins increase the solubility, dissolution rate, and wettability of poorly water-soluble drugs; (ii) cyclodextrins perturb the membrane fluidity to lower the barrier function, which consequently enhances the absorption

of drugs including peptide and protein drugs through the nasal and rectal mucosa; (iii) cyclodextrins prevent the degradation or disposition of chemically unstable drugs in gastrointestinal tracts as well as during storage; and (iv) competitive inclusion complexation with third components (bile acid, cholesterol, lipids, etc.) release the included drug.

In some cases this results in improved bioavailability, increasing the pharmacological effect allowing a reduction in the dose of the drug administered. Inclusion complexes can also facilitate the handling of volatile products. This can lead to a different way of drug administering, e.g. in the form of tablets.

2.5.2 Control of drug release

From the viewpoint of the optimization of pharmacotherapy, drug release should be controlled in accordance with the therapeutic purpose and the pharmacological properties of active substances.

The plasma drug levels time profiles after oral administration can be classified into the rate-controlled release and the time-controlled release (delayed release type). The rate-controlled release is further classified into three types; i.e. immediate-release, prolonged-release and modified-release. Since the dissolution rate of the poorly water-soluble drugs is mainly responsible for both the rate and extent of oral bioavailability of the drugs, various hydrophilic materials are used to attain the immediate release formulation. The hydrophilic cyclodextrins have been extensively applied to enhance the oral bioavailability of steroids, cardiac glycosides, nonsteroidal antiinflammatory drugs, barbiturates, antiepileptics, benzodiazepines, antidiabetics, vasodilators, etc. [14]. These improvements are mainly ascribable to the increase in solubility and wettability of drugs through the formation of inclusion complexes. On the contrary, the hydrophobic cyclodextrins such as ethylated and acylated cyclodextrins with low aqueous solubility are known to work as prolonged-release carriers of water-soluble drugs [15]. The combined use of cyclodextrin complex and cyclodextrin conjugate will be useful for designing various kinds of time-controlled type oral drug delivery preparations [16]. The release of drug from the drug/cyclodextrin conjugate after oral administration shows a typical delayed-release behavior. Therefore, when the cyclodextrin conjugates are combined with other different release preparations, we can obtain more advanced and optimized drug release system, securing balanced oral bioavailability, and prominent therapeutic efficacy.

Since pharmaceutical preparations are usually composed of considerable amounts of pharmaceutical excipients and additives to maintain the efficacy and safety of the drug molecules, suitable combination of the cyclodextrin complex and the third component can markedly extend the actions of cyclodextrin for the design of advanced drug release formulations [17].

2.5.3 Site-specific drug delivery

Cyclodextrin complexes are in equilibrium with guest and host molecules in water, the degree of the dissociation being dependent on the magnitude of the stability constant. This property of the complex is a desirable quality, because the complex dissociates to free cyclodextrin and drug at the absorption site, and only the drug in free form enters into systemic circulation.

However, the inclusion equilibrium is sometimes disadvantageous when drug targeting is to be attempted, because the complex dissociates before it reaches the organ or tissues to which it is to be delivered. One of the methods to prevent the dissociation is to bind a drug covalently to cyclodextrin. Cyclodextrins are known to be barely capable of being hydrolyzed and only slightly absorbed in passage through the stomach and small intestine; however, they are fermented to small saccharides by colonic microflora and thus absorbed as maltose or glucose in the large intestine. Such biological property of CDs is useful as a source of site-specific delivery of drugs to colon [18].

2.6 Toxicological evaluations

The chemical structure of cyclodextrins (i.e., the large number of hydrogen donors and acceptors), their molecular weight (i.e., >972 Da) and their very low octanol/water partition coefficient (approximately log Po/w between less than -3 and 0) are all characteristics of compounds that do not readily permeate biological membranes [19]. Studies have shown that only negligible amounts of hydrophilic cyclodextrins and drug/cyclodextrin complexes are able to permeate lipophilic membranes such as gastrointestinal mucosa and skin. All toxicity studies have demonstrated that when administered orally cyclodextrins are practically non-toxic due to lack of absorption from the gastrointestinal tract [16]. Administered cyclodextrins are quite resistant to starch degrading enzymes, although they can be degraded at very low rates by α-amylases. α-cyclodextrin is the slowest, and γ-cyclodextrin is the fastest degradable compound, due to their differences in size and flexibility. Degradation is not performed by saliva or pancreas amylases, but by α-amylases from microorganisms from the colon flora. Adsorption studies revealed that only 2-4% of cyclodextrins were adsorbed in the small intestines, and that the remainder is degraded and taken up as glucose. This can explain the low toxicity found upon oral administration of cyclodextrins [20].

However, the lipophilic methylated β-cyclodextrins are surface active and they are to some extent (abaout 10%) absorbed from the gastrointestinal tract and consequently only limited amounts of these lipophilic cyclodextrin derivatives can be included in oral formulations, and they are unsuited for parenteral formulations. Due to toxicological considerations, β-cyclodextrin cannot be used in parenteral formulations and the usage of α-cyclodextrin in parenteral

formulations is severely limited although it can already be found in one marketed formulation [16].

In animal studies, γ-cyclodextrin has been found to be virtually non-toxic when given intravenously [21]. Extensive toxicological studies have been completed for 2-hydroxypropyl-β-cyclodextrin [22] as well as for sulfobutylether β -cyclodextrin [23], both of which can be found in marketed parenteral formulations at relatively high concentrations.
The toxixcity is due to α- e β-CD capacity to destroy cellular membranes because thei can extract cholesterol and phospholipids from membrane [24].

2.7 Computer simulation

In the past years, the use of computational chemistry in the area of cyclodextrins was somewhat limited. The reason is not the lack of interest but is rather because cyclodextrins are relatively large, flexible molecules and often studied experimentally in aqueous environments. The size of cyclodextrins and their derivatives makes applications of quantum mechanics difficult even when symmetry conditions are imposed. Because these macrocycles have many rotatable bonds, there exist an enormous number of conformational states. Moreover, cyclodextrins are usually studied experimentally in aqueous media creating a major hurdle that most computational chemists were not willing to surmount. At this on added the lack of hardwares and softwares to carry out these calculations in a reasonable time period.

The first "modern" computational study of cyclodextrins was published in 1970. The computational method employed was molecular mechanics. Then the chemists understood that did not exist cyclodextrins with fewer than six monomers due to steric repulsion of the $-CH_2OH$ groups within the cavity of cyclopentamers [25].

The first steps made in this field were the understanding of cyclodextrins structure, by comparing the theoretical data with X-ray crystallographic structures. In this way the local minima, the charge distributions, the number of stereoisomers and the possible glucose ring distortions of cyclodextrins were obtained.

Empirical and molecular mechanics methods were used to define the host-guest binding energies in the inclusion complexes formation, whereas molecular dynamics simulations were performed to investigate the structure and dynamics of complexes, allowing the study of cyclodextrinic dimers with several complexation ratio such as that of 2:1 and 2:2, that require the association of two host molecules.

These methodologies allowed to explain the type of the interactions involved in the cyclodextrinic cavity and to rationalize the catalytic ability of the cyclodextrinic microenvironment. An enormous amount of study, in fact,

illustrated the regioselectivity of the host-guest binding by using simple polar guests, helping the interpretation of NMR spectra, and providing models for the position and the orientation of guests in the cavity.

The computational chemistry explained also the molecular recognition and the selectivity of cyclodextrins towards enantiomers, by describing the different binding energies of analytes and the forces responsible of the chiral recognition.

At the moment these methodologies, especially molecular mechanics and molecular dynamics are used to describe the interaction energy of host-guest complexes and to predict their stability in aqueous solution, with a full understanding of complexes structure.

All that is at the basis of a rational design of pharmaceutical formulations, that requires a good knowledge of processes and forces that govern the inclusion phenomena. On this subject structural and thermodynamic informations such as the association constant and changes of enthalpy ($\Delta H°$) and entropy ($\Delta S°$) of binding are provided by molecular mechanics and molecular dynamics that constitute a good support to understand the inclusion phenomena of small molecules and big molecules (polymers) with cyclodextrins [26].

References

1. A. Villiers, *Compt. Rend. Acad. Sci.,* 112 (1891) 536-538.
2. F. Z. Schardinger, *Unters. Nahr. U. Genussm.,* 6 (1903) 865-880.
3. K. Freudenberg, G. Blomquist, L. Ewald, K. Soff, *Ber. Dtsch. Chem. Ges.,* 69 (1936) 1258-1266.
4. D. French, *Adv. Carbohydr. Chem.,* 12 (1957) 189-260.
5. *Einschlussverbindungen (Inclusion Compounds),* F. Cramer, Ed. Springer-Verlag: Berlin, 1954.
6. T. Loftsson, M. E. Brewster, *J. Pharm. Sci.,* 85 (1996) 1017-1025.
7. J. Szetjli, *Chem. Rev.,* 98 (1998) 1743-1753.
8. M. Singh, R. Sharma, U.C. Banerjee, *Biotech. Adv.,* 20 (2002) 341-359.
9. M. V. Rekharsky, M. P. Mayhew, R. N. Goldberg, P. D. Ross, Y. Yamashoji, Y. A. Inoue, *J. Phys. Chem.,* 101 (1997) 87-100.
10. M. V. Rekharsky, Y. Inoue, *Chem. Rev.*, 98 (1998) 1875-1917.
11. R. A. Rajewski, V. J. Stella, *J. Pharm. Sci.,* 85 (1996) 1142-1168.
12. R. A, Hedges, *Chem. Rev.,* 98 (1998) 2035-2044.
13. T. Tokunaga, M. Nambu, Y. Tsushima, K. Tatsuishi, M. Kayano, Y. Machida, T. Nagai, *J. Pharm. Sci.,* 75 (1986) 391-394.
14. K. Uekama, F. Hirayama, T. Irie, *Chem. Rev,.* 98 (1998) 2045-2076.
15. F. Hirayama, K. Uekama, *Adv. Drug Deliv. Rev.,* 36 (1999) 125-141.
16. T. Irie, K. Uekama, *J. Pharm. Sci.,* 86 (1997) 147-162.
17. K. Uekama, F. Hirayama, H. Arima, *J. of Incl. Phen. and Macro. Chem.,* 56 (2006) 3-8.
18. K. Uekama, *Chem. Pharm. Bull.,* 52 (2004) 900-915.
19. T. Loftsson, P. Jarho, M. Másson, T. Järvinen, *Expert Opin. Drug Deliv.,* 2 (2005) 335-351.
20. J. Szetjli, *TIBTRCH,* **7** (1989) 171-174.
21. I. C. Munro, P. M. Newberne, R. R. Young, A. Bär, *Regul. Toxicol. Pharmacol.,* 39 (2004) S3–S13.
22. S. Gould, R. C. Scott, *Food Chem. Toxicol.,* 43 (2005) 1451-1459.
23. R. A. Rajewski, G. Traiger, J. Bresnahan, P. Jaberaboansari, V. J. Stella, *J. Pharm. Sci.,* 84 (1995) 927-932.
24. V. J. Stella, R. A. Rajewski, *Pharm. Res.*, 14 (1997) 556-567.
25. P. R. Sundararajan, V. S. R. Rao, *Carbohydr. Res.,* 13 (1970) 351-358.
26. K. B. Lipkowit, *Chem. Rev.,* 98 (1998) 1829-1873.

TIRDH CHAPTER

MOLECULARLY IMPRINTED POLYMERS

3.1 History of imprinting

Molecular imprinting is not a new science. The earliest reports of imprinting go back to the early 1930s when a Soviet chemist M.V. Polyakov [1] prepared a number of silica gels and observed that when prepared in the presence of a solvent additive the resulting silica demonstrated preferential binding capacity for that solvent. Although Polyakov continued with this work until the1950s his findings were seldom cited outside of Eastern Europe. A later study, also using silica, was to have more of an impact. In 1949 a senior student of Linus Pauling, Frank Dickey, published the results of experiments where silica gels had been prepared in the presence of dyes [2]. Dickey observed that after removal of the "patterning" dye the silica would rebind the same dye in preference to the others. Silica imprinting continued during the 1950s and 1960s but the number of publications in the area remained low. However, in 1972 a step change in molecular imprinting occurred when the group of Guenter Wulff reported that they had successfully prepared a molecularly imprinting organic polymer [3]. Wulff used what is now termed a covalent approach to prepare an organic molecularly imprinted polymer (MIP) capable of discriminating between the enantiomers of glyceric acid. Subsequently, throughout the 1970s and 1980s, Wulff's group published extensively using this approach. The second major break through in organic polymer imprinting occurred in 1981 when Mosbach and Arshady reported that they had prepared an organic MIP using non-covalent interactions only [4]. This approach was termed the non-covalent approach, as opposed to the covalent approach favoured by Wulff, and it was this approach, with its simple, seemingly trivial methodology, that triggered the explosion in molecular imprinting that was to occur during the 1990s. To this day the non-covalent versus covalent debate continues with both sides being championed. However, it is generally accepted that there are pros and cons to both approaches and in 1995 Whitcombe et al. reported an intermediate approach that appeared to combine the advantages of both approaches [5]. This approach relies on covalent interaction during the polymerization stage but no-covalent interactions during rebinding. Importantly, in order to improve subsequent non-covalent binding geometry, Whitcombe's approach incorporated a sacrificial spacer group that was designed to be lost during template removal.

The non-covalent approach however is still by far the most widely used approach in MIP synthesis. Several of its drawbacks can be overcome by the use of stoichiometrically associating monomer-template systems [6-9]. This has

resulted in a range of receptors exhibiting high capacity and effective recognition properties in aqueous media.

3.2 Imprinting approach

Essentially, three approaches currently exist to generate high fidelity imprinted sites, these are distinguishable by the nature of the linkage during synthesis and during rebinding.

The first example of molecular imprinting of organic network polymers introduced by Wulff et al. later, followed by Shea et al. was based on a covalent attachment strategy, i.e., covalent monomer-template, covalent polymer–template [10,11]. This approach has the advantage of a known stoichiometry between the functional monomer and the template. Provided that the template can be recovered in high yields, a high density of well defined sites can be expected. One problem with this approach is the limited number of covalent linkages that satisfy these criteria. Furthermore, considerable synthetic effort may be required to prepare the template and slow kinetics is often observed for rebinding by reformation of the covalent bond. This approach is therefore difficult to combine with applications where fast on-off kinetics is required. In this respect, the use of sacrificial spacers has found more widespread use [5]. Here the functional monomer is bound to the template through a disposable spacer that is removed after polymerization is completed. This results in a disposition of the functional groups allowing rebinding to occur through hydrogen bonding interactions. Therefore, this approach can be more amenable to chromatographic applications and furthermore allows more freedom in the choice of polymerization conditions.

However, the most widely used approach in imprinting involves functional monomers that are chosen to associate non-covalently with the template [12,13]. Here the template is directly mixed with one or several functional monomers followed by polymerization. It can thereafter be easily extracted from the polymer and recycled. Generally, the resulting materials can be directly used to perform separations with high affinity and selectivity for instance as chromatographic stationary phases.

The non-covalent approach has been used more extensively for three reasons: (i) Non-covalent methodology is easier because it does not require synthetic steps toward the prepolymer complex; interactions between monomers and template are easily obtained when all components are mixed in solution; (ii) removal of the template is generally much easier, usually accomplished by continuous extraction; (iii) a greater variety of functionality can be introduced into the MIP binding site using non-covalent methods. This approach is very attractive since it is simple, it delivers MIPs showing high affinity for its target and it is broadly applicable. Thus, using essentially the same procedure, MIPs targeting a large variety of small lipophilic targets can be obtained. Conceivably, a simple commodity

monomer such as methacrylic acid can be used to create good binding sites for a large variety of template structures containing hydrogen bond- or proton-accepting functional groups [14]. Commonly, these binding sites are capable of discriminating subtle structural differences in the template, similar to the selectivity displayed by antibodies.

In all cases the network structure depends upon the type of monomer chemistry (i.e., anionic, cationic, neutral, amphiphilic), the association strength and number of interactions between the monomers and template molecule, the association interactions between monomers and pendent groups, the solvent type and the amount of solvent in the mixture, the reactivity ratios of the monomers, and the relative amounts of reacted monomer species in the structure.

Commonly, the monomers used in the above protocols are commercially available and individually provide typically only weak interactions with the template molecule. This leads to site heterogeneity, low saturation capacity and nonspecific binding. In order to address this issue, the monomer tool box may be extended drawing inspiration from the area of host-guest chemistry. Thus, designed functional monomers are capable of stoichiometrically associating with the template in the imprinting step and subsequently to allow strong binding in the rebinding step. This minimizes site heterogeneity due to the functional monomer-template complex distribution.

The polarity and functionality of the material surface need to be matched to the matrix environment for which the materials are designed. Water compatibility can be achieved by tuning the composition of terpolymers including hydrophilic comonomers or the use hydrophilic crosslinkers. Alternatively, the organic polymer matrix may be entirely replaced by an inorganic one.

The development of bead polymerization techniques serves a twofold objective. First it addresses the technical issues related to the conventional monolith procedure to produce MIPs, e.g., low yields of useful particles, irregular particle sizes, time-consuming crushing sieving techniques. Secondly, packed beds of monodisperse spherical particles will exhibit less band broadening effects than corresponding beds of irregular particles. If the particles are sufficiently small, the binding kinetics can also be expected to strongly improve.

In order to decouple the binding site formation from the generation of a particular morphology, grafting techniques may be applied. Thus starting from a support (e.g. a porous membrane, porous particles) thin layers of imprinted polymers may be grafted on its surface. Combining the grafting with controlled radical polymerization techniques offers a mean to perform this grafting in a controlled manner leading to a tunable polymer film thickness. In contrast to the polymer beads the thin film composites have shown strongly improved mass transfer properties [15].

3.3 Optimization of polymerization parameters

The underlying mechanisms for molecular recognition exhibited by the imprinting effect have been attributed to two factors:

(i) pre-organization of complementary functional groups in the polymer by the template;

(ii) formation of a shape-selective cavity that is complementary to the template.

Thus, the imprinting effect is essentially a threedimensional effect, i.e. it is the effective control of three-dimensional interactions by the template with surrounding functional monomers and the crosslinked matrix. However, measurements of binding and selectivity combine all effects contributing to molecular recognition in MIPs into one figure of merit. This figure of merit is usually in the form of a binding constant K, which is compared for different substrates; or as a selectivity factor α, which is the ratio of binding constants for two different substrates. If the two molecules being compared are not enantiomers, then there are other factors which contribute to differential binding (and hence separation) of these substrates such as size or different partitioning effects due to differences in: polarity, hydrophobicity, dipoles or ionization state, shape and/or conformational effects. Thus, evaluation of the imprinting effect becomes quite complex when comparing several substrates or several different MIPs.

3.3.1 Functional monomer to crosslinking monomer ratio

The requirements of covalent imprinting are different than those for non-covalent imprinting, particularly with respect to ratios of functional monomer (M), crosslinker (X), and template (T).

The covalent molecular imprinting is optimized by maximizing the amount of crosslinking monomer in addition to the template-functional monomer complex. The picture changes for non covalent MIPs. First, an excess of functional monomer utilized increases the amount of nonspecific binding which lowers the overall average selectivity of the MIP. Second, there is a minimum amount of crosslinker necessary to form a rigid enough polymer network that will maintain the fidelity of the binding site. This limits the amount of non-crosslinking functional monomer that can be used for formation of the MIP binding sites. Thus, optimization of functional monomer to crosslinking monomer ratio in non-covalent MIPs must be empirically derived; most reports, however, indicate that an optimum crosslinker percentage can be found in the range of 50% to 80% depending on the functional monomer used [16].

3.3.2 Template concentration

The careful choice of functional monomer is of the utmost importance to provide complementary interactions with the template and substrates. The template (T) concentration can then be optimized with respect to the functional monomer [17]. For covalent molecular imprinting, this is not necessary because the template dictates the number of functional monomers that can be covalently attached; furthermore, the functional monomers are attached in a stoichiometric manner. For non-covalent imprinting, the optimal (T/M) ratio is achieved empirically (similar to the optimization of the X/M ratio) by evaluating several polymers made with different formulations with increasing template.

From the general mechanism of formation of MIP binding sites, formation of each individual "binding site" in the polymer is attributed to an individual template molecule that is surrounded by functional monomers in a pre-polymer complex (scheme 3.1).

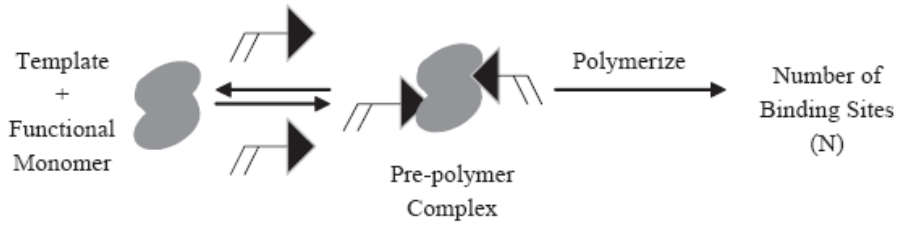

Scheme 3.1 *Relationship between solution complex and specific binding sites made in the MIP.*

It has been postulated, then, that each complex in the pre-polymer solution gives rise to each binding site. Applying Le Chatelier's principle to the complex formed prior to polymerization, increasing the concentration of components or binding affinity of the complex in the pre-polymerization mixture would predict an increase in the pre-polymer complex. Correspondingly, there is an increase the number of final binding sites in the imprinted polymer, resulting in an increased binding or selectivity factor per gram of polymer.

The pre-polymer complex can be increased by increasing either the amount of functional monomer (M) or the amount of template (T), or both. However, increasing the concentration of M results in an equal lowering of the crosslinker (X) concentration; in other words, the (X/M) ratio becomes smaller. As pointed out earlier, there is a limit to how small the (X/M) ratio can become before the MIP formulation falls below a critical amount of crosslinker needed to maintain the fidelity of the binding site. MIP optimization experiments in the literature have shown this ratio to have a lower limit of approximately 1.0, and optimum values around 4.0 [18]. On the other hand, the pre-polymer complex can also be increased by increasing the template concentration. This is an interesting prospect

because the template can in theory be increased to very high concentrations without having any change on the composition of monomers in the final polymer. This is because the template is not covalently incorporated into the final polymer, and is removed at the end of the imprinting process. One strategy, then, to maximize the pre-polymer complex would be to increase the template concentration high enough to drive the complex equilibrium toward complex, while keeping the (X/M) ratio at the optimum 4.0. In other words, once all of the functional monomer is complexed, any further addition of template will have no functional monomer to complex with, and thus is not expected to increase in the number of binding sites (assuming a binding site requires at least one functional monomer).

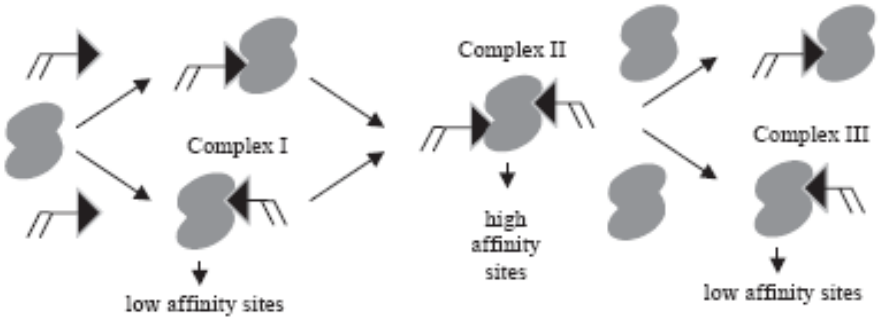

Scheme 3.2 *Template/functional monomer complexes for templates capable of binding two functional monomers.*

There is a similarity for templates with only one interactive functional group and with two interactive functional groups. So, a hypothetical model for 1-point binding, 2-point binding, and higher order complexes has been proposed. An initial increase in the (T/M) ratio maximizes the formation of the 2-point binding complex by Le Chatelier's principle. However, as the (T/M) ratio increases further, the highly selective sites arising from 2-point binding become substituted by the less selective 1-point binding sites (scheme 3.2). This is because once all of the functional monomer is complexed with template in the one-to-one complex established for solution complexes [19], addition of more template will not add nor otherwise interfere with the complexes made. Thus the number of total binding sites would be anticipated to stay the same after this critical amount of template is reached, and remain unchanged with the addition of any more template. This would suggest a similar underlying mechanism for binding site formation, since all other materials' properties remain unchanged [17]. Thus, multiple functional monomer interactions in the final polymer, regardless of the pre-polymer stoichiometry, appear to be responsible for the high-affinity binding sites seen for non-covalently imprinted polymers.

The trends in binding and selectivity in non-covalently imprinted polymers are explained best by a model that incorporates multiple functional monomers within the highest affinity binding sites. The increased number of binding interactions in the polymer binding site may account for greater fidelity of the site, and thus impart greater affinity and selectivity to the site (scheme 3.3). This would suggest that the number of functional groups in the polymer binding site is not determined directly by the solution phase pre-polymer complex; rather, it is determined during polymerization. Because of the difficulty of characterizing the binding site structures during and after polymerization, the actual events determining the final binding site structure are still unknown. Thus, the (T/M) ratios must still be empirically optimized by evaluation of a series of MIP formulations with various template concentrations at a fixed (X/M) ratio. As a general guideline, reports in the imprinting literature empirically comparing MIP performance versus (T/M) ratio have often found best results for (T/M) ratios in the range of approximately 0.5-0.25, depending on the template used [17, 18]. However, if more than one functional monomer is used, the process of optimization becomes exponentially more complex.

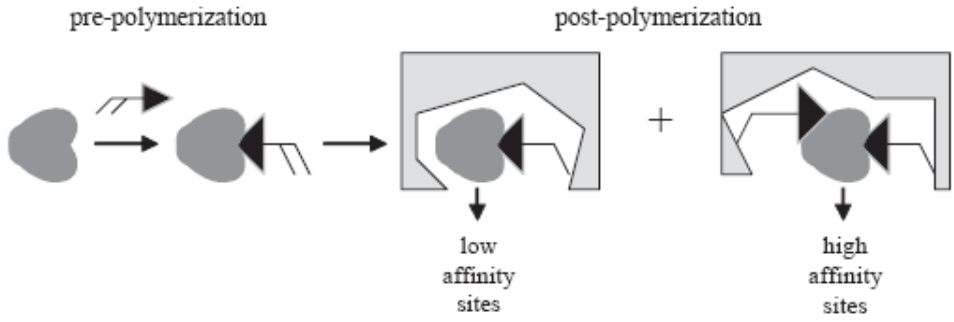

Scheme 3.3 *Model for templates with only one interaction in solution but multiple interactions with the final polymer arising during polymerization.*

3.3.3 Solvent effects

Solvent plays an important role in the formation of the porous structure of MIPs, which are a subset of a larger class known as macroporous polymers [20,21]. The morphological properties of porosity and surface area are determined by the type of solvent, referred to as "porogen", used in the polymerization. Porosity arises from phase separation of the porogen and the growing polymer during polymerization. Porogens with low solubility phase separate early and tend to form larger pores and materials with lower surface areas. Conversely, porogens with higher solubility phase separate later in the polymerization providing materials with smaller pore size distributions and greater surface area. It does not

appear, however, that binding and selectivity in MIPs is dependent on a particular porosity. MIPs made without any porogen do not exhibit any selectivity because substrate cannot access the polymer.

Another important role for solvent in the formation of MIPs is the effect it has on the complexation of functional monomers with the template before, during, and after polymerization. Before (and during) polymerization, the extent of the non-covalent prepolymer complex is affected by the polarity of the porogen solvent. Less polar solvents such as chloroform or benzene will increase complex formation by Le Chatelier's principle, facilitating polar non-covalent interactions such as hydrogen bonding or bridging of ionic salts. On the other hand, more polar solvents tend dissociate the non-covalent interactions in the pre-polymer complex, especially protic solvents that afford a high degree of disruption to hydrogen bonds.

An important discovery in MIPs is that after polymerization, the rebinding performance is optimized when carried out in the same solvent used for imprinting [22, 23]. The underlying cause for this effect has been postulated to arise from differences in solvation of the polymer structure in the binding site microenvironment. Different solvation properties of different solvents, such as chloroform and acetonitrile, may play a role in determining shape and distance parameters that are built into the forming polymer. In order to recreate and maintain these shape and distance parameters, it is possible that optimum rebinding conditions require the same, or very similar, solvation conditions used for polymerization.

3.3.4 Temperature effects

Several studies have shown that polymerization of MIPs at lower temperatures forms polymers with greater selectivity versus polymers made at elevated temperatures. The reason for this has again been postulated on the basis of Le Chatelier's principle, which predicts that lower temperatures will drive the pre-polymer complex toward complex formation, thus increasing the number and, possibly, the quality of the binding sites formed.

3.4 Evaluation

The quality of the receptor mechanism of imprinted polymers can be assessed via a number of parameters. The significant parameters in determining how well a polymeric network can recognize a given molecule are binding affinity (i.e., the equilibrium association or dissociation constant between the ligand molecule and the network), selectivity (i.e., the ability to differentiate between the ligand and other molecules), and the binding capacity (i.e., the maximum ligand bound per mass or volume of polymer). To a lesser extent, binding or imprinting

ratios (i.e., the ratio of recognitive network template bound compared to control network) highlights the recognition properties at a specific concentration.

Binding affinity is a measure of how well the template molecule is attracted to the binding site or how well a ligand binds or is held to the receptor macromolecule. Considering equilibrium theory of receptor-ligand interactions, the dissociation constant, K_d, provides a quantitative measure of this level of attraction. The formation of the macromolecular-ligand complex can be described by the following representation:

$$[M]+[L]\leftrightarrow[ML] \tag{3.1}$$

where [M] represents the concentration of macromolecular binding sites (i.e., recognitive network), [L] represents the concentration of ligand or template molecule, and [ML] represents the ligand-macromolecular complex. The equilibrium binding constant or association constant, K_a, and the equilibrium dissociation constant, K_d, are represented by Eq. 3.2:

$$K_a = K_{complex} = \frac{K_f}{Kr} = \frac{1}{K_d} = \frac{[ML]}{[M][L]} \tag{3.2}$$

where k_f and k_r are the forward and reverse rate constants, respectively. Ligands with low K_d or high K_a values bind tightly to the receptor and have high affinity. Conversely, high K_d and low K_a values are indicative of weak binding systems.

Equilibrium binding parameters can be estimated from binding isotherms analyzing adsorbed or bound molecule versus solute concentration.

Selectivity, α, can be determined by a ratio of the equilibrium association or dissociation constants between two molecules (one which differs from the template in chemical functionality, orientation of chemical functionality, or physical size). Typical selectivities of non-covalent imprinted polymers are in the range of 1.1 to 8 [24], and imprinted polymers with high association constants typically display high selectivities.

$$\alpha = \frac{K_{a,template\_molecule}}{K_{a,other\_molecule}} \tag{3.3}$$

Since recognition requires three-dimensional orientation, most techniques limit the movement of the memory site chemistry via macromolecular chain relaxation such as swelling phenomena by using high ratios of crosslinking agent to functional monomers. As an increase in crosslinking monomer content leads to a decrease of the average molecular weight between crosslinks, the macromolecular chains become more rigid. In less crosslinked systems, movement of the macromolecular chains and the spacing of functional groups will

change, as the network expands or contracts depending on the chosen rebinding solvent (thermodynamic interaction parameters characterizing the segment-solvent interaction) or application solution environment. This process is reversible and transiently affects the binding behaviour and also leads to sites with varying affinity and decreased selectivity [25].

3.5 Characterization: surface area, porosity and MIP swelling

The morphology of MIPs, shown in figure 3.1, arises from nuclei that form around the initiator which grow to 10-30 nm in diameter which then aggregate to form microspheres, that aggregate themselves into larger clusters that form the body of beads. The porosity and resulting surface area in MIPs is formed from irregular voids located between clusters of the microspheres (macropores, > 50 nm in diameter), or from the interstitial space of a given cluster of microspheres (mesopores, 2-50 nm in diameter), or even within the microspheres themselves (micropores, < 2 nm in diameter).

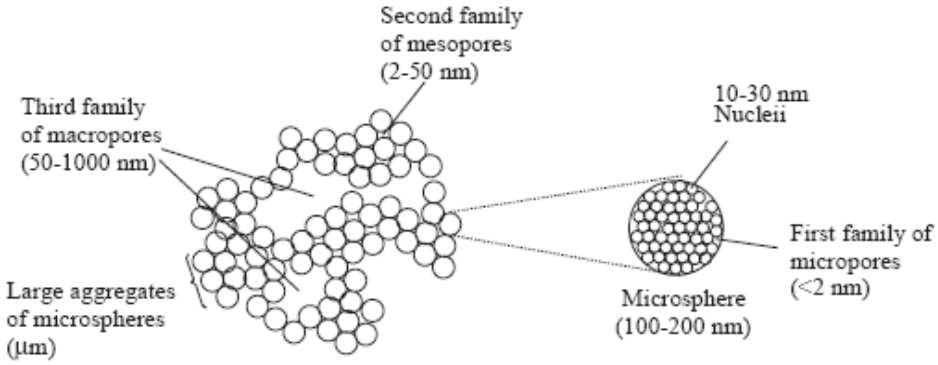

Figure 3.1 *Model of morphology formation that provides porous network in MIPs.*

Typical values for surface area of the imprinted polymers are in the range of 100 to 400 m^2/g. For pore size distribution there are both macropores and mesopores in the range 2 to 100 nm, and micropores of 0.6 to 2 nm in diameter. The most effective variables that control surface area and pore distribution are the percentage of crosslinking monomer, the type and amount of porogen, and the reaction temperature. Although binding and selectivity by MIPs in chromatographic or batch rebinding mode are not dependent on macroporosity, applications in drug delivery may rely on mass-transfer kinetics related to porosity.

Swelling in MIPs has most often been measured using volumetric methods published by Sellergren and Shea [26]. The particles are then photographed in

swollen and unswollen states, and the ratios in area calculated to give the percent swelling. In many cases the particles have irregular shape or else there are wide ranges of different sizes between the particles; therefore, it is best to follow the same particle from the swollen state to the dry state [16].

3.6 Molecular imprinting in drug delivery

Synthetic molecularly selective receptors such as MIPs have broad application in many areas of science but perhaps the area of greatest potential, and probably an area of greatest challenge, is that of therapeutics and medical therapy. Examples of robust near real-time diagnostic sensors, and MIPs with "drug like" effects, such as a cholesterol selective MIPs developed for use as oral adsorbers [27]. In addition MIPs incorporated into membranes are being increasingly investigated in the context of bioseparations and biopurification [28]. But it is in the area of drug delivery that some of the most significant opportunities lie, there is huge potential in drug delivery for technologies that can bring about intelligent drug release or can target a therapeutic pay-load to a particular site of action.

Intelligent drug release refers to the release, in a predictable way, of a therapeutic agent in response to specific stimuli such as the presence of another molecule, whilst drug targeting is best exemplified by the "magic bullet" approach where a drug conjugated to a targeting vector, such as an antibody or a peptide, interacts with specific sites of interactions.

For instance, intelligent controller release could be achieved by the competitive displacement of a drug by a structurally related cross-reactant. This type of direct displacement is probably the simplest way of generating a release profile in response to a second analyte but other "allosteric-like" phenomenon are also plausible (figure 3.2). Thus, the modulation of drug release from an imprinted polymer by a feedback control mechanism can also be considered, such as insulin release when blood glucose level rises above a minimum threshold level.

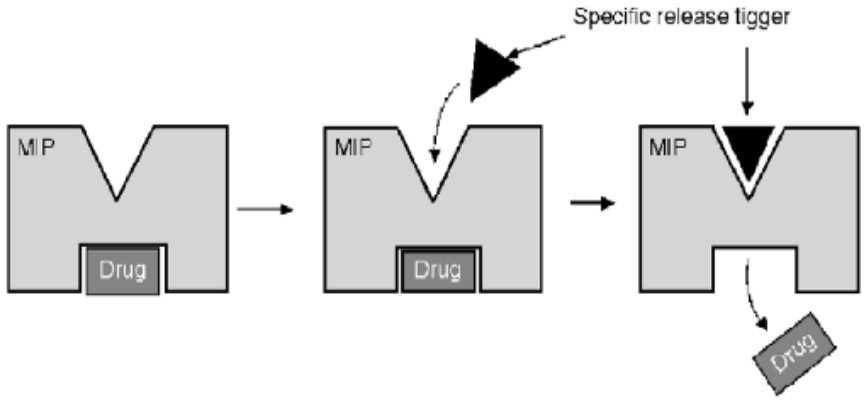

Figure 3.2 *Intelligent "allosteric" drug release from MIP carrier.*

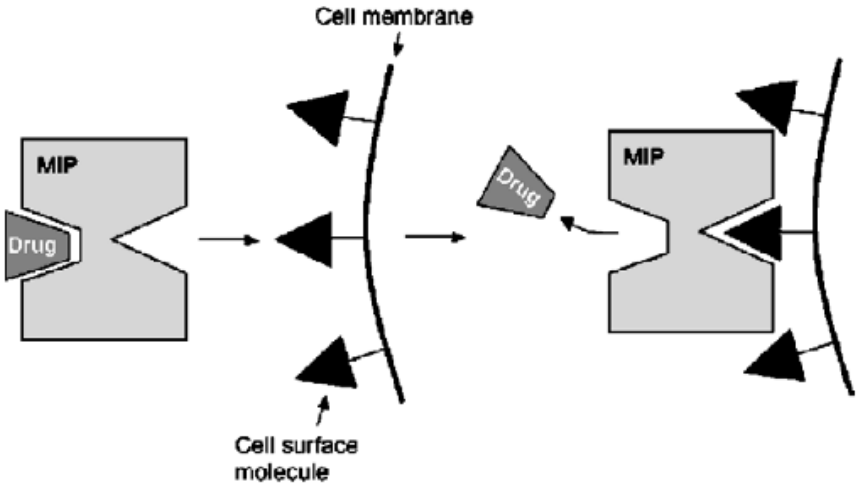

Figure 3.3 *Targeted drug delivery using a molecularly imprinted carrier.*

Using MIPs to target drug delivery is also an exciting concept (figure 3.3). The drug, coupled either covalently or non-covalently to the MIP, would be released when the MIP binds to its target, such as a protein or cell surface receptor, on the surface of a cell. This concept could be extended so that the binding of the MIP to the cell surface would bring about internalisation of the MIP–drug complex and subsequent drug release (figure 3.4).

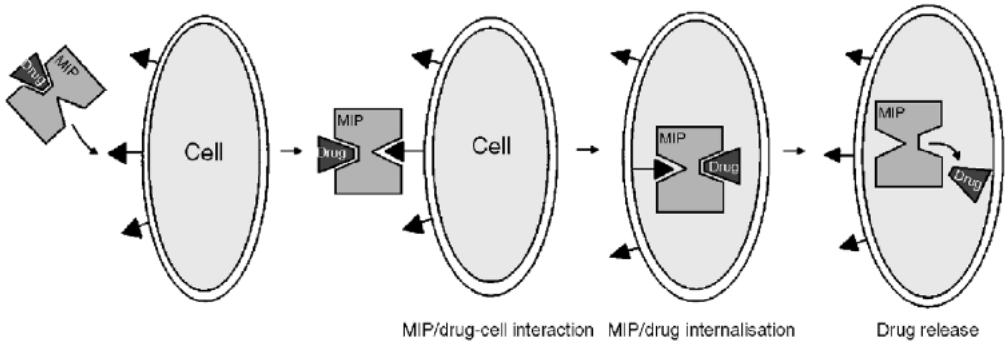

Figure 3.4 *Targeted drug delivery and facilitated internalisation using a MIP.*

Imprinted materials, owing to their cross-linked polymeric nature, inherently act as reservoirs for low molecular weight species. They can potentially increase the residence time of the drug within the body by reducing the rate at which the drug is released. In cases where the drug has a narrow therapeutic window, MIP delivery vehicles might keep the concentration of the drug in the body below the concentration where adverse side effects become dominant. The use of imprinted hydrogels for drug delivery has an added advantage as a change from a collapsed to a swollen state can be chosen to suit the conditions where the

polymer is going to be used to release its load of therapeutic agent. The ability to modulate the release of the imprint in this way would be of great benefit for drugs administered orally in that peptidic or otherwise sensitive therapeutics can be hidden from low pH and protease activity until an environment change at the intended site of action triggers drug release. This can be envisaged in terms of an imprinted hydrogel that collapses to protect its therapeutic payload through the gastroenteric tract but expands to release the drug in the small intestine or the colon.

For a good system should be taken in consideration the following aspect:

i) compromise between rigidity and flexibility. The structure of the imprinted cavities should be stable enough to maintain the conformation in the absence of the template, but somehow flexible enough to facilitate the attainment of a fast equilibrium between the release and the re-uptake of the template in the cavity;

ii) high chemical stability. MIPs for drug delivery should be stable enough to resist enzymatic and chemical attack and mechanical stress.

Additionally, the adaptability of molecular imprinting technology for drug delivery also requires the consideration of safety and toxicological concerns. The presence of residual organic solvents may cause cellular damage. In consequence, hydrophilic polymer networks that can be synthesised and purified in water are preferable to those require organic solvents. A hydrophilic surface also enhances biocompatibility and avoid adsorption of proteins and microorganisms [29].

Currently, a wide range of polymers are being studied for controlled drug delivery, including a number of biocompatible acrylates and vinyl polymers, so the step change from current best practice is not great. In addition, biodegradable polymers, and the potential for biodegradable MIPs, would provide further flexibility in polymer morphology and the resulting dosage form. It is therefore feasible that a working system might comprise a surface imprinted nanoparticulate MIP, selective for some cell surface epitope, conjugated to the active drug [15, 30].

3.7 Computer simulation

An understanding of the physical rules governing the formation of monomer-template complexation is fundamental in being able to rationally design polymerisation systems with high selectivity and affinity. Given that one understands the physical parameters governing the formation of intermolecular interactions (i.e. in the polymerisation process) then one would be able to understand the polymer recognition properties better.

The nature of the template and monomers and the polymerisation reaction itself determine the quality and performance of the polymer product. Moreover, the quantity and quality of the molecularly imprinted polymer recognition sites is

a direct function of the mechanisms and extent the monomer–template interactions present in the pre-polymerisation mixture. Thus, semi-empirical approaches on the prediction of ligand-receptor binding constants, and on the detailed factorisation of energetic contributions to binding.

In principle, the broad range of functional monomers currently available makes it possible to design an MIP specific for any type of stable chemical compound. The application of previous methods to select the best monomers for polymer preparation is not trivial in practice. The problem lies in the technical difficulty of performing detailed thermodynamic calculations on multi-component systems and the amount of time and resources required for the combinatorial screening of polymers. To check a simple two-component combination of 100 monomers one has to synthesise and test more than 5000 polymers which is a very difficult task. This task will be further complicated by the possibility that these monomers could be used in monomer mixtures in different ratios. One potential solution to the problem of polymer design lies in molecular modelling and in performing thermodynamic calculations with the aid of a computer. Molecular modelling and molecular dynamics simulations are advancing the fundamental understanding of biorecognition processes. Given the current state-of-the-art in rationally designing MIPs, such simulations may enable selecting combinations of template, functional monomers, cross-linkers, and solvents providing the most stable complex in the pre-polymerization solution, which will then be selected for molecular dynamics simulations investigating the interaction and conformation of the pre-polymerization complex. However, the molecular modelling approaches discussed above are not fully comprehensive, as the effects of cross-linkers and the correct ratio of the involved molecules are not yet taken into account. It can be expected that establishing models including all the reaction species at the correct ratios will provide better understanding on the role of the different constituents during the imprinting process, which provides a more realistic simulation environment in closer analogy to the experimental conditions present in the pre-polymerization solution.

The main paradigm of molecular imprinting can be described in statement that the strength and type of interactions, existing between monomers and template in monomer mixture will determine the recognition properties of the synthesised polymer. The assumption is that the complexes formed in monomer mixture will somehow survive the polymerisation stage and their structure will be preserved in the synthesised polymer. Thus, instead of modelling the polymer, a model of the monomer mixture and the interactions taking place in solutions between monomers, crosslinker, template and solvent was carried out instead reducing the computational time significantly. The interactions between monomers and template models can be quantified and used for rational selection of monomers for polymer preparation. With molecular modelling the design of functional monomers and its screening against target compounds is relatively easy

to perform, so also determine the optimal type and ratio of the template and the monomers recommended for MIP design.

References

1. M. V. Polyakov, *Fiz. Khim.,* 2 (1931) 799-805.
2. F. H. Dickey, *Proc. Natl. Acad. Sci.***,** 35 (1949) 227-229.
3. G. Wulff, A. Sarhan, *Angew. Chem.,* 84 (1972) 364.
4. R. Arshady, M. Mosbach*, Macromol. Chem. Phys.-Makromol. Chem.,* 182 (1981) 687-692.
5. M. J. Whitcombe, M. E. Rodriguez, P. Villar, E. N. Vulfson, *J. Am. Chem. Soc*., 117 (1995) 7105-7111.
6. G. Wulff, T. Gross, R. Schönfeld, *Angew. Chem. Int. Ed. Engl.,* 36 (1997) 1962-9164.
7. C. Lübke, M. Lübke, M. J. Whitcombe, E. N. Vulfson, *Macromolecules* 33 (2000) 5098-5105.
8. P. Manesiotis, A. J. Hall, M. Emgenbroich, M. Quaglia, E. de Lorenzi, B. Sellergren, *Chem. Commun.,* 20 (2004) 2278-2279.
9. B. Sellergren, *J. Chromatogr.* A, 673 (1994) 133-141.
10. G. Wulff, A. Sarhan, *Angew. Chem. Int. Ed. Engl.,* 11 (1972) 341-344.
11. K. J. Shea, T. K. Dougherty, *J. Am. Chem. Soc.,* 108 (1986) 1091-1093.
12. L. Andersson, B. Sellergren, K. Mosbach, *Tetrahedron Lett.,* 25 (1984) 5211-5214.
13. B. Sellergren, B. Ekberg, K. Mosbach, *J. Chromatogr.,* 347 (1985) 1-10.
14. B. Sellergren, M. Lepistoe, K. Mosbach, *J. Am. Chem. Soc.,* 110 (1988) 5853-5860.
15. B. Sellergren, C. J. Allender, *Adv. Drug Deliv. Rev.*, 57 (2005) 1733-1741.
16. D. A. Spivak, *Adv. Drug. Deliv. Rev*., 57 (2005) 1779-1794.
17. H. Kim, D. A. Spivak, *J. Am. Chem. Soc.,* 125 (2003) 11269-11275.
18. B. Sellergren, *Makromol. Chem.,* 190 (1989) 2703-2711.
19. E. A. Yerger, G. M. Barrow, *J. Am. Chem. Soc.,* 77 (1955) 4474-4481.
20. *Synthesis and Separations Using Functional Polymers,* A. Guyot, in: D.C. Sherrington, P. Hodge - Ed. John Wiley & Sons, New York, 1989, CAP 1.
21. L. Lloyd, *J. Chromatogr.,* 544 (1991) 201-217.
22. D. A. Spivak, K. J. Shea*, J. Am. Chem. Soc.,* 119 (1997) 4388-4393;
23. M. Kempe, K. Mosbach, *Anal. Lett.,* 24 (1991) 1137-1145.
24. G. Wulff, *Angew. Chem. Int. Ed. Engl.,* 34 (1995) 1812-1832.
25. J. Z. Hilt, M. E. Byrne, *Adv. Drug Deliv. Rev.*, 56 (2004) 1599-1620.
26. B. Sellergren, K. J. Shea, *J. Chromatogr.,* 635 (1993) 31-49.
27. B. Sellergren, J. Wieschemeyer, K.-S. Boos, D. Seidel, *Chem. Mater.,* 10 (1998) 4037-4046.
28. M. Ulbricht*, J. Chromatogr. B,* 804 (2004) 113-125.
29. C. Alvarez-Lorenzo, A. Concheiro, *J. Chromatogr. B*, 804 (2004) 231-245.
30. M. E. Byrne, K. Park, N. A. Peppas, *Adv. Drug Deliv. Rev.*, 54 (2002) 149-161

FOURTH CHAPTER

THEORETICAL METHODS

4.1 Docking

The primary task of docking is to find the correct binding position and orientation of a ligand complexed to a receptor. A detailed understanding of the interactions between receptors and their ligands is essential for interpreting many biochemical phenomena and is of paramount practical relevance in pharmaceutical and medicinal sciences.

Given the structures of a ligand and a receptor, the task of computational docking is to predict the correct binding mode of the interacting partners. In other words, the geometry of the complex corresponding to the lowest free energy of binding must be found.

Whatever the nature of the binding partners and whatever the approach used for docking, certain problems must be addressed by any docking method, and some features are common to all procedures. In the simplest form, they may be summarized as "searching and scoring." Any docking method needs to explore the configuration space available for the interaction between two specified molecules. A straightforward systematic search is usually unfeasible even if the degrees of freedom are limited to translational and rotational ones by treating the molecules as rigid bodies. More elaborate search techniques are thus required and should be both accurate (not miss any good solutions) and efficient (not waste any time in uninteresting regions). The other problem in any docking procedure is to evaluate and rank the configurations generated by the search process. Hence, alternative scoring functions that model ΔG_{bind} as accurately as possible, i.e., provide good correlations with experimental binding affinities, must be used.

Kuntz *et al.* divide the docking problem into three basic sub problems [1]. First, docking must find useful ways for representing molecules and molecular properties. Then, docking requires methods for the juxtaposition of ligand and protein, i.e., for generating orientations. Finally, docking needs schemes for the evaluation of complementarity. All three issues are closely related and depend in part on each other. Nevertheless, this distinction is very useful for classifying the existing docking procedures.

The first way to characterize docking methods is by representation of the molecules to be docked. This choice is in part already determining for the subsequent docking strategy. A general distinction can be made between abstract descriptions on the one hand and atomic representations of the structure on the other. Most approaches use abstract descriptions of the receptor to reduce the macromolecular structural information to a manageable yet representative amount.

Geometric shape descriptors are widely used and include, for example, sphere representations of amino acids [2], negative sphere images of the binding site [3], molecular surface cubes [4], surface normals at sparse critical points [5], and cross-sectional slices represented as polygons [6]. The geometric descriptors may in part be associated with other properties of physicochemical relevance (e.g., hydrogen bond donors and acceptors). Instead of geometric descriptions, grid representations may be used for the macromolecular structure. This generally refers to so-called affinity grids, which are calculated on the basis of force field potentials for van der Waals and electrostatic interactions [7-9]. The representation of the macromolecular target often implies the same descriptive method for the ligand. In some cases, however, the ligand may be treated in full atomic detail with flexible torsions while only the receptor structure is simplified. This normally applies to the energy grid techniques. Full atomic description of the entire system is in general used only during an eventual refinement phase. One reason for such post-processing is to somehow include flexibility after an initial complex structure generation under the rigid body assumption.

The inclusion of flexibility is an important issue in docking, because lock-and-key-type binding between rigid bodies is not sufficient to describe all aspects of protein-ligand interactions and significant conformational changes may occur on binding ("induced fit"). Consequently, different ways have been studied to account for conformational flexibility not only in the ligand.

The treatment of flexibility is actually a problem pertaining to the second important aspect of docking which regards the search algorithm, i.e., the sampling of the configuration space to perform the match between the docking partners. The emphasis is on automated docking procedures. Automated procedures may roughly be classified as geometric or combinatorial on the one hand and energy driven on the other, although both methods tend to optimize a function which somehow models the real free energy of binding. If the molecules are represented by geometric descriptors, least-squares fitting procedures may be used to achieve matches between complementary surface patterns [10]. A hierarchical search of geometrically compatible triplets of surface normals on each molecule has been proposed. Three-dimensional correlation techniques using Fourier correlation algorithms are in wide use [11]; a variant is vector-valued cross-correlation [12]. Combinatorial searches are often applied to explore conformational flexibility and make use of algorithms such as dead-end elimination [13].

If some kind of energy function serves to guide the search, a variety of methods is available and are often used in the context of other modeling applications as well. Frequently, the algorithms are used in some combined way along the whole docking process. Monte Carlo (MC) techniques are widely applied, either using a simulated annealing scheme [14,15] or in combination with some form of energy minimization [16]. A "global optimization method" involving a combined Brownian and Monte Carlo minimization procedure,

followed by biased probability MC, has been proposed [17]. Molecular dynamics simulations have also found application in the context of docking [18]. Energy minimization is used in different variants, for example, in the form of rigid-body minimization, either for on-the-fly optimization during the docking process [19] or as relaxation of the receptor interface during refinement [20]. Multiple-copy simultaneous search methods can help to speed up energy-based searches [21]; they use numerous ligand copies which are transparent to each other, but subject to the full force of the receptor. Finally, evolutionary programming and genetic algorithms are becoming increasingly popular in docking [22-26].

The third fundamental point of any docking method is the scoring scheme used to rank and evaluate the generated orientations. Usually, this is strictly coupled with a certain kind of molecular representation. However, in post-docking ranking procedures, which are used for degeneracy checking and removal of false positives, the initial simplifications in the molecular models may be partly overcome by more sophisticated approaches. In such cases, increasingly complicated scoring schemes may be applied in a stepwise manner.

One set of scoring schemes is provided by "general indicators," which are not directly energy related and include various measures of surface complementarity. This applies in different forms to the methods that use geometric shape descriptors, as mentioned above. Force-field-based molecular mechanics functions are a second large class, generally combined with grid-based or detailed atomic representations of the molecules and Monte Carlo, molecular dynamics, or energy minimization techniques as search procedures. These potentials essentially provide a measure for steric and electrostatic complementarity, but are not really suitable as direct estimates of binding affinities, unless computationally demanding free energy simulations are carried out. In fact, they were normally not parameterized for such purposes and do not account for entropic effects and (de)solvation enthalpies. This is one of the main reasons that empirical free energy functions are increasingly used as a third variant of scoring schemes [27]. They may include a variety of terms related to atom–atom surface burial, lipophilicity and hydrophobicity, hydrogen bond geometry, entropical loss, and desolvation energy. Some of them have been calibrated explicitly on large experimental data sets of protein–ligand complexes of known three-dimensional structure [28,29].

AutoDock 4.0 [30] is the program used in this work. It is a program for docking small flexible ligands to a rigid receptor. It combines a fast energy evaluation trough precalculated grids of affinity potentials with a hybrid genetic algorithm-local search definite Larmarckian-genetic algorithm or LGA, since it utilizes Larmarckian notion that adaptations of an individual to its environment can be inherited by its offspring. The local searcher modifies the phenotype (that is the conformation) which is allowed to update the genotype: clearly, this contravenes Mendelian genetics observed in nature, but it does improve the

overall performance of the method. The genome consists of floating point genes each of which encodes one state variable describing the molecular position, orientation and conformation.

AutoDock uses an atomic representation of the ligand. Flexible torsions in the ligand may be defined with the utility AutoTors. The protein, in contrast, is treated as rigid and represented by a set of affinity grids. The grids are generated with AutoGrid on the basis of typical force field terms for van der Waals and Coulombic interactions. At every grid point, the interaction energy of a probe atom/probe charge with the whole protein is calculated, supplying a "map" of affinity potentials for each defined atom type, as well as a map for the electrostatic potential. These maps serve as look-up tables for the calculation of the interaction energy during the docking process. To search for suitable sites of interaction, a population of random ligand conformations in random orientations and at random translations is considered, then a docking run consists of a series of generations associated with a number of energy evaluations.

4.2 Molecular Mechanics

Molecular mechanics [31] is a method of computing minimum energy of a molecule in function of relative positions of its atoms. With such method on can find particular geometries and their associated energies or other static properties. This includes finding equilibrium structures, transition states, relative energies, and harmonic vibrational frequencies.

Molecular mechanics uses an empirical fit for reproducing a molecule's potential energy surface (the location and motion of nuclei on such surfaces dictate a molecule's structure and dynamical properties), commonly called a forcefield. The forcefields commonly used for describing molecules employ a combination of internal coordinates and terms (bond distances, bond angles, torsions, etc.), to describe part of the potential energy surface due to interactions between bonded atoms, and nonbond terms to describe the van der Waals and electrostatic interactions between atoms.

For an equilibrium geometry, where all bond distances and angles are such to determine the minimum energy of molecule, this last can be express by the Δx_i variations of coordinates according to the following equation:

$$V = V_0 + \frac{1}{2}\sum_i \left(\frac{\partial^2 V}{\partial x_i^2}\right)_e \Delta^2 x + \frac{1}{2}\sum_{ij}\left(\frac{\partial^2 V}{\partial x_i \, \partial x_j}\right)\Delta x_i \Delta x_j + ... \qquad (4.1)$$

This equation, where the index *e* refers to the equilibrium geometry, defines the potential molecular energy and is harmonic when it is limited to second degree in Δx_i. The second derivatives define the force constants:

$$f_{ij} = \frac{\partial^2 V}{\partial x_i \partial x_j} \tag{4.2}$$

Therefore, by means of molecular mechanics is possible to explore the potential energy surface and find the global minimum in a given space region in function of selected variables.

An important method to study the potential energy is search for stable conformations. The search of minimum energy conformation occurs by applying the $\Delta r_i \approx -\frac{\partial}{\partial r_i} V(r_1, r_2, ..., r_N)$ gradient in the configurations space.

Minimization of a model is done in two steps. First, the energy expression (an equation describing the energy of the system as a function of its coordinates) must be defined and evaluated for a given conformation. Energy expressions may be defined that include external restraining terms to bias the minimization, in addition to the energy terms. Next, the conformation is adjusted to lower the value of the energy expression. A minimum may be found after one adjustment or may require many thousands of iterations, depending on the nature of the algorithm, the form of the energy expression, and the size of the model.

The efficiency of the minimization is therefore judged by both the time needed to evaluate the energy expression and the number of structural adjustments (iterations) needed to converge to the minimum.

There are different algorithms to find minimum [32-34]: *steepest descent, conjugate gradients* e *Newton-Raphson* and modified versions. The choice of which algorithm to use depends on the potential energy surface type, the starting point adopted for minimum search, the precision request in the minimum determination and the size of the model.

The *conjugate gradients* and the *Newton-Raphson* are efficient on harmonic potential energy surfaces and are preferably used when the starting conformation is not more different from that at minimum energy.

The *conjugate gradients* method produces a complete basis set of mutually conjugate directions such that each successive step continually refines the direction toward the minimum. If these conjugate directions truly span the space of the energy surface, then minimization along each direction in turn must by definition end in arriving at a minimum. The conjugate gradient algorithm constructs and follows such a set of directions.

The *Newton-Raphson* method converges more quickly than *conjugate gradients* but is more computationally expensive. In addition to using the gradient to identify a search direction, the curvature of the function (the second derivative) is also used to predict where the function passes through a minimum along that direction. It is reserved primarily for calculations where rapid convergence to an extremely precise minimum is required.

The *steepest descent* method is efficient on not harmonic potential energy surfaces but the convergence at minimum is slow because the gradient is monodirectional. It is the method most likely to generate a lower-energy structure regardless of what the function is or where the process begins. Therefore, the steepest-descents method is often used when the gradients are large and the configurations are far from the minimum. This is commonly the case for initial relaxation of poorly refined crystallographic data or for graphically built models. The convergence is then obtained by using the *conjugate gradients* or the *Newton-Raphson* method.

The actual coordinates of a molecule combined with the forcefield data create the energy expression for the molecule. This energy expression, in the equation 4.3, is the equation that describes the potential energy surface of a particular molecule as a function of its atomic coordinates. The figure 4.1 shows a schematic representation of the equation. The potential energy of a system can be expressed as a sum of valence (or bond), crossterm, and nonbond interactions. The energy of valence interactions is generally accounted for bond stretching (E^r), valence angle bending (E^a), dihedral angle torsion (E^t), and out-of-plane interactions (E^o) terms, which are part of nearly all forcefields for covalent systems (1-4 terms in the figure 4.1). Forcefields generally achieve higher accuracy by including cross terms to account for such factors as bond or angle distortions caused by nearby atoms (5-9 terms in the figure 4.1). Crossterms can include the following terms: stretch–stretch, stretch–bend, bend–bend, torsion–stretch, torsion–bend. The energy of interactions between nonbonded atoms is accounted for by van der Waals (E^{VDW}), electrostatic (E^{elet}) (illustration 10 in the figure 4.1). An important consequence of standard electrostatic and van der Waals parameters are the possible intra and intermolecular hydrogen bonds functions.

$$E = \sum E^r + \sum E^a + \sum E^t + \sum E^o + \sum E^{rr} + \sum E^{ar} + \sum E^{aa} + \sum E^{at} + \sum E^{rt} + \sum E^{elet} + \sum E^{VDW} \qquad (4.3)$$

where:

$$E^r = K_r (r - r_0)^2 ; E^a = K_a (\theta - \theta_0)^2 ; E^t = K_t (1 - \cos 2\phi)^2 ;$$
$$E^o = K_o (\chi - \chi_0)^2 \left\{ E^{rr}, E^{aa}, E^{ra} \right\} = K_c (s - s_0)(s' - s'_0) ;$$
$$\left\{ E^{rt} \right\} = (r - r_0)\, K_c (1 - \cos 2\phi)^2 ; \left\{ E^{at} \right\} = (\theta - \theta_0)\, K_c (1 - \cos 2\phi)^2 ;$$
$$E^{elet} = \sum_{ij} \frac{q_i q_j}{r_{ij}} ; \; E^{VDW} = \sum_{ij} \varepsilon_{ij} \left[2 \left(\frac{r^o_{ij}}{r_{ij}} \right)^9 - 3 \left(\frac{r^o_{ij}}{r_{ij}} \right)^6 \right].$$

The K_r, K_a, K_t, K_o and K_c parameters are the force constants for the corresponding intramolecular deformations; r^* and ε characterize the dimensions of atoms and the van der Waals interaction force; at the end q_i represents the partial charge of each atom. These parameters are calculated from empirically from vibrational and rotational spectra, NMR and crystallographic data, or with ab initio techniques [35-39].

Several force fields are now available. In our work we have used PCFF [39]. The PCFF has been created originally to simulate polycarbonates and has been extended later on more general polymeric systems with several functional groups.

Of course, the results accuracy, obtained with MM technique, depends on the analytical form used and on precision with the force constants are derived.

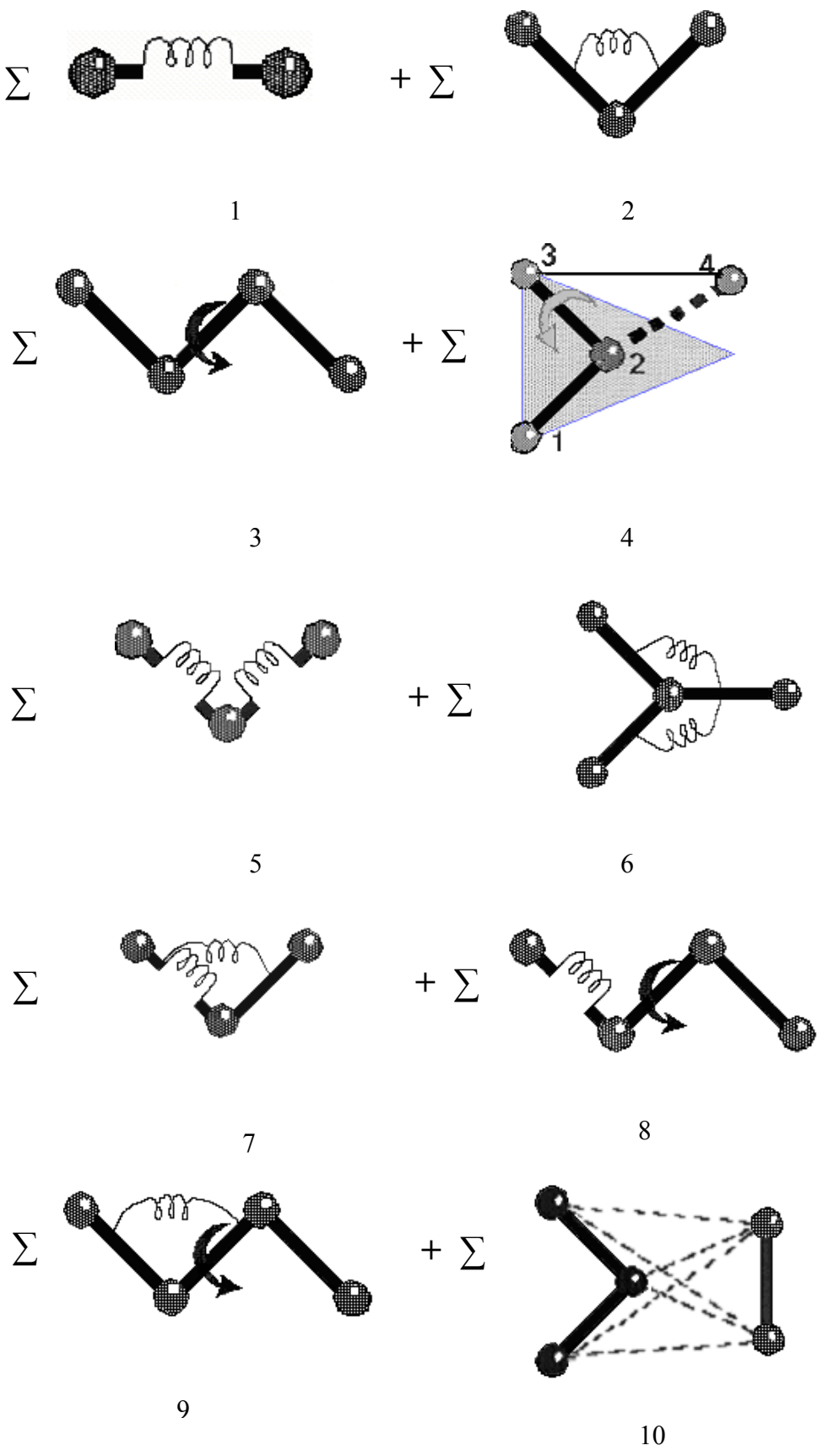

Figure 4.1 *Schematic of a typical empirical force field expression.*

4.3 Molecular Dynamics

Dynamics simulations are useful in studies of the time evolution of a variety of systems at nonzero temperatures, for example, biological molecules, polymers, or catalytic materials, in a variety of states, for example, crystals, aqueous solutions, or in the gas phase. During dynamics simulations, a system undergoes conformational and momentum changes so that different parts of the phase space accessible to the model can be explored. The conformational search capability of dynamics is one of its most important uses. Moreover molecular dynamics simulations allows you to generate statistical ensembles from which various energetic, thermodynamic, structural, and dynamic properties can be calculated such as, for example, diffusion coefficients and protein folding.

Molecular dynamics solves the classical equations of motion for a system of N atoms interacting by using an integration numerical procedure [40, 41]. At its simplest, molecular dynamics solves Newton's familiar equation of motion:

$$F_i(t) = m_i a_i(t) \tag{4.4}$$

where F_i is the force, m_i is the mass, and a_i is the acceleration of atom *i*. The force on atom i can be computed directly from the derivative of the potential energy V with respect to the coordinates r_i:

$$-\frac{\partial V}{\partial r_i} = m_i \frac{\partial^2 r_i}{\partial t_i^{\,2}} \tag{4.5}$$

Notice that classical equations of motion are deterministic. That is, once the initial coordinates and velocities are known, the coordinates and velocities at a later time can be determined. The coordinates and velocities for a complete dynamics run are called trajectory. Although the initial coordinates are determined from crystallographic data or from a previous operation such as minimization, the initial velocities are randomly generated according at the beginning of a dynamics run, according to Maxwell-Boltzmann distribution at the desired temperature.

A standard method of solving an ordinary differential equation such as Eq. 4.5 numerically is the finite-difference method. The general idea is as follows. Given the initial coordinates and velocities and other dynamic information at time t, the positions and velocities at time $t + \Delta t$ are calculated. The timestep Δt depends on the integration method as well as the system itself. Roughly put on the force F_i constant in the time interval Δt. In such way, the problem reduces at an equations system such:

$$\begin{cases} y_0 = \mathrm{y}(\mathrm{t}_0) \\ y_0' = \mathrm{y}'(\mathrm{t}_0) \\ y'' = \mathrm{f}(\mathrm{y}) \end{cases} \tag{4.6}$$

that can solved considering appropriate boundary conditions and where y, y′ and y″ are vectors with 3-N dimensions, whose derivatives are estimated as regards the time.

Between all algorithms available in molecular dynamics, that used in this work is Verlet algorithm [42]. The advantages of Verlet integrators is that this method requires only one energy evaluation per step, requires only modest memory, and also allow a relatively large timestep to be used.

The Verlet algorithm is as follow:

considering v_{middle} as the average of velocity in the time range t and t + Δt, the position at time t + Δt will be:

$$\vec{r}(t + \Delta t) = \vec{r}(t) + \vec{\mathrm{v}}_{\mathrm{middle}} \cdot \Delta t \tag{4.7}$$

considering that the velocity changes linearly during Δt then the average velocity is equal to the instantaneous velocity at the instant t + ½Δt:

$$\vec{v}_{middle} = \vec{v}\left(t + {}^{1}/_{2}\Delta t\right) \tag{4.8}$$

in turn the instantaneous velocity can be calculated from the average acceleration in the range t – ½Δt and t + ½Δt:

$$\vec{\mathrm{v}}\left(\mathrm{t} + {}^{1}/_{2}\Delta \mathrm{t}\right) = \vec{\mathrm{v}}\left(\mathrm{t} - {}^{1}/_{2}\Delta \mathrm{t}\right) + \vec{\mathrm{a}}_{\mathrm{medio}} \cdot \Delta \mathrm{t} \tag{4.9}$$

assuming that the acceleration is linear in the range t - ½Δt and t + ½Δt on obtains:

$$\vec{a}_{middle} = \vec{a}(t) \tag{4.10}$$

from which on obtains the velocity expression:

$$\vec{\mathrm{v}}\left(\mathrm{t} + {}^{1}/_{2}\Delta \mathrm{t}\right) = \vec{\mathrm{v}}\left(\mathrm{t} - {}^{1}/_{2}\Delta \mathrm{t}\right) + \vec{\mathrm{a}}(\mathrm{t}) \cdot \Delta \mathrm{t} \tag{4.11}$$

Combining the last two equations on obtains a different expression for the coordinates:

$$\vec{\mathrm{r}}(\mathrm{t} + \Delta \mathrm{t}) = \vec{\mathrm{r}}(\mathrm{t}) + \vec{\mathrm{v}}\left(\mathrm{t} + {}^{1}/_{2}\Delta \mathrm{t}\right) \cdot \Delta \mathrm{t} \tag{4.12}$$

.

The equations (4.11) (4.12) are called *leapfrog* method because the velocity is out from the step of a quantity equal to middle of the time of the same step (t + ½Δt).

To value the next coordinates the cycle:

1) calculates the acceleration $\left(-\frac{1}{m}\right)\frac{d\vec{v}}{dt}$ at the time t;

2) calculates the velocity at the time t + ½Δt from its value t - ½Δt by means of the equation (4.11);

3) finally determines the coordinates in the range t + Δt from its value at the time t by means of equation (4.12).

A method to accelerate a molecular dymamics calculation is reducing the number of freedom degrees by using geometrical constrains. For example, for macromolecular systems where the number of freedom degrees is high, the reduction occurs by eliminating the stretching vibrations for bonds applying dynamical obligations or maintaining the bending angles constant.

This permits the elimination of any fast vibrational motions by reducing the steps of the numerical integration [43]. In any cases on prefers add others terms, the restrains, to force the system and restrict the calculation field.

In the simulations the temperature and pressures parameters are fundamentals (even if isolated molecules simulated in vacuum don't have a definite pressure). Their control during the simulation can occur in different manners. The constant-temperature, constant-volume ensemble (NVT), also referred to as the canonical ensemble, is obtained by controlling the thermodynamic temperature. Direct temperature scaling should be used only during the initialization stage, since it does not produce a true canonical ensemble (it is not truly isothermal). Any of the other temperature control methods is used during the data collection phase. This is the appropriate choice when conformational searches of models are carried out in vacuum without periodic boundary conditions. The constant-temperature, constant-pressure ensemble (NPT) allows control over both the temperature and pressure. The unit cell vectors are allowed to change and the pressure is adjusted by adjusting the volume (i.e., the size of the unit cell). This method applies only to periodic systems. NPT is the ensemble of choice when the correct pressure, volume, and densities are important in the simulation.

References

1. I. D. Kuntz, E. C. Meng, B. K. Shoichet, *Acc. Chem. Res.,* 27 (1994) 117-123.
2. J. Cherfils, S. Duquerroy, J. Janin, *Proteins,* 11 (1991) 271-280.
3. C. M. Oshiro, I. D. Kuntz, *Proteins,* 30 (1998) 321-336.
4. F. Jiang, S. H. Kim, *J. Mol. Biol.,* 219 (1991) 79-102.
5. R. Norel, S. L. Lin, H. J. Wolfson, R. Nussinov, *J. Mol. Biol.,* 252 (1995) 263-273.
6. G. Ausiello, G. Cesareni, M. Helmer-Citterich, *Proteins,* 28 (1997) 556-567.
7. D. S. Goodsell, A. J. Olson, *Proteins,* 8 (1990) 195-202.
8. B. A. Luty, Z.R. Wasserman, P. F. W. Stouten, C. N. Hodge, M. Zacharias, J. A. Mc Cammon, *J. Comput. Chem.,* 16 (1995) 454-464.
9. Jr. D. Oberlin, H.A. Scheraga, *J. Comput. Chem.,* 19 (1998) 71-85.
10. D. J. Bacon, J. Moult, *J. Mol. Biol.,* 225 (1992) 849-858.
11. H. A. Gabb, R. M. Jackson, M. J. E. Sternberg, *J. Mol. Biol.,* 272 (1997) 106-120.
12. F. Ackermann, G. Herrmann, S. Posch, G. Sagerer, *Bioinformatics,* 14 (1998) 196-205.
13. A. R. Leach, *J. Mol. Biol.,* 235 (1994) 345-356.
14. G. M. Morris, D. S. Goodsell, R. Huey, A. J. Olson, *J. Comput.-Aided Mol. Design,* 10 (1996) , 293-304.
15. P. Cairo, F. Ortuso, S. Alcaro, E. Fontananova, E. Tocci, E. Drioli, *Chem. Phys. Lett.,* 454 (2008) 374-381.
16. A. Caflisch, S. Fischer, M. Karplus, *J. Comput. Chem.,* 18 (1997) 723-743.
17. M. Totrov, R. Abagyan, *Nature Struct. Biol.,* 1 (1994) 259-263.
18. N. Nakajima, J. Higo, A. Kidera, H. Nakamura, *Chem. Phys. Lett.*, 278 (1997) 297-301.
19. D. A. Gschwend, I. D. Kuntz, *J. Comput.-Aided Mol. Design*, 10 (1996) 123-132.
20. R. M. Jackson, H.A. Gabb, M. J. E. Sternberg, *J. Mol. Biol.,* 276 (1998) 265-285.
21. R. Rosenfeld, Q. Zheng, S. Vajda, C. DeLisi, *J. Mol. Biol.,* 234 (1993), 515-521.
22. G. Jones, P. Willett, R. C. Glen, *J. Mol. Biol.,* 245 (1995) 43-53.
23. C. M. Oshiro, I. D. Kuntz, J. S. Dixon, *J. Comput.- Aided Mol. Design,* 9 (1995) 113-130.
24. D. E. Clark, D. R. Westhead, *J. Comput.-Aided Mol. Design,* 10 (1996) 337-358.
25. G. Jones, P. Willett, R. C. Glen, A. R Leach, R. Taylor, *J. Mol. Biol.,* 267 (1997) 727-748.
26. D. R. Westhead, D. E. Clark, C. W. Murray, *J. Comput. - Aided Mol. Design,* 11 (1997) 209-228.

27. A. Wallqvist, D. G. Covell, *Proteins,* 25 (1996) 403-419.
28. H.-J. Böhm, *J. Comput.-Aided Mol. Design,* 8 (1994) 243-256.
29. H.-J. Böhm, *J. Comput.-Aided Mol. Design,* 12 (1998) 309-323.
30. G.M. Morris, D.S. Goodsell, R.S. Halliday, R. Huey, W.E. Hart, R.K. Belew, A. J. Olson, *J. Comp. Chem.,* 19 (1998) 1639-1662.
31. *Molecular Mechanics*, N. L. Allinger, U. Bunker, Monography n° 177, Ed. American Chemical Society: Washington, DC, 1982.
32. *Computational Advances in Organic Chemistry: Molecular Structure and Reactivity*, Ogretir and Csizmadia, Ed. Kluwer: Dordrecht, 1991.
33. *Pratical Methods of Optimization*, R. Flectcher, Ed. John Wiley e Sons: New York, 1980, vol. 1.
34. *Principles of Numerical Analysis*, A. S. Householder, Ed. Mc Graw-Hill: New York, 1953.
35. *Molecular dynamics structures*, J. Hermans, Ed. Polycrystal Western Spring, 1985.
36. O. Ermer, *Structure and bonding,* 27 (1976) 161-211.
37. J. S. Weiner, P. A. Kollmann, D. A. Case, C. C. Singh, C. Ghio, G. Alagona, S. Profeta, P. Weiner, *J. Am. Chem. Soc*., 106 (1984) 765-784.
38. S. J. Weiner, P. A. Kollman, D. T. Nguyen, D. A. Case, *J. Comp. Chem.,* 7 (1986) 230-252.
39. H. Sun, S. J. Mumby, J. R. Maple, A. T. Hagler, *J. Am. Chem. Soc.*, 116 (1994) 2978-2987.
40. W. F. van Gunsteren, H. J. C. Berendsen, *Mol. Phys.,* 34 (1977) 1311-1327.
41. *Computer Simulation of Liquids*, M. P. Allen, D. J. Tildesley, Oxford University Press, 1987.
42. L. Verlet, *Phys. Rev.,* 159 (1967) 98-103.
43. J. P. Ryckaert, G. Ciccotti, H. J. C. Berendsen, *J. Comput Phys.,* 23 (1977) 327- 341

PART II

Results

FIFTH CHAPTER

β-CYCLODEXTRIN INTERACTIONS WITH THREE DRUGS USED IN INFLAMMATORY PATHOLOGIES: AN EXPERIMENTAL AND THEORETICAL STUDY

5.1 Introduction

Cyclodextrins (CDs) are a group of structurally related cyclic oligosaccharides that are formed by enzymatic degradation of starch. CDs have a hydrophilic external surface and a hydrophobic internal cavity that enables the complexation of lipophilic 'guest' drug molecules. The complexation affects many of the physicochemical properties of the drug without affecting their intrinsic lipophilicity or pharmacological properties [1-3]. CDs are widely used in the pharmaceutical field because they enhance the solubility in aqueous solvent, the stability, the bioavailability of drug molecules and reduce the toxic effects of drugs. Often the CD's formulation improves the selective transfer and/or reduces side effects. CDs act as drug carriers delivering the necessary amount to the targeted site for a necessary time period, both efficiently and precisely [4-8].

The determination of the inclusion geometry is a difficult step and represents one of the highest challenges in the host-guest chemistry. The encapsulation of guests into host cavities usually has two associated relevant problems: guest's conformational changes and multiple possible inclusion geometries. Guests normally contain more than one functional group and for this reason can be differentiated by inclusion into a host with one site preferred over others. The rational design of pharmaceutical cyclodextrin formulation requires a good knowledge of the encapsulation process. Structural information, such as the geometries of the complex and thermodynamic data, such as the variation in the enthalpy (ΔH), are necessary to draw a complete picture of CD-drug interaction. Several modeling methodologies have been used for a better understanding of the inclusion process. Indeed, the theoretical studies can strengthen and supplement the experimental conclusions, and vice versa, providing information on the driving forces responsible for complexation processes [9-17].

The aim of the present work is to complete the characterization of the interactions between the βCD, one of the more common CDs with seven glucose units, and three nonsteroid anti-inflammatory drug molecules with a wide range of actions, with both experimental methods and theoretical studies involving molecular mechanics (MM).

The drugs investigated, shown in scheme 5.1, were the 5-aminosalicylic acid (**1**), an anti-inflammatory drug, currently used in the treatment of inflammatory bowel disease, which is a light and oxygen sensitive, the

sulfasalazine (**2**), a prodrug of 5-aminosalicylic acid linked with an azo bond to an inert carrier (sulfapyridine), and the diflunisal (**3**) a salicylic acid derivative which has anti-inflammatory and analgesic activities. It is well established that the CDs reduce the irritation caused by nonsteroidal anti-inflammatory drugs to gastrointestinal mucosa and that CDs stabilize and protect unstable compounds from degradation [6].

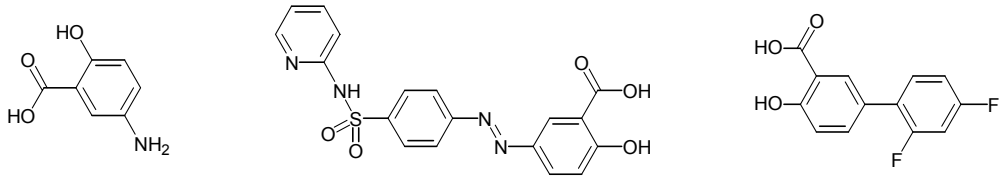

(1) **(2)** **(3)**

Scheme 5.1 *Molecular structures of drugs **1** (5-aminosalicylic acid), **2** (sulfasalazine) and **3** (diflunisal).*

In the literature, some experimental data have shown that **1**-**3** are able to complex with βCD [18-22]. We have employed two different experimental methods in the determination of thermodynamic quantities for the complexation reactions of CDs, i.e., differential scanning calorimetry (DSC) at solid state, and spectrophotometry. Calorimetry was used because is a direct method for the determination of the reaction enthalpy [2]. The disappearance of the melting endotherm of the guests in the DSC curves of the mixtures has been considered, as often used in the literature [23-25], as an indication of the host-guest interaction, as also the reduction of the ΔH of dehydration due to the inclusion of the guest. Moreover, when the guest is an aromatic compound which has a strong absorption band in the UV-vis region, spectroscopic methods can be widely used to determine the stability constants in solution [26,27]. The changes in the absorbance of the guest in the presence of increasing concentrations of the host have been elaborated using the Benesi-Hildebrand linear model for a 1:1 complex [26]. Then to establish in which way the drugs form complexes this work first report a detailed theoretical analysis. The molecular modeling study has been carried out by using the MOLINE docking approach [28] followed by full energy minimization steps. In order to compare different parameter sets, the final optimization has been performed taking into account two different force fields such as AMBER* [29], as implemented in MacroModel ver. 7.2 [30], and PCFF [31], included into the INSIGHT package [32]. A comparison between the theoretical data and the experimental results is reported in this manuscript.

5.2 Experimental

5.2.1 DSC analysis

DSC has been used for studying the thermal behaviour of 1:1 molar ratio physical mixtures of compounds **1-3** with βCD. βCD has been used as received from Sigma-Aldrich without further purification. Transition temperature and enthalpy have been measured at the first heating by a Perkin–Elmer Pyris Diamond DSC (from 30 to 250°C; heating rate 15°C/min; in nitrogen flux) using aluminium pan with lids, but uncrimped. Sample masses have been between 1 and 3 mg.

5.2.2 Determination of Equilibrium Constant

The Benesi-Hildebrand equation (5.1) has been used to determine the stability constant (K) for an assumed binary complex through UV-Vis absorption experiments

$$\frac{\Delta A}{b} = \frac{[guest]K\Delta\varepsilon[CD]}{1+K[guest]} \qquad (5.1)$$

where b is the path length and Δε represents the difference between the molar absorptivities of the free and complexed guest in the UV-Vis absorption experiments. This equation has been applied due to the change in the absorbance, ΔA, with increasing βCD concentration. These experiments have been carried out in a thermostatic bath at 25 °C. The stability constants of the complex βCD·guest, have been obtained from the linear double-reciprocal plot [27], considering the difference in the absorbance ΔA^{-1} values versus the βCD concentration $[\beta CD]^{-1}$.

5.2.3 Preparation of the guests - βCD solid mixtures

The mixtures of βCD and guest drug molecules have been prepared by shaking and mixing with a vortex mixer (2000 rpm) for 10 min 1:1 molar ratio mix of the two components.

5.2.4 Preparation of the guests - βCD solid solutions

For each guest a standard volume (4 ml) of a stock solution in water ($8.00\cdot10^{-4}$ mol/L for **1**; 2.51 10^{-6} mol/L for **2** and $4.16\cdot10^{-5}$ mol/L for **3**) has been added to standard volumes (7 ml) of βCD solutions at increasing concentration (unbuffered solutions). This procedure ensures a constant concentration of the guest. The solutions have been stirred with a fast magnetic stirrer for 24 h, for an

elapsed time that has ensured the achievement of equilibrium during the formation of inclusion complexes, at 25 ± 1°C and then has been analyzed by UV-vis spectroscopy. The absorbance has been measured for **1** at wavelength (λ_{max}) of 298 nm, for **2** at 360 nm and for **3** at 252.5 nm. The changes in absorbance ($\Delta A = A - A_0$) at the same λ_{max} between the guest solution in the presence of the βCD (A) and without the βCD (A_0) have been calculated.

5.2.5 Molecular modeling

The theoretical study has been carried out using a three-step approach. In the first step, conformational properties of compounds **1-3** have been evaluated by means of the Monte Carlo (MC) search applying 5000 iterations to all rotatable bonds available in each guest molecule. All unique conformations have been energy minimized by using the AMBER* force field with all-atoms notation. Water solvent effects have been taken into account by means of the GB/SA (generalized Born/surface area) implicit solvation model as implemented in the MacroModel package. The conformations have been selected with a Boltzmann probability higher than 0.01% producing a total of 5 unique conformations for compound **1**, 82 for **2** and 21 for **3**.

In the second step the molecular recognition of all conformations of compound **1-3**, within 5 kcal/mol above the global minimum energy structure, has been investigated with respect to the βCD using the software MOLINE [28]. The energy contributions have been computed by using the AMBER* force field. At this stage the water environment has been mimicked by using a dielectric constant equal to 80.

For each conformer 65712 configurations have been generated. The structure have been consequentially clustered and optimized reporting 948, 4289 and 1435 configurations for βCD complexes respectively with compounds **1**, **2** and **3**.

In the third step, the minimum energy complexes, within 3 kcal/mol above the global minimum, have been submitted to the full energy refinement. In order to investigate the accuracy of molecular mechanics techniques two force fields, AMBER* and PCFF, have been adopted for this energy optimization and their results have been compared. AMBER* calculation have been performed taking into account the water solvent effects by means of the implicit model of solvation GB/SA.

The Truncate Newton Conjugate Gradient algorithm has been chosen for AMBER* optimizations with a convergence criterion fixed to 0.2 kcal/mol Å.

PCFF calculations have been performed using the InsightII/Discover software of Accelrys [32] with the dielectric constant set to 80. Conjugate gradient algorithm with a termination gradient of 10^{-2} kcal/mol has been selected for PCFF optimizations.

All conformations, with an RMS (root mean square of distance) lower than 0.25 Å, computed after the energy minimization, both from AMBER* and from PCFF, have been considered as duplicate structures and, consequently, removed from the configuration ensembles.

The optimisation performed with AMBER* has produced respectively 12, 516 and 137 configurations for complexes with compounds **1**, **2** and **3**. Instead, PCFF force field has yielded 49, 240 and 128 configurations.

In order to evaluate the accuracy of the PCFF force field for the βCD, this molecule has been subjected to a NVT-MD (constant number of atoms, constant volume, constant temperature) of 700 ps with time step of 1 fs, at 300 K. The conformational analysis has been carried out collecting snapshots every 50 ps and in correspondence of potential energy peaks. The sampled structures have been optimized and the lowest energy minimum structure has been superimposed on those obtained from calculations performed by using the cvff force field (being amply used in literature for in vacuo and in solution calculations of CDs) [10,12, 33] and on those determined from X-ray [34]. The comparison showed a quite good agreement of all models.

5.3 Results and Discussion

5.3.1 Calorimetric determinations

DSC analyses have been done for the pure components and for 1:1 molar ratio physical mixtures. Indeed, the thermal behaviour of the mixtures has provided an indication of possible inclusion of the potential guests into the cavity of the cyclodextrin. The results of the thermo-analytical curves of the mixtures have been compared, in figure 5.1a-c, with those of the pure compounds in order to observe indications of the host-guest interactions. This, because, it is considered to be a proof of the inclusion formation, although not entirely conclusive, the disappearance of the melting peak of the guest molecule in the DSC curve of the complex [23-25]. In figure 5.1a-c the decreasing in the endotherm associated with βCD dehydration in all the physical mixtures in comparison with the pure βCD has been observed, indicating that all drug molecules interacted with the cyclodextrin.

The analysis of the DSC curve of the pure βCD has indicated a broad endotherm peak, from 82 to 116 °C, that may be attributed to the loss of water as observed in different studies [19,23-25]. After this peak only a small exo effect, corresponding to the βCD phase transition (219-223 °C), has been observed.
The inclusion of a guest in the CD cavity may displace some or all water molecules originally in the cavity or in the surrounding environment, so the changes in the dehydration endotherms observed in the ΔH of the mixtures can be used as an additional indicator of the inclusion occurrence [19,23-25].

The difference in $\Delta H_{dehydr.}$ of the mixture respect to pure βCD (283 J g^{-1}) has been defined as

$$\frac{\Delta H_{dehydr.}(\beta CD:guest) - \Delta H_{dehydr.}(\beta CD)}{\Delta H_{dehydr.}(\beta CD)} \cdot 100 \qquad (5.2)$$

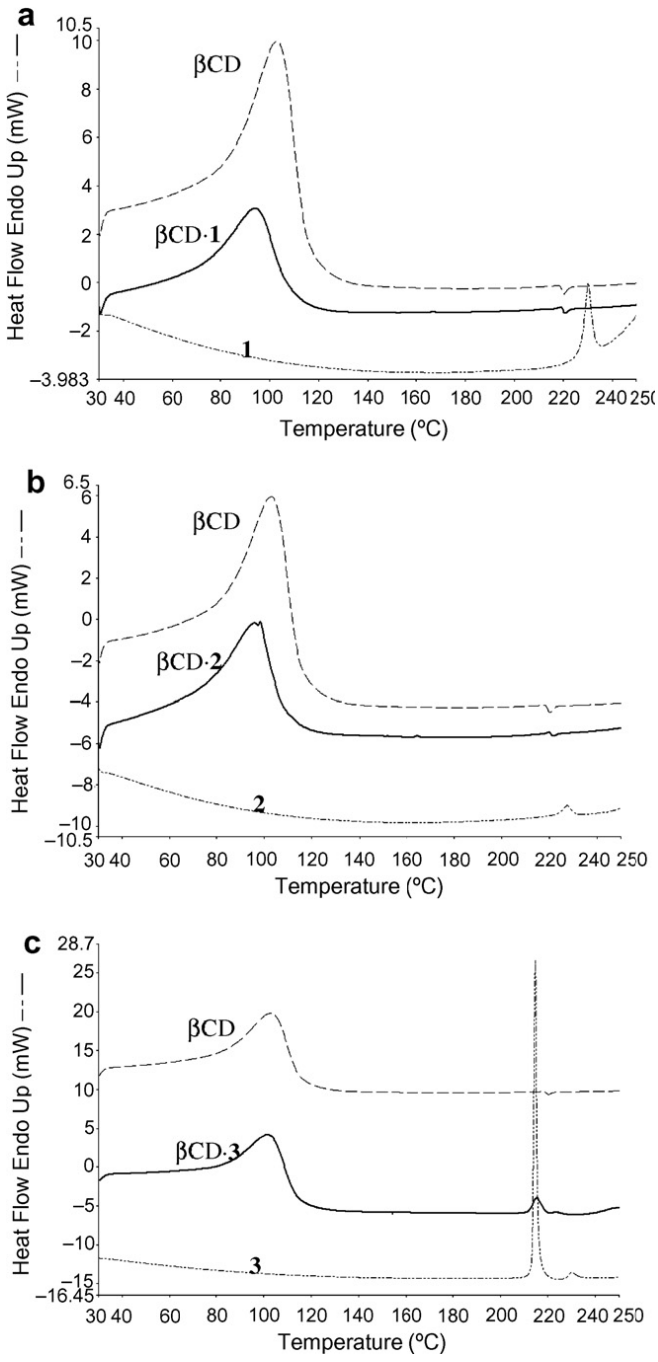

Figure 5.1 *DSC curves for a) βCD, **1** and βCD·**1**; b) βCD, **2** and βCD·**2**; c) βCD, **3** and βCD·**3**. All physical mixtures are considered on 1:1 molar ratio.*

The curve in figure 5.1a shows a strong interaction between βCD and **1**, confirmed by the strong reduction in the $\Delta H_{dehydr.}$ (28.3%), by the decrease of the dehydration endotherm of βCD and, finally, by the disappearance of the endotherm peak of pure **1**. Figure 5.1b points out the interaction between **2** and βCD as indicated by the reduction in the enthalpy of dehydration (18.4%). Further the disappearance of the endotherm peak of the pure compound **2** (at onset 224 °C), as previously ascertained by X-ray and IR data [21], has been observed. The curve for the mixture βCD·**3**, in figure 5.1c, has indicated a partial reduction of dehydration of βCD, a decreasing of the melting endotherm of the pure compound **3**, but not its complete disappearance. This is a proof of the presence of the pure **3** in the physical mixture, that has not completely interacted within the cyclodextrin. This phenomenon could explain the minor reduction of $\Delta H_{dehydr.}$ in comparison with the other two guests (13.1%).

The different $\Delta H_{dehydr.}$ percentage can be explained in terms of a minor steric hindrance of **1** which more easily goes into the βCD cavity than the larger **2** and **3** molecules also in solid state, causing a major displacement of water molecules from the βCD and, consequently, a higher reduction of $\Delta H_{dehydr.}$ for βCD.

5.3.2 Thermodynamic parameters of the complexes

Table 5.1 reports the experimental complexation constants for the βCD·drug analysed. The value obtained for the βCD·**3** complex is in good agreement with the reported value by Sideris et al. [22] of $7.83(\pm0.38)\cdot10^4$ M^{-1} obtained by using ion-selective electrode potentiometry. The strongest interaction has appeared with the larger molecule **2** followed by **3**. The least stable interaction has been found for compound **1**. These data well agree with the solubility trend of drugs in water: **2** shows the minor solubility with respect to **3** and **1**. The lower K value of **1** could be due to the presence of several polar groups attached on an aromatic ring which induce a better solubilisation in the bulk solution in comparison to that of other drugs. An increase in the apolar character of the molecule results in an increase in the complexation constant.

Complex	$\Delta H_{binding}$ MOLINE	$\Delta H_{binding}$ AMBER*	$\Delta H_{binding}$ PCFF	K_{exp} (M^{-1})
βCD·**1**	-11.71	-16.55	-26.79	$1.68(\pm0.45)\cdot10^3$
βCD·**2**	-19.05	-22.57	-37.05	$1.34(\pm0.07)\cdot10^5$
βCD·**3**	-16.52	-18.29	-33.05	$7.39(\pm0.41)\cdot10^4$

Table 5.1 *Complexation enthalpies of the complexes between the βCD and **1**, **2** and **3** computed with the different theoretical methodologies and experimental equilibrium constants determined by UV-Vis spectroscopy.*

(Energy values are reported in kcal/mol. Experimental stability constants for the complexes in water at 25 °C.).

5.3.3 Theoretical analysis

Calculation have been performed in order to obtain global informations about the geometry of the host-guest complexes and to find the intermolecular interactions between cyclodextrins and the three drug molecules. The evaluation of the **1**-**3**·βCD recognition has been performed taking into account CD flexibility and induced fit phenomena by means of full minimizations carried out using AMBER* and PCFF.

The computational protocol best fitting the experimental stability constant trend has been evaluated based on the correlation with the computed complexation enthalpy differences [11,14,15,35] calculated for absolute minima (table 5.1). The binding energy of complexes has been calculated as follows:

$$\Delta H_{bin} = \mathrm{H}_{\mathrm{G}\bullet\mathrm{CD}} + \left(\mathrm{H}_{\mathrm{G}} + \mathrm{H}_{\mathrm{CD}}\right)_{frozenincomplex} \qquad (5.3)$$

where G is the guest, CD is the β-cyclodextrin, G·CD is the final inclusion compound and ΔH_{bin} is the difference between the energy of the optimized complex and the sum of the energies of the isolated molecules extracted from the complex in the same conformation. The negative values upon complexation indicate that the drugs form a stable complex with βCD under conditions such as those considered here. The order of interaction is the same with the different theoretical methodologies: βCD·**2** > βCD·**3** > βCD·**1**. Every single approaches in molecular modelling was correct to draw a picture of energetic behaviour of the complexes. All force fields are able to reproduce the experimental trend found in the measurement of stability constants (table 5.1). In details, the difference between the enthalpy values calculated with the different theoretical approaches (MOLINE, AMBER, PCFF) were in the same order of magnitude. In order to describe the recognition process at the molecular level dummy atoms, representative of ring centroids, have been used for the calculation of significant geometrical descriptors. Two dummy atoms have been considered, respectively, as centroids for the primary and the secondary –OH groups located onto the βCD. The theoretical analysis has indicated the groups of guest molecule that give the better interactions with βCD providing the orientation of the drugs into βCD cavity; moreover it has evidenced the formation of hydrogen bonds between host and guests.

5.3.3.1 βCD·2 complex

Compound **2** (figure 5.2) shows an 'L' shape, the pyridine residue representing the short side (Pyr) and the phenyl ring with the azo bond and the salicylic moiety representing the long side of the 'L' (5asa). Figure 5.2 illustrates that the majority of conformations (80% of the total) have shown the salicylic moiety out of the secondary rim (5asa Sec) and only a small percentage has been found with the pyridinic part on the secondary rim (Pyr Sec). The minima are in the range of the most populated complex conformers.

Both AMBER* and PCFF minima are characterized by the stabilization effect of intermolecular hydrogen bond(s) between the sulfamidic moiety and βCD (table 5.2). These interactions could explain the highest experimental stability constants and the maximum binding energy.

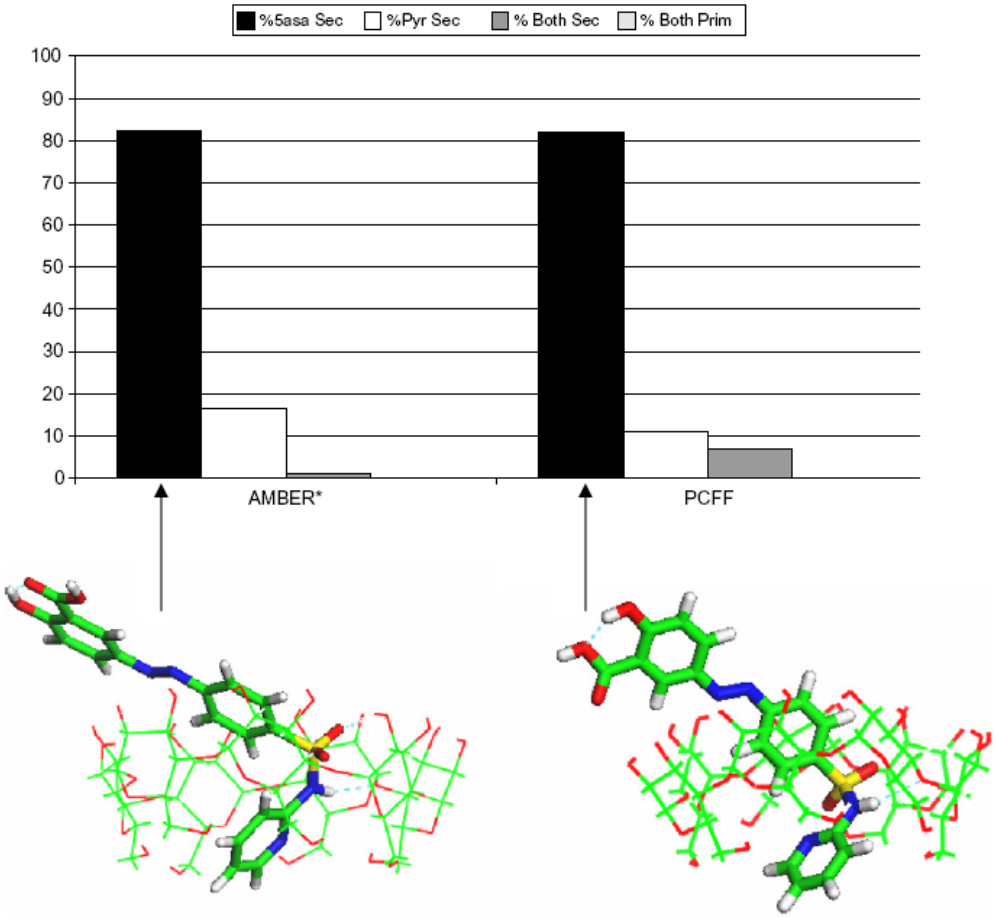

Figure 5.2 *Different orientation of* ***2*** *into βCD cavity, expressed as Boltzmann probability percentage at room temperature, obtained with AMBER* and PCFF force fields. The terms Prim and Sec refer to the primary and secondary rim of CD. Pyr is the pyridine residue of compound* ***2****, 5asa is the salicylic moiety of* ***2****. Also are indicated the global minimum conformers of* ***2*** *obtained with AMBER* and PCFF force fields.*

Complex	H Bond AMBER* (CD-guest)	H Bond PCFF (CD-guest)
βCD·**1**	-	O···(H-O-C=O)- O-H···(O=C-O-H)
βCD·**2**	O···(H-N)- O-H···(O=S=O)-	O···(H-N)-
βCD·**3**	O-H···(O-C=O)- | H	-

Table 5.2 *The intermolecular hydrogen bonds formed between βCD and the three drugs **1**, **2** and **3**.*

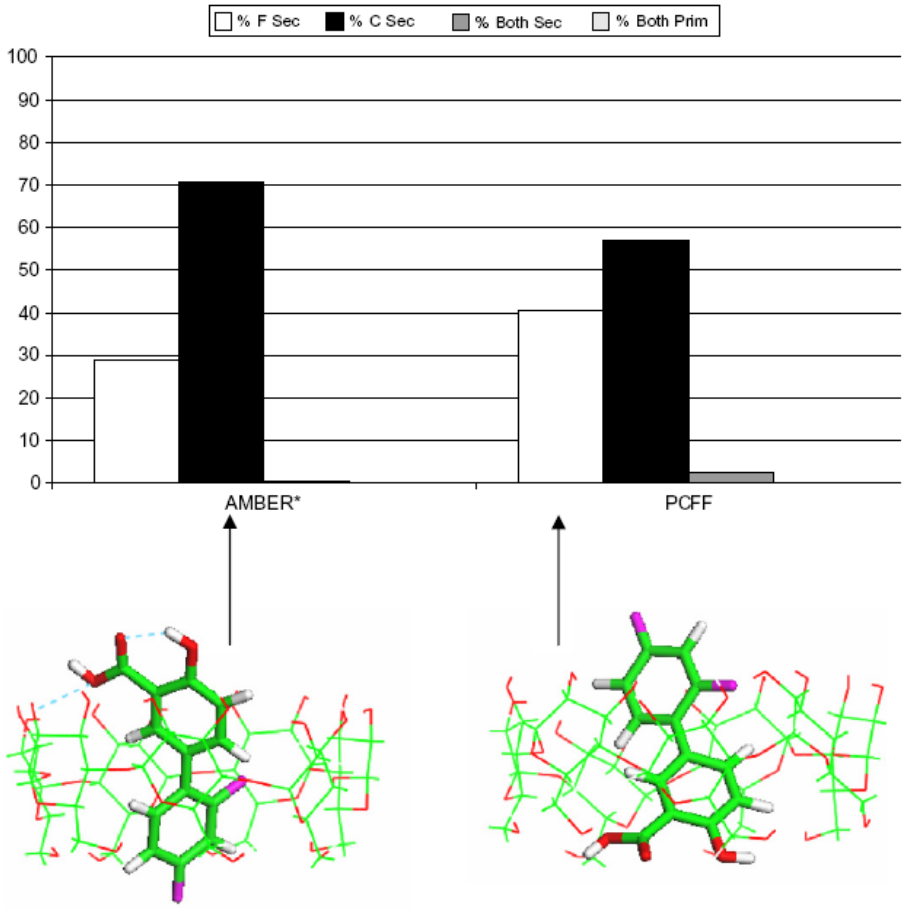

Figure 5.3 *Different orientation of **3** into βCD cavity, expressed as Boltzmann probability percentage at room temperature, obtained with AMBER * and PCFF force fields. The terms Prim and Sec refer to the primary and secondary rim of CD. C is the –COOH group of salicylic moiety and F is the fluorinated ring of compound **3**. Also are indicated the global minima with AMBER * and PCFF force fields.*

5.3.3.2 βCD·3 complex

The geometrical descriptors used for the complexation of **3** have been expressed in terms of the salicylic moiety –COOH (C) and of the fluorinated moiety (–F), directed toward the primary rim (C Prim/F Prim) and toward the secondary rim (C Sec/F Sec).

The inclusion of **3** has shown that the –COOH group is directed to the secondary rim (C Sec) of cyclodextrin with a Boltzmann percentage between 55% and 70% (figure 5.3). The other configurations, with the Boltzmann population in the range of 30-40%, revealed that is the fluorinated ring oriented in this direction (F Sec). The minimum of AMBER* is in the range of the most populated complex conformers. Inversely the minimum of PCFF is collapsed from the less populated region.

The aromatic rings are always included into βCD cavity but only in AMBER* conformations the complexes are stabilized by the presence of hydrogen bonds (table 5.2).

5.3.3.3 βCD·1 complex

The inclusions of **1** into βCD have been described in terms of the guest –COOH group directed toward the primary rim (C Prim) and toward the secondary rim (C Sec) and of the $–NH_2$ of guest's group addressed to the primary rim (N Prim) and to the secondary rim (N Sec).

In figure 5.4 are indicated the sides of **1** molecule entered into the cavity according to the different Boltzmann percentages. With PCFF all orientations of **1** are equally probable, with the exception of **1** parallel to the primary small side (Both Prim). AMBER* force field selected only one conformation, i.e. structures with N Sec orientation. In this case is only the minimum PCFF complex stabilized by means of hydrogen bonds (table 5.2).

In general **1** penetrates completely into the cavity, but the conformers at minimum energy obtained with the diverse approach have different orientations into the cavity indicating that **1**, due the small dimensions, can rotate and adopt several positions with quite similar energies. This extra mobility, in comparison with other drugs, could explains the highest reduction of $\Delta H_{dehydr.}$ at solid state.

The presence of several polar groups attached on the aromatic ring reduces the hydrophobic character of **1** that results more soluble in the bulk solution so to explain the smallest experimental stability constant and the smallest values of binding energy.

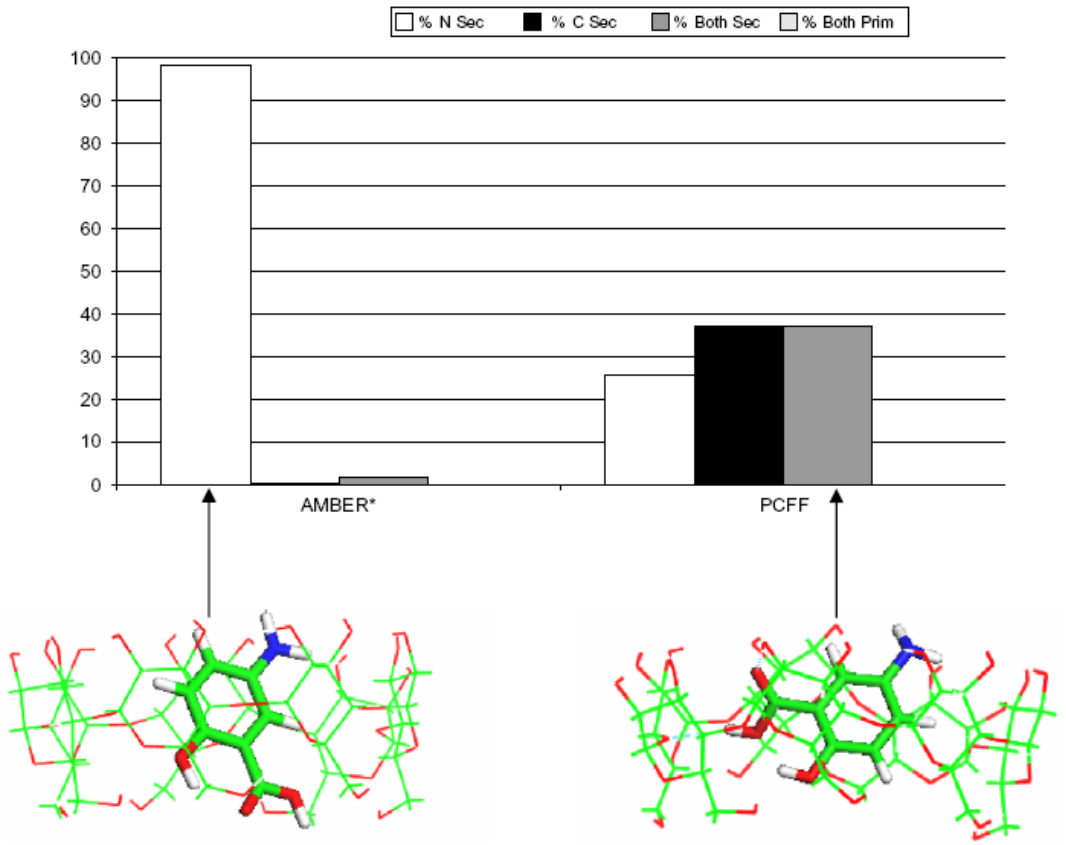

Figure 5.4 *Different orientation of **1** into βCD cavity, expressed as Boltzmann probability percentage at room temperature, obtained with MOLINE, AMBER* and PCFF force fields. The terms Prim and Sec refer to the primary and secondary rim of CD. C is the –COOH group of compound **1** and N is –NH_2 group of **1**. Also are indicated the absolute minimum conformers of **1** obtained with AMBER* and PCFF force fields.*

5.4 Conclusion

The encapsulation process of βCD with 5-aminosalicylic acid, sulfasalazine and diflunisal has been characterized both experimentally and theoretically. Structural information, such as the geometries of the complexes, and thermodynamic data, i.e. the variation of the enthalpy, have been considered to draw a complete picture of the CD-drug interactions. In the solid state **1** goes into the βCD cavity more easily than the larger **2** and **3** molecules as shown by the biggest difference in $\Delta H_{dehydr.}$ percentage from DSC analysis. Conversely, in solution the stability constants of the complex βCD·guest, measured by using UV–vis spectroscopy, show that the strongest interaction appears with the larger molecules **2** and **3** followed then by compound **1**. The geometry of each complex

has been determined theoretically, differentiating the preferred inclusion of functional groups.

The molecular modelling approaches used pointed out that the drugs form stable complexes with βCD as indicated by the negative values in the complexation enthalpy differences, calculated for each optimized structure. The order of interaction is the same with the all different force fields: βCD·**2** > βCD·**3** > βCD·**1**. The results are in good agreement with the experimental data found in the measurement of stability constants.

References

1. *Comprehensive Supramolecular Chemistry Cyclodextrin,* vol3, J. Szejtli, Ed. Elsevier, Oxford, 1996.
2. M. V. Rekharsky, Y. Inoue, *Chem. Rev.,* 98 (1998) 1875-1917.
3. J. Szejtli, *Chem. Rev.,* 98 (1998) 1743-1753.
4. K. Uekama, F. Hirayama, T. Irie, *Chem. Rev.,* 98 (1998) 2045-2076.
5. M. Singh, R. Sharma, U. C. Banerjee, *Biotechnol. Adv.,* 20 (2002) 341-359.
6. V. J. Stella,V.M. Rao, E. A. Zannou, V. Zia, *Adv. Drug Delivery Rev.,* 36 (1999) 3-16.
7. T. Loftsson, D. Duchene, *Int. J. Pharm.,* 329 (2007) 1-11.
8. V. J. Stella, R. A.Rajewski, *Pharm. Res.,* 14 (1997) 556-567.
9. B. Lipkovicz, *Chem. Rev.,* 98 (1998) 1829-1873.
10. C. B. Lebrilla, *Acc. Chem. Res.,* 34 (2001) 653-661.
11. S. Alcaro, C. A. Ventura, D. Paolino, D. Battaglia, F. Ortuso, L. Cattel, G. Puglisi, M. Fresta, *Bioorg. Med. Chem. Lett.,* 12 (2002) 1637-1641.
12. A. Mele, G. Raffaini, F. Ganazzoli, A. Selva, *J. Inclusion Phenom. Macrocyclic Chem.,* 44 (2002) 219-223.
13. M. T. Faucci, F. Melani, P. Mura, *Chem. Phys. Lett.,* 358 (2002) 383-390.
14. M. Oana, A. Tintaru, D. Gavriliu, O. Maior, M. Hillebrand, *J. Phys. Chem. B,* 106 (2002) 257-263.
15. L. M. A.Pinto, M. B. de Jesus, E. de Paula, A. C. S. Lino, J. B. Alderete, H. A. Duarte, Y. Takahata, *J. Mol. Struct.,* 678 (2004) 63-66.
16. R. Consonni, T. Recca, M. A. Dettori, D. Fabbri, G. Delogu, *J. Agric. Food Chem.,* 52 (2004) 1590-1593.
17. S. Chelli, M. Majdoub, M. Jouini, S. Aeiyach, F. Maurel, K. I. Chaneching, P. -C. Lacaze, *J. Phys. Org. Chem.,* 20 (2007) 30-43.
18. N. Zerrouk, J.M. Ginès Dorado, P. Arnaud, C. Chemtob, *Int. J. Pharm.,* 171 (1998) 19-29.
19. M. K. Rotich, M. E. Brown, B. D. Glass, *J. Therm. Anal. Calorim.,* 73 (2003) 687-706.
20. S. Agotonovic-Kustrin, B. D. Glass, M. E. Brown, M. K. Rotich, *J. Therm. Anal. Calorim.,* 77 (2004) 391-402.
21. L. Filip, D. Bogdan, M. Boijta, M. Bogdan, *Physica,* (2001) special issue, http://www.itim-cj.ro/PIM/2003/2001/Volum/PosterMolecula/PM21.doc
22. E. E. Sideris, G. N. Valsami, M. A. Koupparis, P. E. Macheras, *Eur. J. Pharm. Sci.,* 7 (1999) 271-278.
23. M. K. Rotich, M. E. Brown, B. D. Glass, *J. Therm. Anal. Cal.,* 73 (2003) 671-686.
24. P. Mura, F. Maestrelli, M. Cirri, S. Furlanetto, S. Pinzauti, *J. Therm. Anal. Cal.*, 73 (2003) 635-646.

25. J. Orgoványi, L. Pöppl, K.H. Ottá, G.A. Lovas, *J. Therm. Anal. Cal.,* 81 (2005) 261-266.
26. H. A. Benesi, J. H. Hildebrand, *J. Am. Chem. Soc.,* 71 (1949) 2703-2707.
27. Y.L. Loukas, *J. Pharm. Biomed. Anal.,* 16 (1997) 275-280.
28. S. Alcaro, F. Gasparrini, O. Incani, S. Mecucci, D. Misiti, M. Pierini, C. Villani, *J. Comput. Chem.,* 21 (2000) 515-530.
29. D. Q. McDonald, W. C. Still, *Tetrahedron Lett.,* 33 (1992) 7743-7746.
30. F. Mohamadi, N. G. J. Richards, W. C. Guida, R. Liskamp, M. Lipton, C. Caufield, G. Chang, T. Hendrickson, W. C. Still, *J. Comput. Chem.,* 11 (1990) 440-467.
31. H. Sun, S. J. Mumby, J. R. Maple, A. T. Hagler, *J. Am. Chem. Soc.,* 116 (1994) 2978-2987.
32. Discover and InsightII User Guide, Version 400p+, Accelrys: San Diego, CA, 1999.
33. A. T. Hagler, E. Huler, E. Lifson, *J. Am. Chem. Soc.,* 96 (1974) 5319-5327.
34. J. A. Hamilton, M. N. Sabesan, *Carbohydr. Res.,* 102 (1982) 31-46.
35. A.C.S. Lino, Y. Takahata, C. Jaime, *J. Mol. Struct. (Theochem),* 594 (2002) 207-213.

SIXTH CHAPTER

MODELLING OF DRUG RELEASE FROM POLYMER CYCLODEXTRIN SYSTEM

6.1 Introduction

The primary purpose of drug delivery systems is to deliver the necessary amount of drug to the targeted site both efficiently and precisely [1]. The desirable attributes of drug carriers in drug delivery system are the multi-functional properties such as controlled-release, targeting, and absorption enhancing abilities [2-4].

In recent years, controller drug delivery formulations have become much more sophisticated, with the ability to do more than simply extend the effective release period for a particular drug, such as respond to changes in the biological environment and deliver, or cease to deliver, drugs based on these changes.

From the safety viewpoint, bio-adaptability is an important necessity, and high quality, cost performance, etc. are required for drug carriers. Cyclodextrins (CDs) [5-8] have such characteristics. They are a group of structurally related cyclic oligosaccharides that are formed by enzymatic degradation of starch. CDs have a hydrophilic external surface and a hydrophobic internal cavity that enables the complexation of lipophilic 'guest' drug molecules.

CDs are widely used in the pharmaceutical field because they are fairly bioadaptable and hardly absorbable from gastrointestinal tracts, they interact with specific components of biomembrane such as cholesterol and lipids, their macrocyclic ring survives small intestine, but they are biodegradable in colon and large intestine, and more functional CD derivatives are available to modify the physicochemical and inclusion properties of the host molecules [1,9,10]. CDs enhance the solubility, the stability and the bioavailability of drug molecules, also they improve the selective transfer and/or reduction of side effects. The principal advantages of natural CDs as drug carriers are: a well-defined chemical structure, the availability of CD's different cavity sizes, low toxicity and low pharmacological activity and, finally, the protection of the included drug from biodegradation [11-14].

The incorporation of cyclodextrins into polymeric drug delivery systems can influence the mechanisms by which drug is released. The incorporation of cyclodextrins into polymeric matrices overcome the well know problem of "burst" release [14]. The aim of this work has been the study of the release of two drug molecules used in the treatment of Crohn's disease, one inflammatory bowel disease (IBD), from a β-cyclodextrin (βCD) encapsulated on the surface of a polymeric membrane of PEEK-WC by using molecular dynamics (MD)

simulations. The incorporation of the βCD in the PEEK-WC was thought to relate the versatility of the cyclodextrins with the protection furnished by a polymeric core. The reason is that the glycosidic bonds of CDs are cleaved in strong acids. To avoid the breaking of the cyclodextrins they were inserted in a polymeric matrix of a modified polyetheretherketone (PEEK-WC) (scheme 6.1c), PEEK-WC, a polymer with high chemical stability and low affinity for plasmatic proteins, [15-16], already used as implant material. In this way the complex βCD·drug should reach the colon protected.

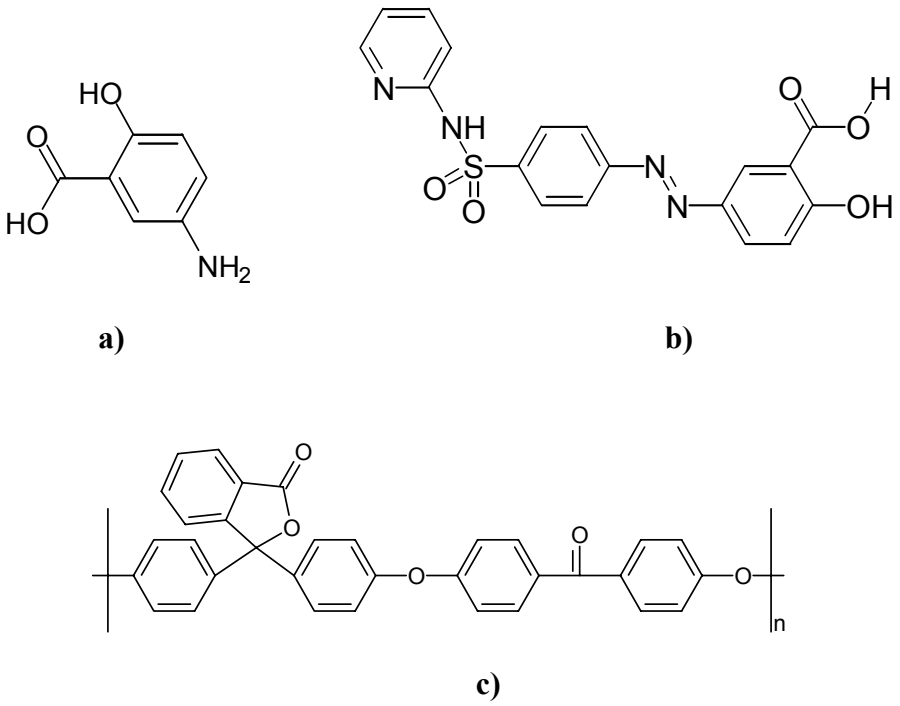

Scheme 6.1*: Structures of drugs a) 5-aminosalicylic acid (5asa), b) sulfasalazine (SF) and c) PEEK-WC.*

The drugs analysed, shown in Scheme 6.1**,** are: 5-aminosalicylic acid (5asa), an anti-inflammatory drug light and oxygen sensitive and sulfasalazine (SF), a prodrug of 5asa: 5asa is linked with an azo bond to an inert carrier (sulfapiridine) and it is activated by colonic bacterial azoreductase. The complexation of these drugs with βCD has already been proved by experimental methods [17-20] and investigated in a combined theoretical and experimental work [21].

The calculations can provide information on the driving forces responsible for freeing processes. The behaviour of the complexes pure and immobilised in polymeric membrane has been analysed when they are in contact of a water solution.

6.2 Computational Details

The computations were performed by using the INSIGHTII (400P+) molecular modelling package of Accelrys [22] using the PCFF force field (ff) [23]. The accuracy of the PCFF force field for the βCD has been validated in a previous paper [21]. Then all simulations of βCD complexes supported on polymer were carried out with PCFF force field due to the versatility of such force field in describing well polymer properties.

6.2.1 Preparation of βCD·drug models

The initial structures of the βCD, of 5asa and SF molecules (see scheme 6.1) were built and, as described in a previous paper [21], a complete characterization of the interactions between the CD and the molecules has been performed. Structural information, such as the geometries of the complexes, and thermodynamic data, i.e. the variation of the enthalpy, have been considered.

6.2.2 Preparation of polymer-βCD·drug models

The polymeric matrices containing βCD on the surface have been prepared using the following procedure:
1) In a first stage the repeat unit of PEEK-WC (poly (oxap-phenylene-3,3-phtalido-p-phenylenxoxa-p-phenylenexoxi-p-phenylene) was built.
2) Then chains containing the number of repeat units were made using the Polymerizer module of the Accelrys software. The chains were grown as for an atactic polymer and then subjected to a static structure optimisation via the steepest descent energy minimisation until the maximum energy gradient at any atom was below 10 kJ/mole nm.
3) An initial amorphous packing of PEEK-WC model with chain segments was successively constructed. For this purpose the "self-avoiding" random walk method of Theodorou and Suter [24,25], which implements a modification of the rotational isomeric state (RIS) was employed.
In order to minimize chain end effects, each simulation box contained only one minimized polymer sequence of 51 monomer units (i.e. 3000 atoms) rather than several confined to the same volume, which would lead to increased density of chain ends. On the same line of thought, the use of single-chain polymers representing bulk amorphous systems is common and has been proven to be quite accurate in replicating the behavior of experimental polymeric systems [24, 26-28]. The polymer chains were grown at 303 K under periodic boundary conditions effective in only two dimensions (x and y in this case). In the third dimension penalty surface potentials force the non-periodic (z) coordinates of the constituent atoms in a layer of a thickness that results from the other two box-lengths and the

expected/intended density of the system. The general shape of such a surface penalty potential term U_z is:

$$U_z = \mathrm{K}_z \sum_i \frac{1}{z_i^m} + \frac{1}{(z_i + z_{\max})^m} \qquad (6.1)$$

with z_i and z_{max} are the z-coordinate of the i^{th} atom and the length of the basic volume element in *z*-direction, respectively. K_z and m are constants. The summation runs over all atoms of the system. The shape of this potential term leads to prohibitively high energy penalties for atoms whose z-coordinates come close to the minimum (z = 0) or maximum (z = z_{max}) z-coordinate of the basic volume element. K_z is usually chosen by trial and error in a way that there is no atom with a z-coordinate closer than about 1 Å to z = 0 or z = z_{max}.

4) The initial polymer packing models were subsequently equilibrated. Sequences of static structure optimizations and MD simulations combined with force field parameter scaling were utilized for this purpose. Details of these procedures can be found in [29-31]. In this stage the periodic boundary conditions are again effective only in two dimensions utilizing the already mentioned penalty surface potentials. In the beginning, the initial packing models were subjected to sequences of static structure optimizations and NVT-MD runs combined with different procedures of force field scaling. After this stage, the experimental density was reached by increasing the pressure with several cycles of NPT (constant particle number, temperature and pressure) runs at pressures of thousands of bars. Subsequently, simulated annealing with temperatures up to 1000 K was also necessary to equilibrate the compressed systems.

The conformations with minimum energy of complexes βCD·drugs [21] discussed in the previous chapter, were added at the surface of the box of PEEK-WC. Two βCD·drug assemblies were included into the simulation box when the polymer was at a very low density, to each side of the box, due to the 2D periodic boundary conditions. CD·drug assemblies were included into the simulation box when the polymer was at a very low density. To avoid distortions of all the systems from the minimum conformation and to avoid the release of drug molecules from βCD, several restraints were applied. In particular, a force of 10^5 N along the *z* direction of the box was applied, and the dihedral angles of the torus cavity and the hydroxyl groups of βCD, the twisting angles of both the drugs, and the distances among guests and host were fixed. As the complexes were incorporated into the polymer the box was cut so as to increase the density of the polymer-complexes system. Then the packing model was then subjected to NVT-MD runs to equilibrate the system. This last procedure was repeated several times to finally reach a density of about 1.23 g/cm^3, that is the density of the pure PEEK-WC polymer. In this case we considered that the contribution of the CD was minimal in comparison to the molecular weight of the polymer chain.

To study the interactions at the interface, the polymeric models were combined with a cubic water box with side a = 30 $Å^3$ and containing 700 water molecules, employing periodic boundary conditions. The pure liquid models were also constructed using the amorphous cell module of the Accelrys software using the same procedure as described before for the polymer model: a two-dimensional periodic basic volume element was filled with the solvent molecules. The molecules were inserted in random sequence at random positions and with random orientations. The subsequent equilibration was achieved by similar procedures as for the polymers.

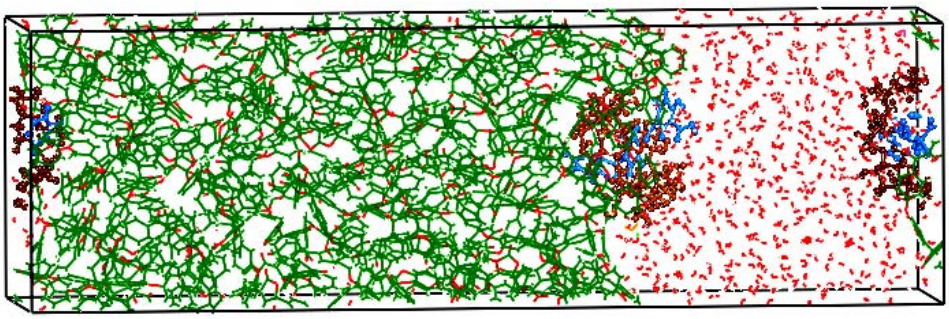

***Figure 6.1** βCD-SF included on the PEEK-WC surface model in water.*

After the complete refinement of each individual box the polymer and the water boxes were layered onto each other. Due to the influence of the applied penalty surface potentials, immediately after the surface formation there is a small empty slit between the polymer and the watery solution. To resolve this problem 45 ps of MD simulation were performed at 300 K with NVT ensembles at a very low time step of 0.1 fs to allow for a gentle equilibration of polymer atoms and solvent molecules into these slits and towards the real system density. The final dimensions of models were 30 x 30 x 96 $Å^3$. In figure 6.1 is shown the structure of βCD·drug(SF) included on the PEEK-WC surface model.
Through the dynamics, the thermostat described by Andersen et al. [32] and the Berendsen [33] pressure control method were applied.

6.2.3 MD of polymer-βCD·drug models

The structures prepared as described previously were used for MD simulations in order to study the behavior of drug molecules in contact with the watery solution. The MD simulation was performed for 1,5 ns on the polymer-βCD-5asa and the polymer-βCD-SF system. The trajectories have been saved every 500 fs.

Concerning the diffusivity behavior, the diffusion coefficients were calculated from the slope of the plots of the mean square displacements of gases versus time using the Einstein relation:

$$D = \frac{1}{6N_\alpha} \lim_{t\to\infty} \left\langle \left| \mathbf{r}_i(t) - \mathbf{r}_i(0) \right|^2 \right\rangle \qquad (6.2)$$

where N_α is the number of diffusing molecules of type α, $\mathbf{r}_i(0)$ and $\mathbf{r}_i(t)$ are the initial and final positions of molecules (mass centres of particle *i*) over the time interval *t*, and $\left\langle \left| \mathbf{r}_i(t) - \mathbf{r}_i(0) \right|^2 \right\rangle$ is the mean square displacement (MSD) averaged over the possible ensemble.

6.3 Results and Discussion

The goal of this work was the analysis of the mechanisms responsible of the release of two anti-inflammatory drugs from the cyclodextrins included in polymers. The idea was to relate the host-guest capacity of complexation of the cyclodextrins to the protection furnished by a polymeric material/membrane.

6.3.1 Stability of the polymer-βCD·drug complexes

In order to explain the results obtained with the cyclodextrins included in the matrix of PEEK-WC we investigated qualitatively the interactions of drugs with CD and the effect of inclusion.

At a starting stage of the simulations we have fixed the CD-guest obtained minima and put on the surface of the membrane. A check of the possible deformations of the inclusion in the matrix of PEEK-WC has been performed. We observed (not shown in the paper) that the cavity remains almost unchanged in the optimised complex.

The stability of the complexes was considered valuing the binding energy. Generally, the computational protocol that best fit the experimental stability constant trend for simple host-guest complexes is evaluated based on the correlation with the computed complexation enthalpy differences [34-37] calculated for absolute minima (table 6.1). The binding energy of complexes has been calculated as follows:

$$\Delta H_{bin} = H_{\text{PEEK-WC}/\beta\text{CD·drugs}} - \left(\sum H_{\beta CD} + \sum H_{drugs} + H_{\text{PEEK-WC}} \right)_{frozenincomplex} \qquad (6.3)$$

where ΔH_{bin} is the difference between the energy of the optimized complex and the sum of the energies of the isolated molecules extracted from the complex in the same conformation.

An introductory statement is needed. Due to the impossibility to search the absolute minimum for the polymer, given the nature of the material, we are unable to explore all conformational states. Moreover, their contribution to potential energy is only due to the bonding terms because of the large mass which cancels itself in the net contribution.

Complex	$\Delta H_{binding}$
βCD·5asa*	-26.79
PEEK-WC/βCD·5asa	17,78
βCD·SF*	-33.05
PEEK-WC/βCD·SF	-6,04

Table 6.1 *Complexation enthalpies of the complexes βCD·drug taken from [21] and PEEK-WC/βCD·drug. (Energy values are reported in kcal/mol).*

The negative values upon complexation indicate that the drugs form a stable complex with βCD (under conditions such as those considered here).
The qualitative results show that the affinity of the drugs put into the CD on the polymeric structure is in the order of PEEK-WC/βCD·SF > PEEK-WC/βCD·5asa.
The only comparison that could be done is about the order of stability. The energies of the single βCD·drugs are in the same trend showing the same order of interaction, βCD·SF > βCD·5asa.
In the case of the system polymer-βCD·SF, the variation of interaction energy indicate that the SF remains included into CD cavity when the cyclodextrin is supported by polymeric matrix with the diazo bridge and the 5asa moiety outside βCD cavity. The βCD·5asa complex alone shows a bigger stability in comparison to the same complex put on the surface of the polymer offering the suggestion of possible release of 5asa when put on a polymer. The cyclodextrin inserted in PEEK-WC has its primary hydroxyls in contact with the polymeric wall and more interacting with the guest. This should imply a destabilizing effect between host and guest, and a variation in the release of drugs.

6.3.2 MD analysis of polymer-βCD·drug complexes

The simplest way of studying diffusion of individual molecules is to inspect their paths through space. A procedure often chosen in the literature is to analyze the mean squared displacement MSD(t) averaged over all penetrant molecules of a given kind. In order to get a more detailed insight in different modes of penetrant molecules, it can also make sense to investigate displacement $\boldsymbol{R(t) = \sqrt{|r(t) - r(0)|}}$ and MSD(t) for individual molecules [38].

The release of drug on MD simulations was valued considering the distance between the centroid of geometry of the βCD and 5asa and that of the βCD and SF, respectively. The MSD of the single drugs and of the βCD were analysed.

The system PEEK-WC/βCD·5asa shows the release at about 1 ns of simulation. In figure 6.3 two displacements referring to two molecules of 5asa are indicated due to the 2D periodic boundary conditions. When the 5asa leaves the βCD there is a deformation of CD cavity.

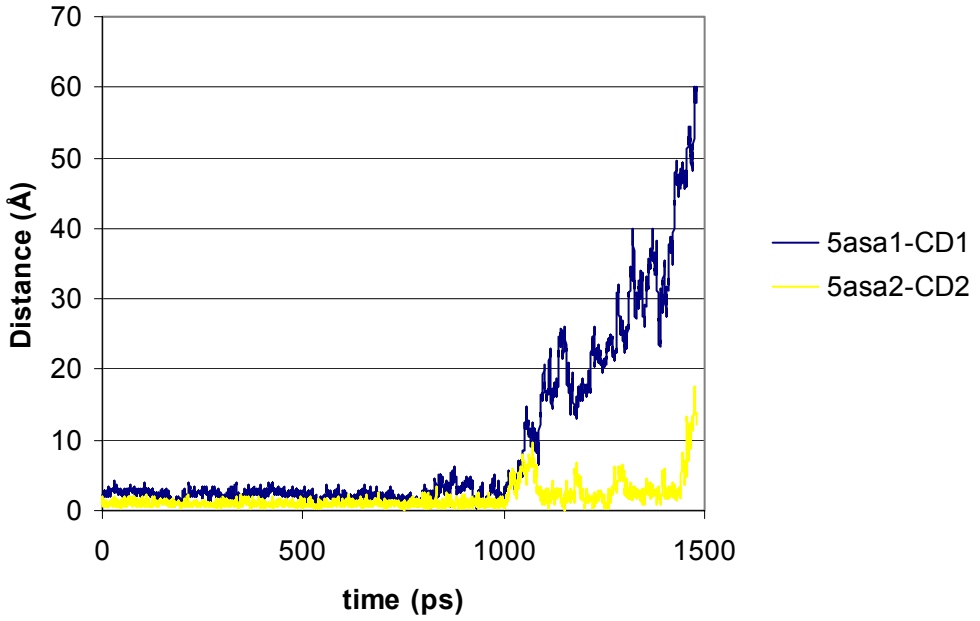

Figure 6.3 *Distance host-guest as a function of the simulation time measured on centroid of geometry between PEEK-WC/βCD and two 5asa from both side of the model, due to the 2D periodic boundary conditions.*

For the PEEK-WC/βCD·SF system instead was not observed any release of drug after 1,5 ns (figure 6.4).

The release of drug can also be seen from the MSD averaged over all atoms of the reference system. In our case we have analysed the MSD averaging on drug, βCD and the PEEK-WC atoms, respectively (figure 6.5). For PEEK-WC/βCD·5asa it was observed that the mobility of the drugs of both side of the polymeric box complex is bigger than that of the CD (not shown in figures for clearness) and of the polymer. The minimum mobility of the polymer is due to the thermal motion of the polymeric chain because the PEEK-WC is a glassy stiff material. The MSD of the βCD is of the same size order of the polymeric matrix MSD, this indicates that the cyclodextrins are not released from the surface and that their anchorage on matrix surface is good nevertheless it is not a chemical bond. It should be noted that it is not possible to say that no release is obtainable

in absolute terms, because of the limited simulation time used. Nevertheless, it is evident the difference in behaviour with 5asa because their departure from the cavity is reached immediately.

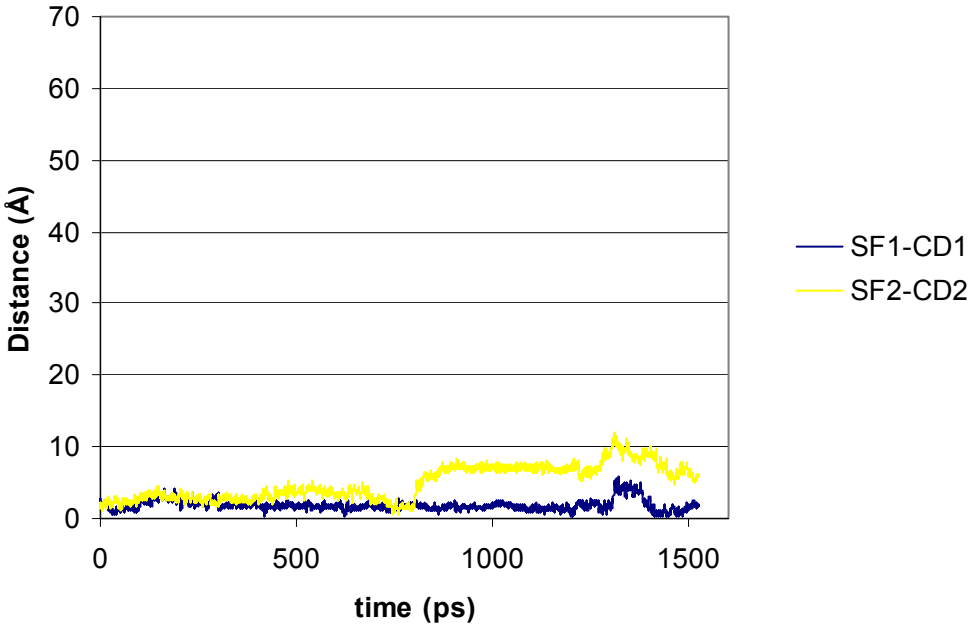

Figure 6.4 *Distance host-guest as a function of the simulation time measured on centroid of geometry between PEEK-WC/βCD and two SF from both side of the model, due to the 2D periodic boundary conditions.*

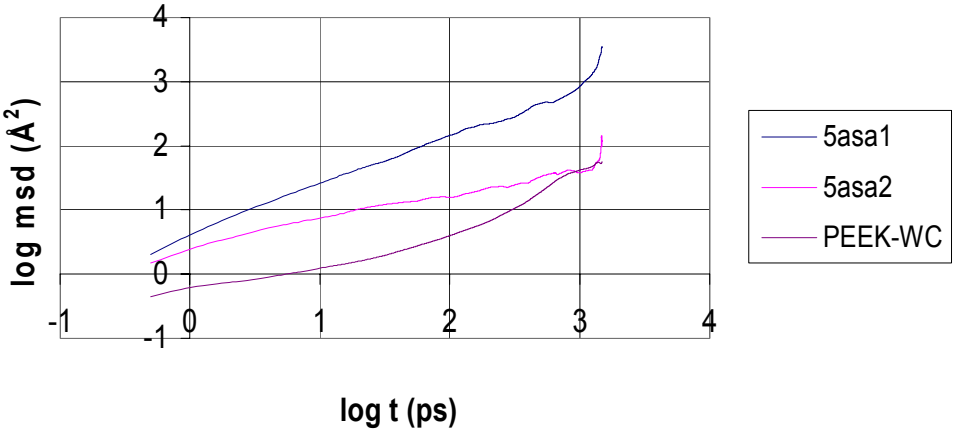

Figure 6.5 *Mean-square displacements of neutral 5asa molecules and of polymer chain.*

Figures 6.6 and 6.7 show the normalized density profiles of 5asa and SF, at the beginning and at the end of the simulations.

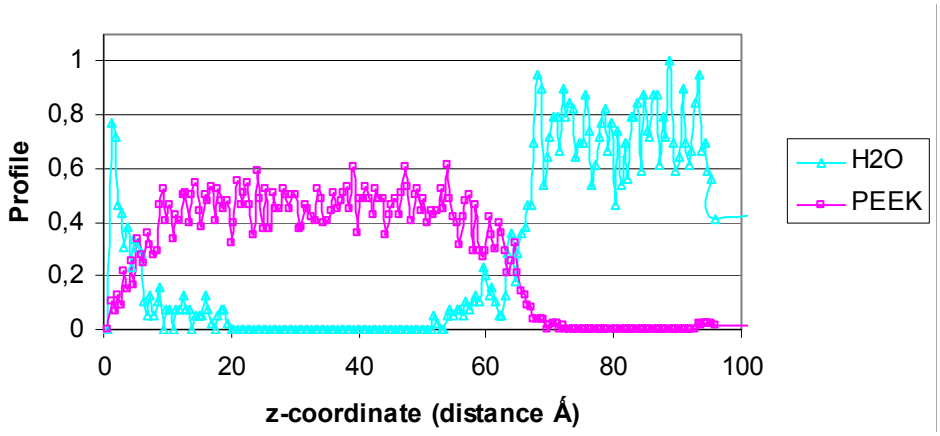

a)

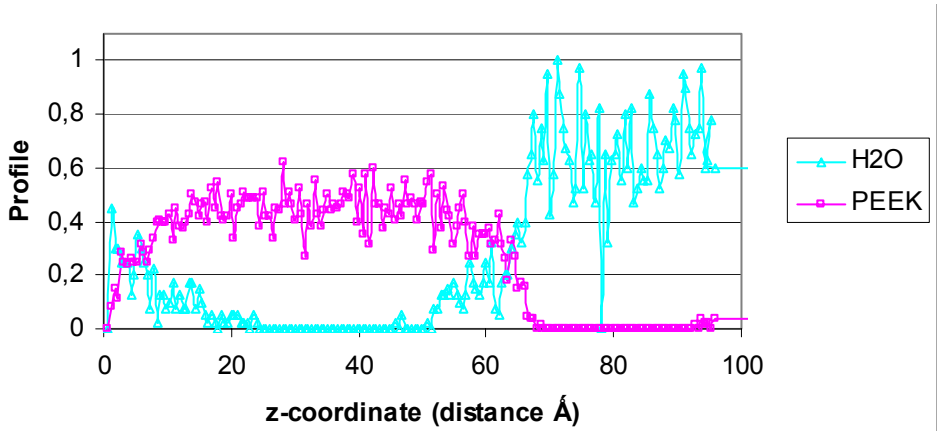

b)

Figure 6.6 *Density profiles of 5asa a) at the beginning of the simulation and b) at the end of the simulation.*

In all shown normalized density profiles the maximum density values of each participant is set to one for sake of a better compatibility. At the beginning the boundary between polymer and water is artificially high.
During the simulation time few water molecules enter in the polymer surface but without showing a swelling behaviour that has not been observed experimentally. The concentration of water inside the polymer seem to be the same (apart some statistics) and is not dependent on the system studied.

The displacement of the water molecules during the exit of the drug was analysed in details to get insight into the mechanism of the release of 5asa from the cavity (figure 6.8). It was observed the entry of one water molecule into the βCD cavity between 1070 and 1080 ps of simulation time and immediately after the exit of drug from the complex. Later on also the water molecule leaves the βCD. The water molecule breaks the hydrogen bonds that form among βCD and 5asa destabilizing the interactions between host and guest.

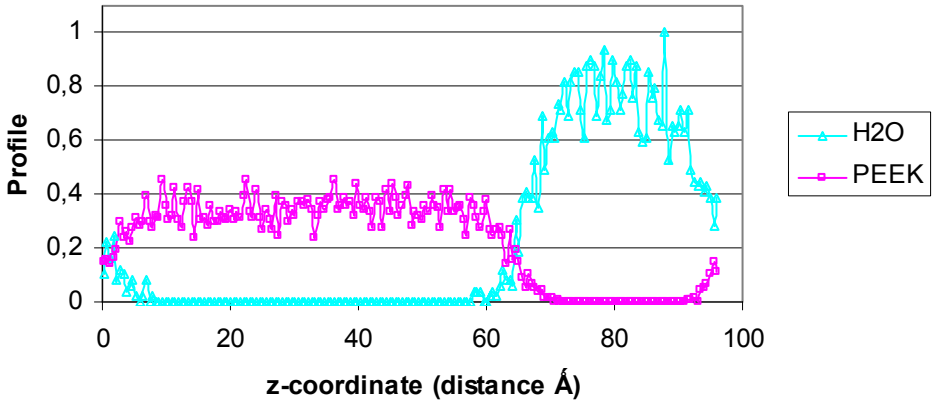

a)

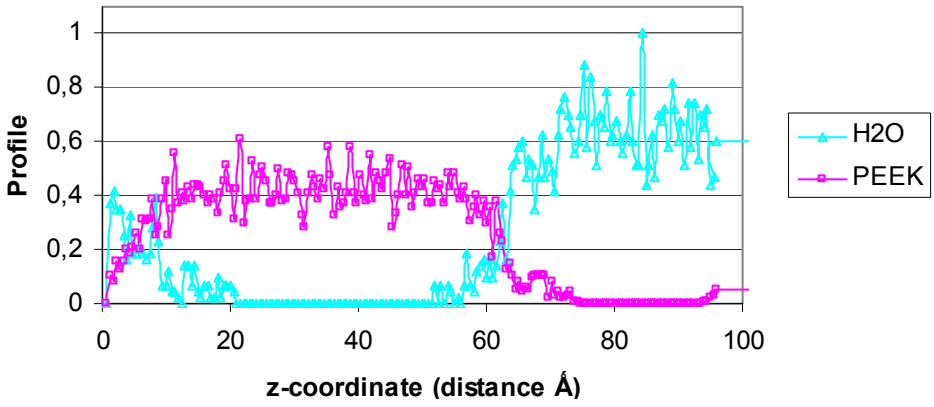

b)

Figure 6.7 *Density profiles of SF a) at the beginning of the simulation and b) at the end of the simulation.*

6.4 Conclusions

The behavior of the complexes of βCD and of 5-aminosalicylic acid (5asa) and sulfasalazine (SF), a prodrug of 5asa, immobilized in polymeric membrane, a biocompatible modified polyetheretherketone (PEEK-WC), was investigated theoretically simulating the behavior of both systems when they are in contact with a water solution. The molecular dynamics on the polymeric system formed by adding on the surface of PEEK-WC the βCD·drug complex showed the release of 5asa drug in a water solution and the possibility to delivery the drug included.

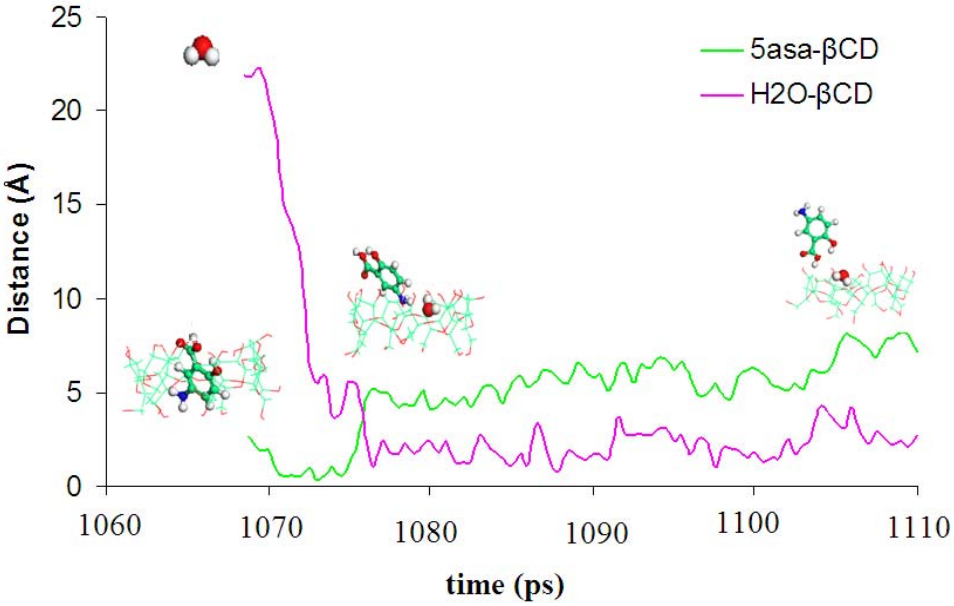

Figure 6.8 *Release of 5asa from PEEK-WC/βCD system by one water molecule measured as the distance between the 5asa and the water molecule from the βCD cavity in the simulation time.*

References

1. K. Uekama, F. Hirayama, T. Irie, *Chem. Rev,.* 98 (1998) 2045-2076.
2. K. Uekama, F. Hirayama, H. Arima, *J. Incl. Phen. and Macro. Chem.,* 56 (2006) 3-8.
3. F. Hirayama, K. Uekama, *Adv. Drug Deliv. Rev.* 36 (1999) 125-141.
4. K. Uekama, *Chem. Pharm. Bull.,* 52 (2004) 900-915.
5. A. Villiers, *Compt. Rend. Acad. Sci.,* 112 (1891) 536-538.
6. F. Z. Schardinger, *Unters. Nahr. U. Genussm.,* 6 (1903) 865-880.
7. M. V. Rekharsky, Y. Inoue, *Chem. Rev.*, 98 (1998) 1875-1917.
8. J. Szetjli, *Chem. Rev.,* 98 (1998) 1743-1753.
9. T. Irie, K. Uekama, *J. Pharm. Sci.,* 86 (1997) 147-162.
10. M.E. Davis, M.E. Brewster, *Nat. Rev. Drug Disc.,* 3 (2004) 1023-1035.
11. M. Singh, R. Sharma, U. C. Banerjee, *Biotechnology Advances*, 20, (2002), 341-359.
12. T. Loftsson, *Nordic Industrial Fund*, (1998), 1-39.
13. V. J. Stella, R. A. Rajewski, *Pharm. Res.,* 14 (1997) 556-567.
14. D. C. Bibby, N. M. Davies, I. G. Tucker, *Int. J. Pharm.,* 198 (2000) 1-11.
15. L. De Bartolo, A. Gugliuzza, S. Morelli, B. Cirillo, A. Gordano, E. Drioli, *Mat. Sci. For.*, 5 (2005) 257-268.
16. A. Katzer, H. Marquardt, J. Westendorf, J. V. Wening, G. Van Foester, *Biomaterials,* 23, (2002), 1749-1759.
17. N. Zerrouk, J.M. Ginès Dorado, P. Arnaud, C. Chemtob, *Int. J. Pharm.,* 171 (1998) 19-29.
18. M. K. Rotich, M. E. Brown, B. D. Glass, *J. Therm. Anal. Calorim.,* 73 (2003) 687-706.
19. S. Agotonovic-Kustrin, B. D. Glass, M. E. Brown, M. K. Rotich, *J. Therm. Anal. Calorim.,* 77 (2004) 391-402.
20. L. Filip, D. Bogdan, M. Boijta, M. Bogdan, *Physica*, special issue, (2001).
21. P. Cairo, F. Ortuso, S.Alcaro, E. Fontananova, E. Tocci, E. Drioli, *Chem. Phys. Lett.,* 454 (2008) 374-381.
22. InsightII 4.0.0.P+, Polymerizer, Discover, Amorphous Cell, Builder Modules 2001, Accelrys Inc., San Diego, CA, USA, 2001.
23. H. Sun, S. J. Mumby, J. R. Maple, A. T. Hagler, *J. Am. Chem. Soc.,* 116 (1994) 2978-2987.
24. R. H. Gee, L. E. Fried, R. C. Cook, *Macromolecules,* 34 (2001) 3050-3059.
25. D. Hofmann, M. Heuchel, Yu. Yampolskii, V. Khotimskii, V. Shantarovich, *Macromolecules*, 35 (2002) 2129-2140.
26. D. Hofmann, M. Entrialgo-Castano, A. Lerbret, M. Heuchel, Y. Yampolskii, *Macromolecules* 36 (2003) 8528-8538.
27. E. Tocci, D. Hofmann, D. Paul, N. Russo, E. Drioli, *Polymer,* 42 (2001) 521-533.

28. E. Tocci, P. Pullumbi, *Mol. Simul*., 32 (2006) 145-154.
29. L. Fritz, D. Hofmann, *Polymer,* 38(1997) 1035-1045.
30. D. Hofmann, L. Fritz, D. Paul, *J. Memb. Sci.,* 144 (1998) 145-159.
31. L. Fritz D. Hofmann, *Polymer,* 39 (1998) 2531-2536.
32. T. A. Andrea, W. C. Swope, H. C. Andersen, *J. Chem. Phys.,* 79 (1983) 4576-4584.
33. H. J. C. Berendsen, J. P. M. Potsma, W. F. Gunsteren, A. Di Nola, J. R. Haak, J. Chem. Phys. 18 (1984) 3684-3690.
34. S. Alcaro, C. A. Ventura, D. Paolino, D. Battaglia, F. Ortuso, L. Cattel, G. Puglisi, M. Fresta, *Bioorg. Med. Chem. Lett.,* 12 (2002) 1637-1641.
35. M. Oana, A. Tintaru, D. Gavriliu, O. Maior, M. Hillebrand, *J. Phys. Chem. B,* 106 (2002) 257-263.
36. L. M. A. Pinto, M. B. de Jesus, E. de Paula, A. C. S. Lino, J. B. Alderete, H. A. Duarte, Y. Takahata, *J. Mol. Struct.,* 678 (2004) 63-66.
37. A.C.S. Lino, Y. Takahata, C. Jaime, *J. Mol. Struct. (Theochem),* 594 (2002) 207-213.
38. D. Hofmann, J. Ulbrich, D. Fritsch, D. Paul, *Polymer,* 27 (1996) 4773-4785.

SEVENTH CHAPTER

MOLECULAR RECOGNITION OF NARINGIN BY POLYMERIC MEMBRANES ENTRAPPING β-CYCLODEXTRIN: A THEORETICAL STUDY

7.1 Introduction

The recognition properties of O-octyloxycarbonyl-β-cyclodextrin (OβCD) (figure 7.1) immobilized on the surface of an amorphous polyetheretherketone known as PEEK-WC membranes towards naringin, a flavanone responsible for the main bitterness of the grapefruits, has been investigated by using Docking, Molecular Mechanics (MM) and Molecular Dynamics (MD) methods.

Excessive bitter taste reduces the quality of commercial fruit juices. For this reason the removal of the bitter components is an important industrial goal. Several experimental techniques have been used to decrease the concentration of bitter components in citrus juice including also βCD polymers [1-3]. Modelling methodologies have been applied for a better understanding of the inclusion process so as to characterize the interactions between the naringin and the OβCD from a structural and energetic point of view.

The thermodynamic and structural basis for the OβCD-naringin inclusion complex has been described. Docking and MM methods have characterized the encapsulation process defining the molecular moieties responsible for the interactions and the thermal behaviour of the complexes. The molecular modelling study has been carried out by using the MOLINE docking approach [4] followed by energy minimisation of the generated configurations by using PCFF force field [5].

A 1.3 ns of MD simulation has shown the encapsulation of naringin into OβCD cavity from a water solution.

The molecules analyzed, shown in scheme 7.1**,** are: naringin, O-octyloxycarbonyl-β-cyclodextrin and the monomer of PEEK-WC.

7.2 Method of computation

The theoretical study has been carried out using a three-step approach. In the first step, conformational properties of flavonone has been evaluated by means of the Monte Carlo (MC) search applying 5000 iterations to all rotatable bonds available in the guest molecule. All unique conformations have been energy minimized by using the AMBER* force field [6] with all-atoms notation. Water solvent effects have been taken into account by means of the GB/SA (generalized

Born/surface area) implicit solvation model as implemented in the MacroModel package [7]. The conformations have been selected with a Boltzmann probability higher than 0.01%.

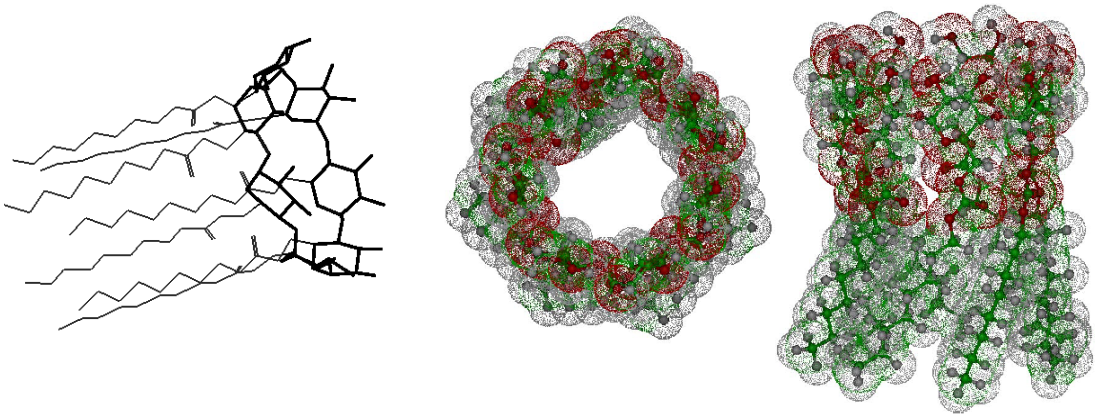

Figure 7.1 *Structure of O-octyloxycarbonyl-β-cyclodextrin (OβCD).*

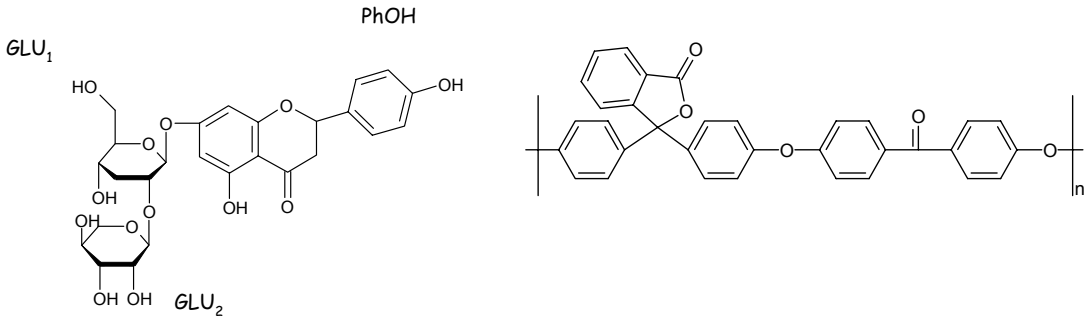

Scheme 7.1 ***N****aringin structure and repeat unit of poly (oxa-p-phenylene-3,3-phtalido-p-phenylene-oxa-p-phenylenexoxi-p-phenylene) PEEK-WC. In naringin labels of the glucose units and phenol moiety have been added.*

In the second step the molecular recognition of all conformations of naringin, within 5 kcal/mol above the global minimum energy structure, has been investigated with respect to the OβCD using the software MOLINE [8]. The energy contributions have been computed by using the AMBER* force field. At this stage the water environment has been mimicked by using a dielectric constant equal to 80.

For each conformer several configurations have been generated. The structures have been consequentially clustered and optimized reporting 79 configurations for the complex.

In the third step, the minimum energy complexes, within 3 kcal/mol above the global minimum, have been submitted to the full energy refinement. For this energy optimization the PCFF force field [9] has been used and the calculations have been performed using the INSIGHTII/Discover software of Accelrys [10]

with the dielectric constant set to 80. Conjugate gradient algorithm with a termination gradient of 10^{-2} kcal/mol has been selected for PCFF optimizations.

All conformations, with an RMS (root mean square of distance) lower than 0.25 Å, computed after the energy minimization, have been considered as duplicate structures and, consequently, removed from the configuration ensembles. Thus the optimisation has produced 63 configurations, all in the energetic range of ΔE=15 kcal/mol.

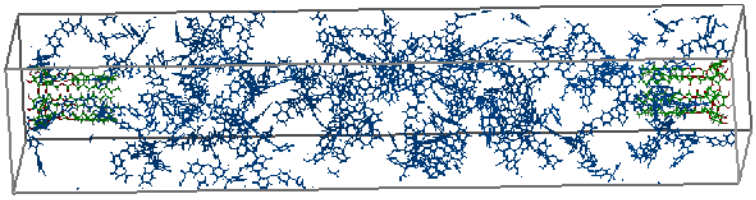

Figure 7.2 *OβCD included on the PEEK-WC surface model at the initial stage of the equilibration procedure.*

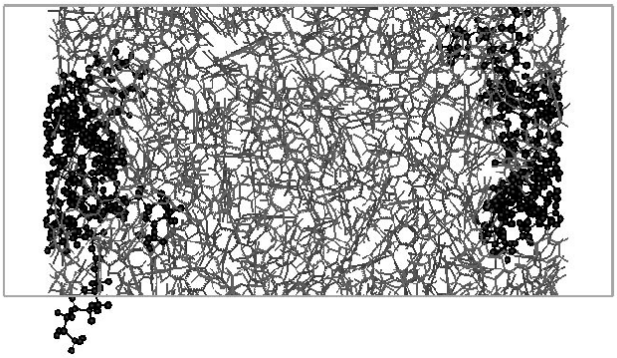

Figure 7.3 *OβCD included on the PEEK-WC surface model.*

The procedure for the preparation of the polymeric matrices containing OβCD on the surface is similar to that described in the previous chapter. Here we will describe it briefly:

1) In a first stage the repeat unit of PEEK-WC (poly (oxap-phenylene-3,3-phtalido-p-phenylenxoxa-p-phenylenexoxi-p-phenylene) was built.

2) Then chains containing the number of repeat units were made using the Polymerizer module of the Accelrys software. The chains were grown as for an atactic polymer and then subjected to a static structure optimization.

3) An initial amorphous packing of PEEK-WC model with chain segments was successively constructed. For this purpose the "self-avoiding" random walk method of Theodorou and Suter [11,12] , which implements a modification of the rotational isomeric state (RIS) was employed. The initial packing model was built at low density (see figure 7.2). Solvent molecules have been included in the Amorphous Cell and low initial density of 2D packed cells. The scaling of

conformation energy terms and nonbonded interactions in the force field have been performed using NVT-MD. Then the equilibration procedure was applied using surface potential at, NVT at T= 750 K, NVT at T= 550 K and NVT at T= 303 K, respectively. The final length of the polymer box was of about 31 Å (figure 7.3). Total number of atoms is of 7738.

7.3 Results and discussion

Calculation have been performed in order to obtain global information about the geometry of the host-guest complexes and to find the intermolecular interactions between cyclodextrins and naringin. The evaluation of the OβCD recognition has been performed taking into account CD flexibility and induced fit phenomena by means of full minimizations carried out using PCFF. The principal conformations of the inclusion complexes are shown in figure 7.4.

The binding energy of complexes has been calculated as follows:

$$\Delta H_{bin} = \mathrm{H}_{\mathrm{G\bullet CD}} + \left(\mathrm{H}_{\mathrm{G}} + \mathrm{H}_{\mathrm{CD}}\right)_{frozenincomplex} \qquad (7.1)$$

where G is the guest, CD is the β-cyclodextrin, G·CD is the final inclusion compound and ΔH_{bin} is the difference between the energy of the optimized complex and the sum of the energies of the isolated molecules extracted from the complex in the same conformation. The negative values upon complexation indicate that the guest forms a stable complex with OβCD under conditions such as those considered here. Table 7.1 reports the theoretical complexation constants for the OβCD·naringin analysed.

The strongest interaction has appeared when the phenol moiety (OβCD·**1**) is inserted into the cavity followed by OβCD·**2**, that is when the phenol part is only partly included into the cavity. The less stable interaction has been found for compound OβCD·**3**, a glucose moiety of naringin included.

Complex	$\Delta H_{binding}$ (Kcal/mol)
OβCD·**1**	-9.56
OβCD·**2**	-7.42
OβCD·**3**	-0.05

Table 7.1 *Complexation enthalpies of the complexes between the OβCD and naringin.*

The cyclodextrin inserted in PEEK-WC has the octyloxycarbonyl chain in contact with the polymeric wall. Fontananova et al. [3] indicated that the β-cyclodextrin derivative, entrapped in polymeric membrane, maintains the

recognition properties of β-cyclodextrin and its ability to form an inclusion complex with naringin.

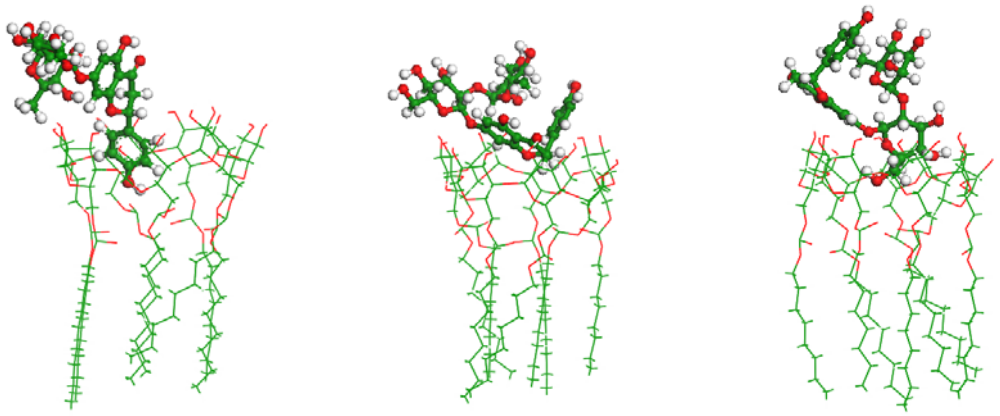

a) **b)** **c)**

Figure 7.4 *Three obtained minima of OβCD/naringin complexes: a)* OβCD·**1**, b) OβCD·**2**, c) OβCD·**3**.

The simplest way of studying diffusion of individual molecules is to inspect their paths through space. A procedure often chosen in the literature is to analyze the mean squared displacement (MSD) averaged over all penetrant molecules of a given kind. In order to get a more detailed insight in different modes of penetrant molecules, it can also make sense to investigate displacement $R(t) = \sqrt{|r(t) - r(0)|}$ and MSD (t) for individual molecules [13].

The encapsulation of drug on MD simulations was valued considering the movement of the OβCD, PEEK-WC and naringin, respectively. Their mean-square displacements were analyzed in Figure 7.5 and Figure 7.6. The displacements referring to figure 7.5 indicates that one of the two molecules of naringin is encapsulated into the cavity. For this reason there no differences in the MSD curves. In figure 7.6 a second molecule of naringin is moving freely in water during the simulation time.

7.4 Conclusions

The Docking and Molecular Mechanics provide information on the geometry and the energy of complexation of OβCD·naringin: the driving force for the host-guest complexation is due to the van der Waals interaction of the aromatic systems.

The Molecular Dynamics calculations can furnish details on the complexation of naringin on the PEEK-OβCD surface.

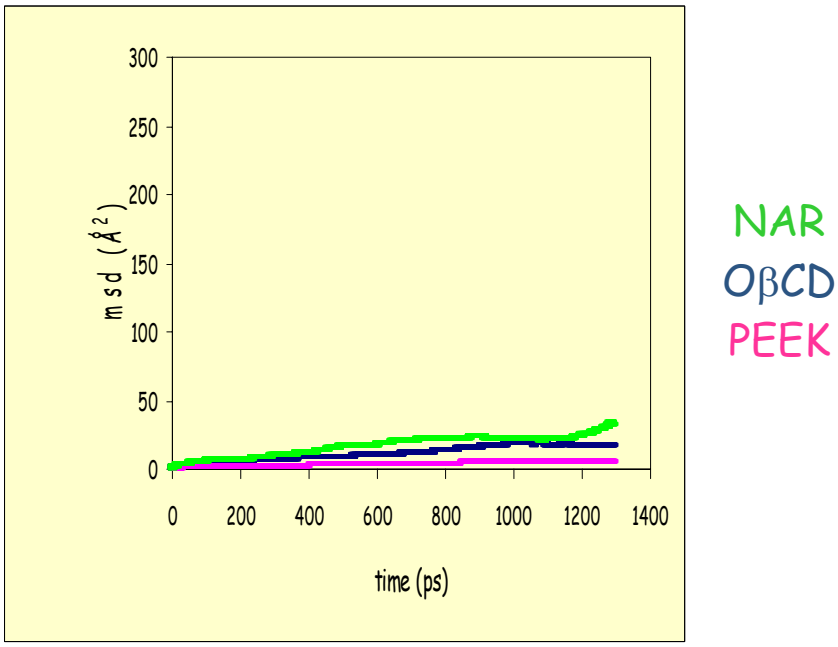

Figure 7.5 *Mean squared displacement MSD(t) of naringin, OβCD and polymeric chain.*

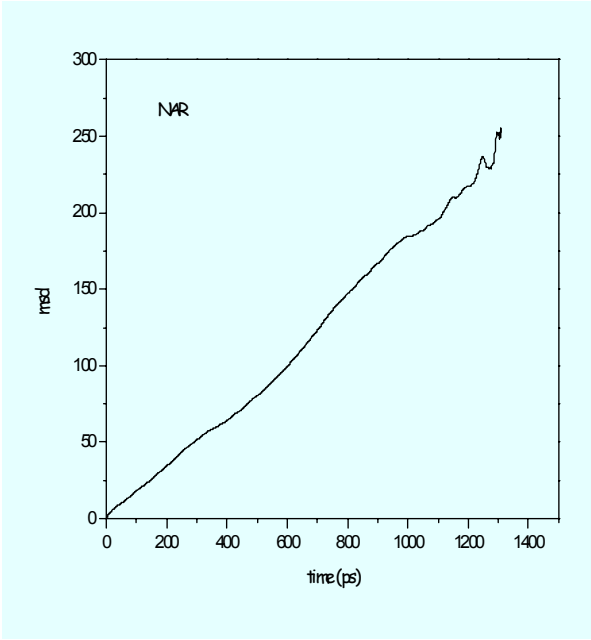

Figure 7.6 *Mean squared displacement MSD(t) of the freely moving naringin.*

References

1. P. E. Shaw, J: H: Tatum, C. W. Wilson, *J. Agric. Food Chem.*, 32 (1984) 832.
2. P. E. Shaw, B. S: Buslig, *J. Agric. Food Chem.*, 34 (1986) 837.
3. E. Fontananova, A. Basile, A. Cassano, E. Drioli, *J. Incl. And Macro. Chem.*, 47 (2003) 33.
4. S. Alcaro, F. Gasparrini, O. Incani,, S. Mecucci, D. Misiti, M. Pierini, C. Villani, *J. Comput. Chem.*, 21 (2000) 515.
5. H. Sun, S. J. Mumby, J. R. Maple, A. T. Hagler, *J. Am. Chem. Soc.*, 116 (1994) 2978.
6. D. Q. McDonald, W. C. Still, *Tetrahedron Lett.,* 33 (1992) 7743-7746.
7. F. Mohamadi, N. G. J. Richards, W. C. Guida, R. Liskamp, M. Lipton, C. Caufield, G. Chang, T. Hendrickson, W. C. Still, *J. Comput. Chem.,* 11 (1990) 440-467.
8. S. Alcaro, F. Gasparrini, O. Incani, S. Mecucci, D. Misiti, M. Pierini, C. Villani, J. Comput. Chem., 21 (2000) 515-530.
9. H. Sun, S. J. Mumby, J. R. Maple, A. T. Hagler, *J. Am. Chem. Soc.,* 116 (1994) 2978-2987.
10. Discover and InsightII User Guide, Version 400p+, Accelrys: San Diego, CA, 1999.
11. R. H. Gee, L. E. Fried, R. C. Cook, *Macromolecules,* 34 (2001) 3050-3059.
12. D. Hofmann, M. Heuchel, Yu. Yampolskii, V. Khotimskii, V. Shantarovich, *Macromolecules*, 35 (2002) 2129-2140.
13. D. Hofmann, J. Ulbrich, D. Fritsch, D. Paul, *Polymer*, 27 (1996) 4773-4785.

EIGHTH CHAPTER

COMPUTATIONAL EVALUATION OF MONOMERS AND POLYMERS FOR MOLECULAR IMPRINTING OF 5-FLUOROURACIL FOR USE AS DRUG DELIVERY SYSTEMS

8.1 Introduction

In the treatment and management of disease, the discovery and analysis of new pharmaceutical compounds is vital, but it is equally important to develop novel methods or devices that are able to deliver specific compound at relevant concentrations to the site of action. In particular, the ability to load therapeutically relevant concentrations of drugs within a delivery vehicle and to control the transport properties of drug from the vehicle is essential for a successful therapeutic effect. The today research activities in the field of drug delivery carriers, the major emphasis has being focused toward engineering of architectural design of biomaterials on a molecular level. In this optics molecular simulation techniques are playing an increasingly important role in the designing and the development of materials for various industrial applications. These simulations are likely to benefit the study of materials by increasing our understanding of their chemical and physical properties at a molecular level and by assisting us in the design of new materials and predicting their properties. Simulations are usually considerably cheaper and faster than experiments. Molecular simulations also offer a unique perspective on the molecular level processes controlling structural, physical, optical, chemical, mechanical, and transport properties.

The principle of molecular imprinting is based on cross-linking polymerization in presence of functional monomers around template molecules. After polymerization the template molecule is removed and a cavity of specific shape and functionalities complementary to the target analyte remains in the polymer. It has been demonstrated that the success of the imprinting procedure crucially depends on the creation of strong monomer/template complexes and on the stability of the molecular assemblies during the entire polymerization reactions.

The comprehension at the molecular level of the mechanisms and the nature of the complex phenomena involved in the formation and recognition capability of molecularly selective, robustly stable, imprinted polymers is a hard goal to achieve.

From the theoretical point of view, several are the computational techniques, which can be applied to the study of the various steps leading to the formation of the molecularly imprinted materials [1-7]. High computational costs,

system sizes and time scales are, however, a limit, which forces the choice of the theoretical method and the definition of models.

With the development of extremely powerful computer hardware and software in the last few decades, computational methods have become an important source of information on the chemical-physical properties of materials. In spite of the advances already made, the development of ever better force fields, calculation algorithms and computer hardware remains a continuous challenge. Molecular dynamics (MD) simulations are a powerful tool to investigate complex systems made of thousands of atoms at reasonable computational costs. The properties of molecules are affected by the surrounding environment and accurate MD simulations must include a proper description of the existing interactions, which are mainly of electrostatic and van der Waals nature, through an appropriate choice of the force field parameters which they are based on. Nevertheless, MD simulations when complemented by other computational techniques and most of all by experimental data can give a clearer picture of the system of interest than can experiments alone.

The aim of the present work is to use different molecular modeling techniques to obtain quantitative/qualitative description of the imprinting process and of the recognition mechanisms.

We were interested to the modelling of monomers-template complexes to study the affinity of template *vs* monomers and the effect of porogenic solvents, but also to focus on the selective recognition parameters of the imprinting system. Finally we wanted to use the systems as controlled release device.

Moreover MD simulations on a polymeric membrane model provided transport properties such as diffusivity, solubility and permeability coefficients of 5-FU, and structural properties such as swelling and free volume. Simulations of the formation of imprinted polymers for 5-fluorouracil (5-FU), as molecular template, are proposed, using combined MD, molecular mechanics (MM), and docking computational techniques. 5-FU is an anticancer agent that is widely used in the clinical treatment of several solid cancers, such as breast, colorectal, liver and brain cancer. Because of its high rate of metabolism in the body, the maintenance of a high serum concentration improves its therapeutic activity, but this requires its continuous administration. However, concentration above a certain limit produces a severe toxic effect, and this must be avoided [8,9].

In order to evaluate the imprinting effect the binding selectivity of MIP was tested by performing the same experiments using a molecule quite similar in structure to 5-FU, uracil (UR) which differ from 5-FU only in the substituent at position 5 of the ring, and using molecules relatively similar, such as cytosine (CY) and 5-fluorocytosine (5-FC) (see scheme 8.1).

Methacrylic acid (MAA) (scheme 8.2) was chosen as functional monomer to prepare MIPs because it contains carboxylic groups hat can form hydrogen bonds with the template. The study was performed to the formation of MIPs and

then to analyse the recognition properties and, finally the release of the 5-FU from the cavity sites.

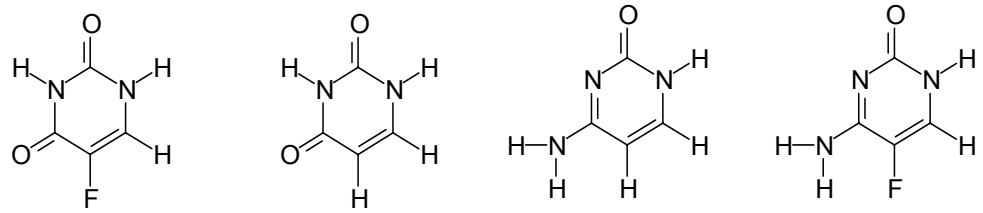

Scheme 8.1 *Chemical structure of a) 5-fluorouracil (5-FU) and of the analogues studied in this paper: b) uracil (UR), c) cytosine (CY), and d) 5-fluorocytosine (5-FC).*

Simulations were carried out for different monomeric molecular systems (clusters) to assess the interaction energies, closest approach distances and the functional groups between the monomers and template implicated in the cavity formation.

Solvent plays an important role in the formation of the porous structure of MIPs. To show the effect that it has on the complexation during the pre-polymerization step, we have completed the study of clusters of 10 MAA molecules and 5-FU considering molecules of dimethylformamide (DMF) in a stoichiometric ratio of one 5-FU molecule and 20 DMF molecules.

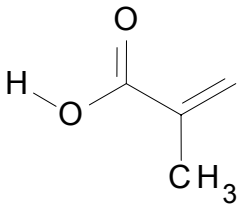

Scheme 8.2 *Chemical structure of methacrylic acid (MAA).*

The study was carried out in two phases. In the first phase 10 MAA monomers interact with the ligand (5-FU or its structural analogues) to investigate the affinity and selectivity of MAA membrane for the template 5-FU.

In this phase the solvent effects of dimethylformamide (DMF) during pre-polymerization was considered simulating a cluster of 10 MAA monomers, one 5-FU molecule and 20 DMF molecules.

The second phase of simulations considers a box of polymethacrylic acid (PMAA) (scheme 8.3) chain with 9 5-FU molecules at contact with a water solution to investigate the drug release. In fact the water molecules destroy the hydrogen bonds between the template and the functional groups of polymer.

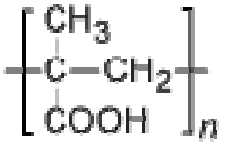

Scheme 8.3 *Chemical structure of polymethacrylic acid (PMAA) repeat unit.*

8.2 Experimental section

8.2.1 Simulation procedures

Molecular mechanics (MM) calculations and MD simulations carried out with Material Studio/Discover (4.0) software of Accelrys Inc. (San Diego, CA) [10] employing PCFF force field [11]. Indeed, previous study showed a satisfactory performance of this force field for the molecular simulation of organic molecular clusters of monomers and polymers [5,6-12]. This force field is parameterized for a large class of organic molecules including H, C, O, S, P, F, Cl and Br, allowing it to be applied to bio- and synthetic polymers. PCFF force field gives accurate geometries for various polymeric systems and can be used to calculate and minimise the energy of simulated monomeric and polymeric systems. Amorphous polymer packings were constructed using the Theodorou/Suter method [13,14] as implemented in the Amorphous Cell module [15]. All calculations were carried out on the supercomputer CINECA BCX cluster (Bologna, Italy) and on PC.

8.2.2 Molecular mechanics

The PCFF provides a potential energy interaction function (E_{total}) that accounts for both bonded (E_b) and non-bonded (En_b) interactions. The bonded terms typically include harmonic bond stretching (E_s), harmonic angle bending (E_a), torsional (E_t), and inversion (E_i) energies. Non-bonded terms typically contain van der Waals (E_{vdW}), electrostatic (Coulombic) and hydrogen bond (10-12 potential) (E_{hb}) interactions. In practice it is common to choose a suitably large cut-off distance for the long-range non-bonded interactions. The Mie 6-12 potential [16], that is often referred to in the literature as the Lennard-Jones 6-12 potential function ($u=A/r^{12}-B/r^6$), was used to calculate the non-bonded van der Waals interactions. A and B are parameters which determine the size of the attraction ($-B/r^6$) and the repulsion (A/r^{12}) interactions between the atoms which are separated by a distance r equal to the sum of r_i and r_j, where r_i and r_j are van der Waals radii of the non-bonded atoms i and j.

Four molecular clusters consisting each of one ligand, 5-FU, UR, CY and 5-FC, respectively, with 10 molecules of MAA monomers, were designed. Each

molecular cluster was optimised and the values of the total potential energy (and of its components were obtained).

Then NVT-MD (runs at constant number of particles, temperature and volume) simulations were performed at 300 K, for each system.

MD calculations simulate the natural motions of all atoms in a molecular system over time at non-zero temperature and the MD algorithm makes use of Newton's equation of motion, thus giving a complete dynamic description of the polymeric material. In order to ensure that the simulations are carried out for sufficient time, which is one of the most important criteria in equilibrating the system and then to accurately predict its equilibrium properties, the simulation time of NVT MD calculations was 10 ns, and the output frequency was every 2000 steps. The time step of 1 fs (femtosecond) is taken to be constant for all the simulations. In this MD study the model system exchanges energy with a heat bath in order to maintain a constant temperature. The thermostat described by Andersen et al. [17] was used for isothermal-isobaric NVT MD simulations. For all the simulations the dielectrical constant was kept constant at value of 1. After the achievement of an energy asymptotic value, the sampling of structures of the MD trajectory was performed.

The conformational analysis was carried out collecting snapshots after 500 ps of simulations, every 250 ps and in correspondence of potential energy (E_{pot}) peaks. The extracted structures, 48 of 5-FU, 49 of UR, 49 of CY and 48 of 5-FC, respectively, were optimized by using steepest descent, conjugate gradients (with a termination gradient of 10^{-2} kcal/mol) and Newton-Raphson algorithms with a termination gradient of 10^{-3} kcal/mol.

Binding affinity, that is a measure of how well the template molecule is attracted to the binding site, was calculated [18], from the interaction energy between the ligand and the monomers. Theoretically it was assumed that the monomer (the template) giving the highest ΔE with the given template (monomer) should also give the polymer with the highest affinity.

On the absolute minima of each molecular cluster the interaction energy was calculated in order to estimate the interaction energy between the ligand and the corresponding monomers in the following manner:

$$\Delta E = E_{cluster} - \left(\sum E_{monomers} + E_{ligand}\right) \qquad (8.1)$$

where $E_{cluster}$, is the total energy of the simulated cluster (monomers and ligand), $\sum E_{monomers}$ is the total energy of the ten monomers (without the ligand) and E_{ligand} is the total energy of the ligand [5].

To estimate the porogenic solvent effects in the pre-polymerization step on the energy minimum conformation 20 DMF molecules were added to the cluster with the 5-FU ligand. The solvent molecules number was chosen to simulate an excess of solvent as experimentally occurs. Then a MD-NVT simulation run and

the following conformational analysis were performed for 10 ns, as described above. The extracted structures, 52 in total, were optimized by using steepest descent, conjugate gradients (with a termination gradient of 10^{-2} kcal/mol) and Newton-Raphson algorithms with a termination gradient of 10^{-3} kcal/mol. In the case of molecular cluster containing solvent molecules the interaction energy becomes:

$$\Delta E = E_{cluster} - \left(\sum E_{monomers+solvent} + E_{ligand}\right) \qquad (8.2)$$

where $\sum E_{monomers+solvent}$ is the sum of monomers energy and solvent molecules energy [6].

8.2.3 Docking

Selectivity and recognition capability were tested inserting the 5-FU and their analogues into the binding cavity found for 5-FU by means of a docking study [7,18] by using AUTODOCK 4.0 program [19]. This program starts with the ligand molecule in an arbitrary conformation, orientation, and position, and finds favourable dockings in a ligand-binding site, using Lamarckian genetic algorithm. Three binding energy terms were taken into account in the docking step: the van der Waals interactions, the hydrogen bonding and the Coulomb interactions. Non-polar hydrogens were removed from the ligand, and their partial atomic charges were united with the bonded carbon atoms. Gasteiger charges were calculated. The grid maps around the MIP cavity were calculated using AUTOGRGRID 4.0 with 40x40x40 points, and a grid spacing of 0,375 Å. Parameters in AUTODOCK were assigned default values. For each ligand 50 runs were performed [20-22]. The simulations were carried out in vacuum. The final docked conformations were grouped into families of similar ligand orientations comparing the root mean square deviation (rmsd) between the coordinates of the atoms. The criterion employed to cluster structures as similar was 0,5 Å intervals of ligand rmsd.

8.2.4 Generation and equilibration of polymer structures

Two independent atomistic bulk models of polymethacrylic acid (PMAA) were prepared. The applied basic techniques of packing and equilibration have been described in detail elsewhere [23-25].
Briefly, the procedure is given below:
1) After preparing atomistic repeating units of PMAA (see scheme 8.2), a single polymer chain with 634 repeat units was constructed. The construction of the polymeric model started from the spatial disposition of MAA monomers interacting with the 5-FU molecule in the minima structure found by means of

previous sampling procedure and then introducing the others monomer units and finally linking between them. Cross-linking density is not expected to significantly alter the pre-polymerization equilibrium, so the influence of cross-linking agents was neglected to avoid too much data in the computational system. In fact, in evaluation of MIP, the analogues and the template are similar to both in structure and volume and we can focus on the cavity sites between the monomers and the template without considering to the cross-linker.

2) For the initial packing of each PMAA model, a polymer chain was grown under 3-dimensional periodic boundary conditions at 308 K and at a density of about 10% of the experimental value in a simulation box. Periodic boundary conditions were applied to minimise the artificial effects caused by the finite size simulation system. 9 5-FU molecules and 619 water molecules were also added. The solvent molecules match the 20% in weight. In this way the model should correspond better to the experimental films [26].

Three independent initial configurations were generated for each polymer. The chain was grown following the Theodorou/Suter method [13,14], based on the Rotational Isomeric State (RIS) model of the Amorphous Cell Program of Material Studio [15]. One single long chain was utilized to reduce the influence of chain ends on the simulations. This procedure to represent bulk amorphous systems is common and has been proven to be quite accurate in replicating the behavior of experimental polymeric systems [24,25].

3) An equilibration procedure was carried out consisting of simulated annealing runs (NVT-MD dynamics at different temperature) (NVT-MD are runs at constant number of particles, temperature and volume) for 150 ps. Subsequently, compression (runs at constant number of particles, temperature and pressure - NPT-MD) at 300K and pressure of 1bar were carried out through a set of successive MD simulations for 1,2 ns. During the equilibration procedure restraint forces were applied to the distances between the functional groups of the monomers that created the cavity around the 5-FU molecule and between the monomers and the template to assure the same spatial conformation found in the sampling procedure. Later on the production run only the restraints on the monomers that created the cavity around the 5-FU were used to keep the memory effect of MIP.

The “equilibration” procedure yielded well-equilibrated packing models with stable density fluctuations at a density close enough to the given experimental value under the experimental pressure (1 bar).

The following simulation conditions were used: periodic boundary condition to make the system numerically tractable and to avoid symmetry effects; a cutoff distance of 26 Å for interaction energy functions. The Andersen thermostat [17] was used for temperature control and the Berendsen method [29] was applied to control the pressure of the system during NPT-MD simulations.

4) NPT-MD simulations were performed at T=300 K and p=1 bar for about 2.1 nanoseconds with the Discover package of Accelrys [10] employing a time step of 1 fs for the numerical integration and the coordinates were stored every 500 steps. The obtained packing models have an edge length of about 53,1 Å, which offers a good compromise between calculation velocity and maximum void size that can be analyzed in comparison with boxes of 40 Å, often used in the literature [23]. The aim of using larger cells in our study is to improve the statistics.

8.3 Results and discussion

8.3.1 Computational prediction of MIP's affinity

The strength of intermolecular interactions between ligand and functional monomers and the number of binding (activity) sites in the pre-polymerization mixture are important criteria to establish the affinity of the ligand towards monomers used in the preparation of a MIP.

An introductory statement is needed. As with laboratory experiments, computer simulation experiments can have both systematic and statistical errors, which, however, can be controlled and minimised. Applying MD simulation, the thermo-physical, structural and dynamic properties of polymeric materials can be calculated with an accuracy that strongly depends on the reliability of the potential function, in other words, on the errors arising from the truncation of the intermolecular forces, and statistical errors, arising from insufficiently long sampling period. In practice, MD simulation studies are presently still limited by the speed and storage capabilities of current computers to limited molecular cluster size and computing time scales. In addition, the results of the molecular simulations for any given cluster might converge to different local minima depending on the starting conformation of the system. One of the solutions to this problem was to start from many, widely different initial conformations, and to make sure that the results obtained from them did not differ widely.

To simplify the model, the number of the activity sites was assumed to be equivalent to the number of hydrogen bonds formed between the ligand and the functional monomers, as suggested by Liu *et al.* [18]. Also the influence of cross-linking agent was neglected both to avoid too much data in the computational system and because apparently does not affect the formation of the pre-polymerization complexes [18].

According to the literature [26] reported the complexes are in the ratio of 5-FU and/or analogues: methacrylic acid (MAA) = 1:10. Then the conformations with the lowest energies were used for interaction energy calculation.

The interaction energy calculated (ΔE [kcal/mol]) and the number of hydrogen bonds (H bonds) created by ligand interacting with monomers in the most stable complexes are listed in table 8.1.

It should be pointed out that the interaction energy is an approximation to the enthalpy change or the free energy change in the binding process and hence is a physically significant quantity. Therefore, it appears that at this time calculations of direct interaction energies, ΔE, in MM calculations are a reasonable choice for predicting binding affinities of MIPs and templates. That is, based on the above factors, we can conclude that a large negative value of ΔE for a given monomers-ligand cluster should give a good indication that this particular ligand will form stable complex with the monomers and will be a good candidate for MIP. Thus, as a measure of the complex stability, the interaction (binding) energy calculated was used.

Molecular cluster	ΔE (kcal/mol)	n° H bonds		Bond length
5-FU·10MAA	-53,96	4	C=O ··· (H-O-C=O)- N-H ··· (O=C-O-H)-	1,7 Å 1,9 Å
UR·10MAA	-40,61	3	C=O ··· (H-O-C=O)- N-H ··· (O=C-O-H)-	1,6 Å 1,9 Å
CY·10MAA	-44,38	4	C=O ··· (H-O-C=O)- N-H ··· (O=C-O-H)- -(H-N-H) ··· (O=C-O-H)-	1,7 Å 1,9 Å 1,8 Å
5-FC·10MAA	-44,71	5	C=O ··· (H-O-C=O)- N-H ··· (O=C-O-H)- -(H-N-H) ··· (O=C-O-H)-	1,8 Å 1,9 Å 2 Å

Table 8.1 *Interaction energy and hydrogen bonds between the ligand and the monomers in the molecular cluster in the absolute minima.*

As was already proven, the larger (the most negative value) interaction energy of the molecular system and the stronger hydrogen-bonding interactions product the more stable resulting complex [7,18,30-35].

From the results in table 7.1, it can be concluded that the order of the molecular interactions is as follows: 5-FU-MAA > 5-FC-MAA ~ CY-MAA > UR-MAA. These results show that 5-FU·10MAA is the most stable complex. The active group of MAA formed selective recognition cavities interacting strongly with 5-FU.

As indicated in several previous studies [32,36], hydrogen bonding is the most important interaction in non-covalent imprinted polymers. Thus, in this step, complex level was determined by the number of hydrogen bonds formed between the functional monomer and the template, or non-template. The hydrogen bonds formation is in good accord with the ΔE calculations. In fact there is a strong correlation between the higher number of hydrogen bonds present in molecular

clusters with higher stability.
The formation of hydrogen bonds has been analyzed in all the minimised structures (See figures 8.1-8.5).

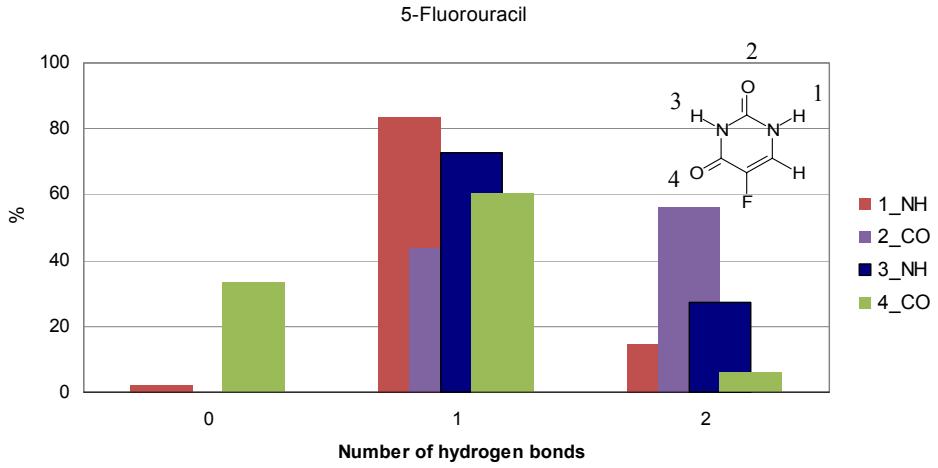

Figure 8.1 *Hydrogen bonds for all the minimised structures of 5-FU.*

In general the couples 5-FU and UR and that of 5-FC and CY could form the same number of hydrogen bonds both, for the presence of the same functional groups. It has been observed, that both 5-FU and 5-FC, form one more hydrogen bond. The explanation is the presence of fluorine atom in the molecular structure. In 5-FU and in 5-FC the fluorine atom is not directly involved in the hydrogen bond formation but plays an important role in the molecular behaviour due to its electron attractor effect. The result for fluorinated molecules is that a greater number of hydrogen bonds between the others functional groups and the MAA monomers are obtained. This is one of the most important factors which lead to the bigger interaction between the MAA and 5-FU and 5-FC.

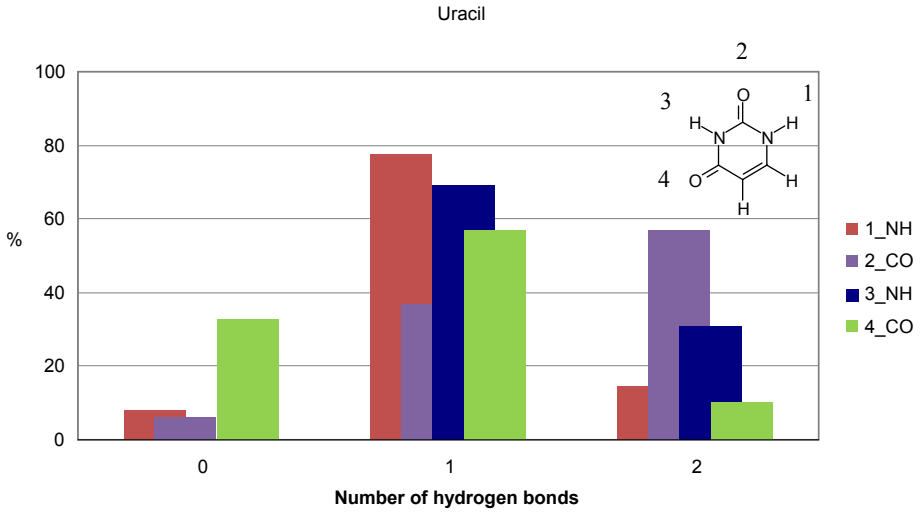

Figure 8.2 *Hydrogen bonds for all the minimised structures of UR.*

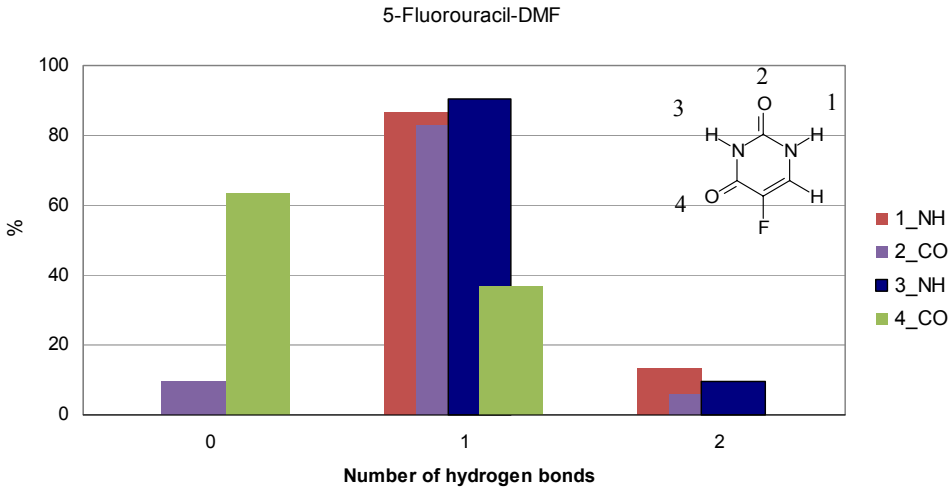

Figure 8.3 *Hydrogen bonds for all the minimised structures of 5-FU in DMF.*

Considering the analogues UR/5-FC, is 1_NH the site responsible for the major number of hydrogen bonds, above 80% for the fluorinated uracil, and below 80% for UR. The hydrogen bonds in which the 3_NH is involved are essentially the same for both analogues. Considering the carbonyl groups, the 2_CO forms more single hydrogen bonds in 5-FU than in UR.

The presence of DMF modifies the total number of hydrogen bonds. Whereas no modification are available for 1_NH, the hydrogen bonds that involve 2_CO double in the case of single bonds, but goes from about 50% to 10% for double hydrogen bonds. 3_NH increases passing from 70% to 90% for single hydrogen bond and is reduced to 1/3 for double hydrogen bonds. Finally the number of interactions of 4_CO is reduced going from 60% to 30%.

The reason of such behavior could be ascribed to the fact that after 10 ns of simulation there is a partial separation of phases, DMF and MAA molecules are non completely miscible, so MAA are more sterically constrained and are not able to lye in bridge position between two functional groups of the template. They are involved in single hydrogen bonds. The 4_CO is the functional moiety of the template more exposed to the solvent. Only one, maximum two molecules of MAA stay in this area: for this reason the hydrogen bonds of 4_CO are less in DMF than in non solvated system.

Considering the analogues CY/5-FC, the number of hydrogen bonds of 1_NH is the almost the same. As before, the percentage of hydrogen bonds increase (to about 80%) in fluorinated cytosine. The 2_CO is less sterically hindered than UR/5-FU. So can be involved in two interactions.

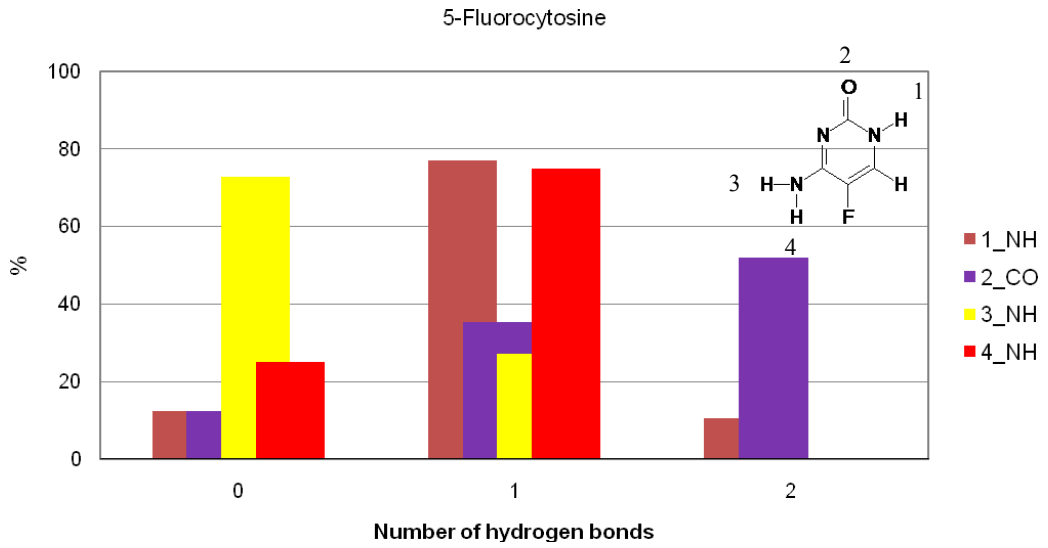

Figure 8.4 *Hydrogen bonds for all the minimised structures of 5-FC.*

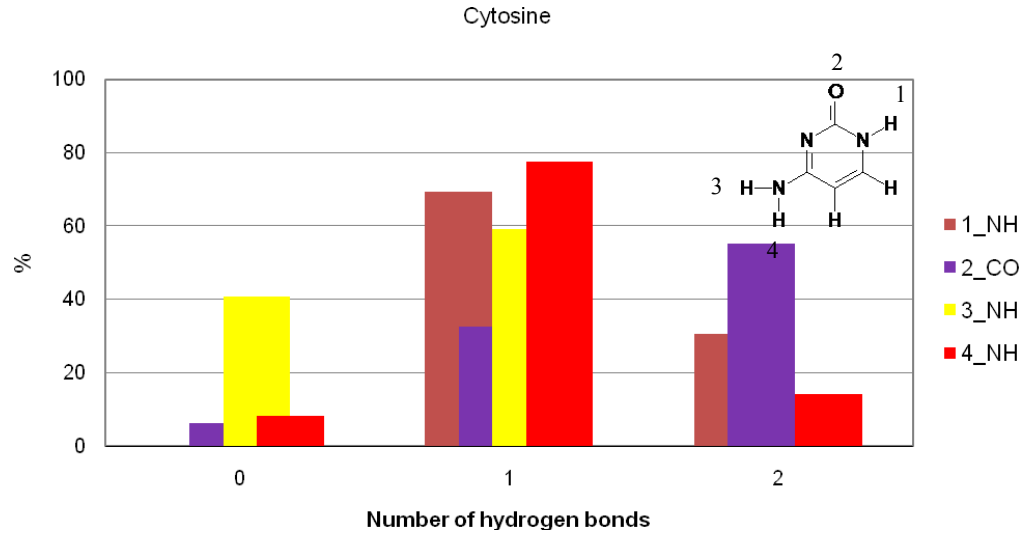

Figure 8.5 *Hydrogen bonds for all the minimised structures of CY.*

The other site responsible for the formation of hydrogen bonds is the hydrogen of the amminic moiety of CY/5-FC. They form, in average, one hydrogen bond ranging from 60% to 70%. If F is into the structure the number of hydrogen bonds is reduced.

The most stable structures of molecular clusters calculated using the MM sampling procedure are shown in figure 7.6. In the most stable 5-FU·10MAA complex (figure 8.6a) there are four hydrogen bonds. The hydrogen-bonding pair consists of two MAA hydroxyl groups and the two carbonylic groups on the 5-FU

molecule. The length of these bonds is 1,7 Å. Additionally, the presence of two hydrogens bonded to two different nitrogens on the 5-FU are responsible of others two weak interaction between two MAA carboxylic oxygens with a length of 1,9 Å.

The most stable UR·10MAA complex (figure 8.6b) shows three hydrogen bonds. The strongest hydrogen bond with a length of 1,6 Å, is the bond between one UR carbonylic oxygen and acidic hydrogen of MAA. This interaction is enhanced by the presence of two weak hydrogen bonds formed between the hydrogens bonded to the two nitrogen atoms of UR. Based on the calculated geometrical parameters of the hydrogen bonding sites, we may deduce that the interaction between 5-FU and MAA is stronger than that between UR and MAA. Really, 5-FU has four main functional groups, two are proton acceptors and two proton donors, such as also UR. Consequently, these molecules could possibly participate in four hydrogen bonds, both. But 5-FU forms really four hydrogen bonds and UR forms only three hydrogen bonds.

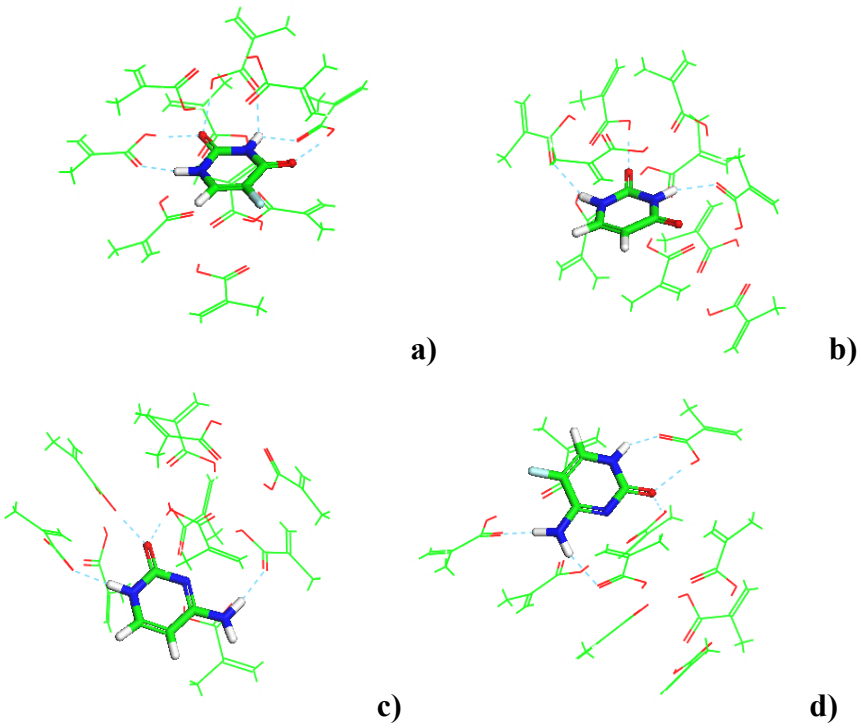

Figure 8.6 *Optimised geometries of the most stable pre-polymerization molecular clusters: a) 5-FU, b) UR, c) CY and d) 5-FC. Hydrogen bonds are shown with blue dashed lines.*

In the most stable CY·10MAA complex (figure 8.6c), the linkage of hydrogen bonds involving MAA molecules as well as proton donor and acceptor sites is formed. In particular we observe two strong H bonds between the

carbonylic oxygen of CY with the MAA hydroxylic group with a length of 1,7 Å, one weak hydrogen bond between the hydrogen linked to nitrogen atom of CY and MAA carboxylic oxygen with a length of 1,9 Å, and finally one hydrogen bond between one hydrogen of CY amminic group and MAA carboxylic oxygen with distance of 1,8 Å.

Finally, in the most stable 5-FC·10MAA complex (figure 8.6d) there are five hydrogen bonds. Two strong hydrogen bonds are formed between the oxygen of 5-FC carbonylic group and MAA hydroxylic group with a length of 1,8 Å, one hydrogen linkage is formed between the hydrogen bonded to nitrogen atom of 5-FC and MAA carboxylic oxygen with a length of 1,9 Å, and two weak hydrogen bonds are created between the two amminic hydrogen of ligand with the MAA carboxylic oxygen with distance of 2 Å.

8.3.1.1 Computer simulation in solvent

The more realistic modelling of the imprinting molecular systems should not only include the substrate but also the effects of the solvent since, nearly all imprinting processes are performed in the presence of the solvent. Solvents with various dielectric constants and hydrogen bonding capacities influence the template/monomer interaction differently.

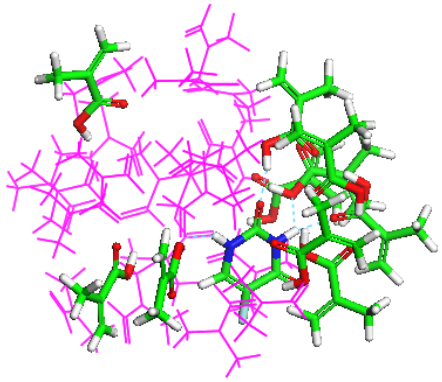

Figure 8.7 *Optimised geometry of the most stable pre-polymerization molecular clusters of 5-FU in presence of DMF solvent (pink colour). Hydrogen bonds are shown with blue dashed lines.*

In this section, MD atomistic simulations were carried out for molecular systems containing solvent in order to investigate the solvent (DMF) effect on template/monomer non-covalent interactions. The monomer/solvent ratio was 1:2 as indicated in the experimental study reported for 5-FU imprinted polymer [26]. At the minimum energy conformation of the molecular clusters containing 10 molecules of monomers and one molecule of 5-FU simulated in precedence, 20 molecules of DMF were added during this phase. The conformation at minimum

energy obtained (figure 8.7) was used to predict the interaction energies between ligand and monomers dissolved in a solvent from Eq. 8.2.

As reported in table 8.2 the solvent molecules interact with the template and functional monomer in solvent environment. And the intermolecular interaction between solvent molecules and the complex is competitive with template-monomer interaction in the complex, as proved from the hydrogen bonds formation between DMF and 5-FU, leading to weakening the interaction between the template and monomer. As result, the interaction energy between template and monomers in DMF is lower than that in gas phase. As the polarity of solvents could affect the conformation of the complex due to the different dielectric constant, the way that monomers recognize the template is different. The interaction energy could reflect the effect of solvent on the complex formation.

Molecular cluster	ΔE (kcal/mol)	n° H bonds		Bond length
5-FU·10MAA	-53,96	4	C=O ··· (H-O-C=O)- N-H ··· (O=C-O-H)-	1,7 Å 1,9 Å
5-FU·10MAA·20DMF	-53,61	3	C=O ··· (H-O-C=O)-MAA N-H ··· (O=C-O-H)-MAA N-H ··· (O=C-O-H)-DMF	1,7 Å 1,9 Å 1,9 Å

Table 8.2 *Interaction energy and hydrogen bonds between the 5-FU and the monomers in molecular cluster with and without DMF solvent.*

8.3.2 MIP's selectivity

In the docking phase the selectivity and recognition capability were tested inserting 5-FU and its analogues into the binding site and evaluating their interactions and binding by visual inspection and empirical energy calculations. The most common approach is to position or dock ligand and receptor molecules together in many different ways and then scores each orientation according to an evaluation function.

The pocket of the active site was defined by including all the monomers atoms found for the minimum energy conformation of 5-FU molecular cluster by previous MM study. The orientation of the ligand was evaluated with an energy scoring function consisting of van der Waals and electrostatic components. In order to describe the physical and chemical environment of the ligand-binding site of the receptor molecule, atomic affinity potentials for each atom type in the receptor molecule in the manner described by Goodford [37] were calculated. The cavity is embedded in a three-dimensional grid and a probe atom is placed at each

grid point. The energy of interaction of this single atom with the cavity is assigned to the grid point. The electrostatic interaction is evaluated similarly.

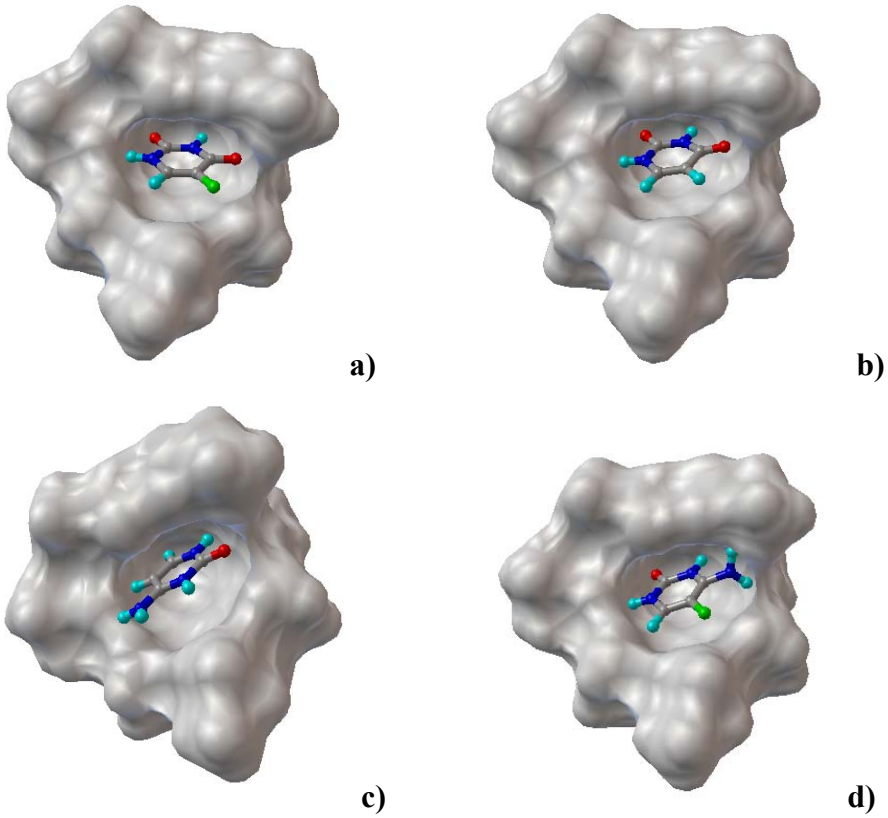

Figure 8.8 *Inclusion geometries of the ligand a) 5-FU, b) UR, c) CI and d) 5-FC in the MAA cavity.*

The figure 8.8 shows the inclusion of the ligands into the MAA cavity. The molecules are accommodated in the binding pocket in such a way to maximize steric interactions and favourable contacts and orientate their hydrogen bond donors, hydrogen bond acceptors and lipophilic groups towards the complementary matching areas. Thus, the -C=O and -NH groups are oriented versus the cavity inner whereas the fluorine atom is directed out (green coloured in the figure 8.8a and 8.8d). As observed in the previous MM study, the fluorine atom is not directly occupied in H bonds formation so that it doesn't interacts with the cavity but plays an important role because is responsible of the orientation of the others functional groups present on the molecule toward the inner cavity.

The three-dimensional structure of the obtained binding sites is closely connected to 5-FU conformation, thus one of its characteristic feature is the shape selectivity. 5-FC and CY molecules larger than 5-FU have reduced selectivity due to steric exclusion effects due to the $–NH_2$ group that sticks out from the cavity, in fact only the molecule ring enters into the cavity. Also smaller substrates, even

though their size does not prohibit entering the binding site, may have also reduced selectivity as in the case of UR, due to less favourable interactions with the walls of the cavity. In fact the absence of fluorine atom involves less favourable interactions.

The key results in a docking calculation are the docked structures found at the end, the energies of these docked structures and their similarities to each other. The similarities of docked structures are measured by computing the root-mean-square-deviation, rmsd, between the coordinates of the atoms. Moreover the reliability of a docking result depends on the similarity of its final docked conformations. One way to measure the reliability of a result is to compare the rmsd of the lowest energy conformations and their rmsd to one another, to group them into families of similar conformations or "clusters". The clustered structures for each ligand are shown in figure 8.9.

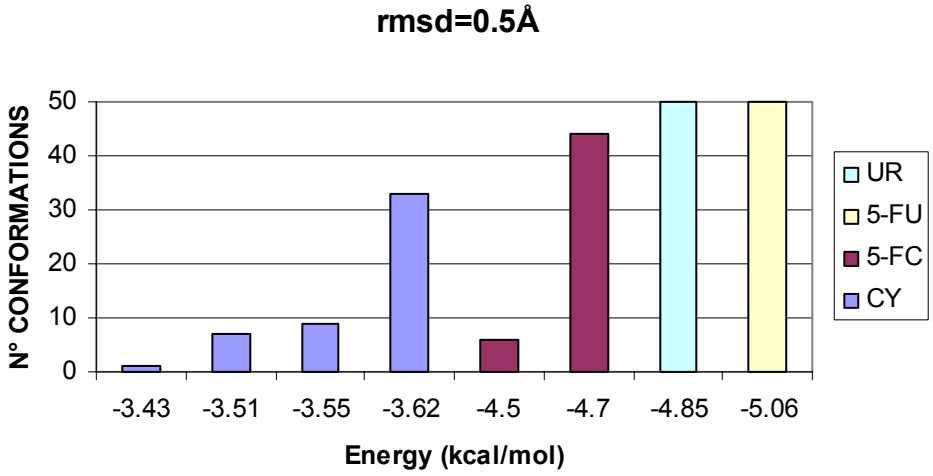

Figure 8.9 *Clusters computed at rmsd=0.5 Å. The bars are sorted by energy of the lowest-energy conformation in that cluster.*

The 5-FU structures are grouped in one cluster because the cavity is closely connected to 5-FU conformation (the cavity was obtained from previous MM study). Also the UR structures are grouped in only one cluster like the 5-FU. This could be explained because there is only one favourite orientation that fits well into 5-FU cavity due to the strong similarity to 5-FU.

On the contrary 5-FC and CY structures are grouped into two and four families, respectively. The reason for that is the presence of the fluorine atom that is responsible of the orientation of the ligand's functional groups towards the cavity to maximize the interactions. Thus 5-FC structures are oriented almost in one direction, whereas CY structures can orient in different ways.

Ligand	$E_{binding}$ (kcal/mol)	E_{vdW} (kcal/mol)	E_{ele} (kcal/mol)
5-FU	-5,06	-4,40	-0,66
UR	-4,84	-4.49	-0,35
5-FC	-3,69	-3,71	-0,25
CY	-3,62	-3,43	-0,46

Table 8.3 *Binding energy, van der Waals and electrostatic contributions calculated for each ligand by using docking procedure.*

In table 8.3 are shown the binding energy for each ligand calculated by using docking procedure. The following observations can be made: in all cases the main contribution to the binding energy derives from the van der Waals contribution whereas electrostatic contribution is very small. This indicates that the selectivity is especially a geometrical question. As reported for 5-FC and CY, that have the smaller binding energy, the hindering $–NH_2$ group prevent the full admission of the molecule in the cavity. On the contrary 5-FU and UR, that have the higher binding energy, can lie totally in the cavity due to small dimensions. The higher binding energy found for 5-FU confirms the correct docking procedure because the pocket of the cavity was defined by including all the monomers atoms found for the minimum energy conformation of 5-FU molecular cluster by previous MM study.

8.3.3 Comparison with experimental data

In the experimental study reported for 5-FU imprinted polymer, the selectivity of the imprinted polymer was evaluated by comparing the binding percentages of 5-FU and its structural analogue UR on the MAA imprinted polymer in organic medium, at pH=1.0 and 7.4 (table 8.4) [26].

The percentage of bound 5-FU by the imprinted polymer was 30% in organic medium, 35% at pH=1.0 and 27% at pH=7.4, but for UR they were only 16% in organic medium, 11% at pH=1.0 and 9% at pH=7.4. The higher binding percentage for 5-FU shows the selectivity of MIP toward 5-FU. The comparison of the binding amounts of substrates on the imprinted polymer shows that study of the selectivity of MIP using conformational analysis is reliable and important. In fact, our computational results show a higher interaction energy between 5-FU and MAA. Therefore, these experimental results confirm the reliability of our computational method.

		SELECTIVITY →	
		%5-FU bind	%UR bind
MIP	AFFINITY ↓	27±3	9 ±3
NIP		9 ±3	10±3

Table 8.4 *Experimental affinity and selectivity of MIP and Non imprinted NIP of 5-FU and UR.*

8.3.4 Computational prediction of MIP's transport properties

The atomistic modelling of PMAA material was used as a tool for understanding the mechanisms of physical processes on molecular levels, gaining insights into the molecular origins of behaviour of bulk polymers.

Figure 8.10 shows the equilibrated 3D periodic cell of PMMA with 20% wt of water containing 9 molecules of 5-FU inserted into 9 cavities. The molecules in CPK represent a molecule of 5FU in a cavity site.

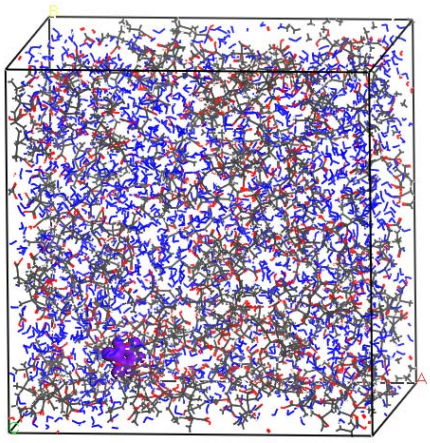

Figure 8.10 *Atomistic bulk models of polymethacrylic acid (PMAA).*

Generally, although an imprinted polymer is a rigid matrix because of cross-linker agents presence, the thermal vibration of the polymer chain segments permit the formation of temporary channels that can be utilized for diffusion of water and template molecules. Moreover, as hydrogen bonding interaction between template and functional monomers is considered among the dominant forces in non-covalent

imprinting, this is largely suppressed at aqueous conditions, thus to permit the diffusion of template agent in the imprinted matrix.

To analyze the possible release from this system, the movement (diffusion) of 5-FU molecules was controlled.

The constants of diffusion can be obtained in principle from diffusion trajectories r(t) of template determined during a MD simulation of imprinted polymer model. The diffusion coefficient for the respective template and water molecules can then be calculated from the mean squared displacement MSD(t) = < | r(t) –r(0) |^2 > of a given molecule averaged over all possible time origins t = 0 and all simulated trajectories of the diffusing molecules:

$$D = \frac{\left\langle \left| r(t) - r(0) \right|^2 \right\rangle}{6t} \qquad (8.3)$$

This so called Einstein equation can of course also be used to determine D value from MD simulation.

Diffusion coefficients can be calculated using Eq. 8.3 only if a random-walk motion for the diffusing particles is assumed. At very short times of simulation, of the order of ps, penetrants execute, indeed, ballistic motion as they rattle in cavities. Anomalous diffusion, in which molecules still follow correlated paths, depends on how fast the penetrant diffuses. The slope of the mean square displacements curve vs time starts off steeply, since fast jumps present an easy way for a gas molecule to move some distance, but never levels off to a straight line, as slower jumps now can only help the penetrant move further.

The displacements of the nine molecules of 5-FU were calculated on the equilibrated 3D models by performing dynamic runs on NPT ensemble.

The 5-FU mean squared displacements curves (MSD) *vs* time of simulation are showed in Figure 8.11. It is evident from the showed MSD curves that the release of 5FU is prevented because the mobility of 5FU is reduced. Only one molecule shows a certain movement (in blue in figure). Only one diffusion coefficient was calculated from curves of figure 8.11, and the quite small value is of $3{,}33 \cdot 10^{-9}$ cm^2/s.

Drug molecules have been analyzed into the cavity. In details we have checked a molecule of 5-FU in figure 8.12.

From the analysis of the figure it is possible to notice that there are strong interactions between 5-FU and PMAA chain by means of several hydrogen bonds. Also a water molecule that is in the surroundings of the cavity interacts with 5-FU with an hydrogen bond. These interaction prevent the release of the drug. A consideration has to be done on simulations times: these results indicate only that to analyze such system the simulations have to be longer in time.

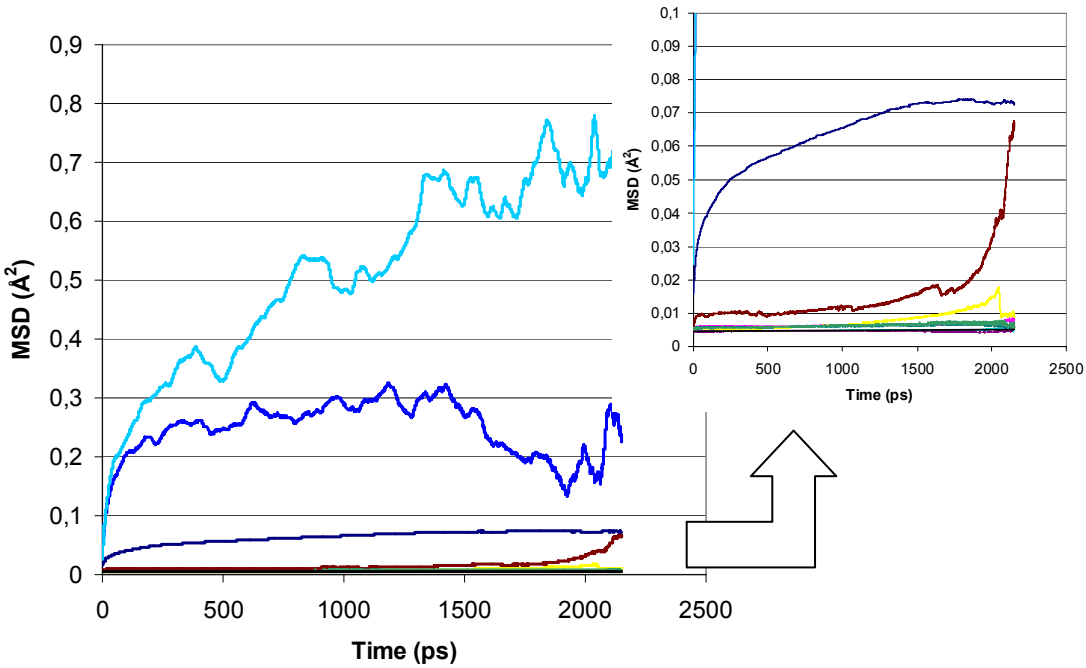

Figure 8.11 *Mean squared displacements curves (MSD) of 5-FU calculated on the equilibrated 3D models by performing dynamic runs on NPT ensemble.*

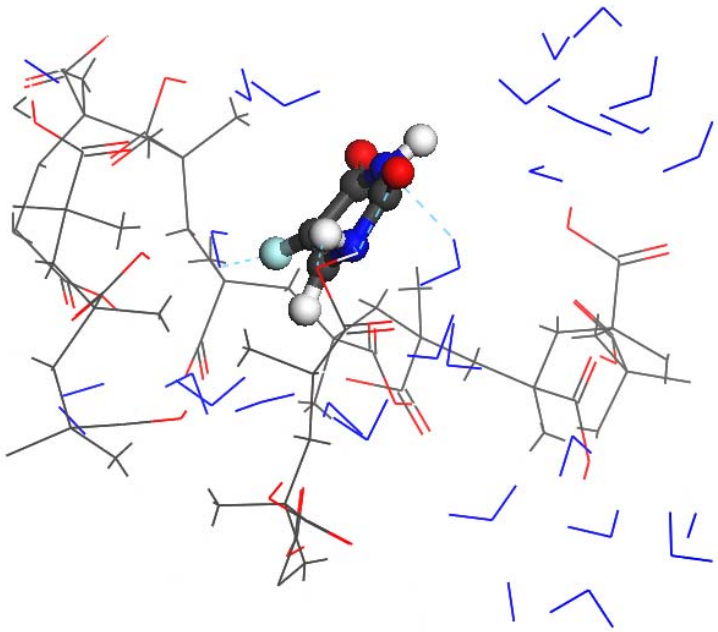

Figure 8.12 *5-FU molecule in the MIP cavity, water molecules are shown in blue lines and polymer chain are coloured in gray sticks.*

8.4 Conclusions

It is extremely difficult to characterize the binding site structures of MIPs together with the number and type of functional groups of the binding cavities, which are not necessarily determined during the pre-polymerization phase but rather during the complex mechanisms taking place in the polymerization process.

The computational model employed focused on the aggregation of a specific template with a preformed polymer on the basis of intermolecular interactions between the template and the polymer building blocks. The simulations used were able to verify the most important characteristic properties of a putative MIP binding site, that are selectivity and binding affinity.

Moreover atomistic modelling of material structure was a tool for understanding the mechanisms of physical processes on atomic and molecular levels, gaining insights into the molecular origins of behaviour of bulk polymers.

In the present work the molecular clusters of 5-FU template agent, or its structural analogues, and MAA monomers were investigated by extensive NVT-MD simulations in order to obtain a better insight about the molecular imprinting formation, mechanism and properties of molecularly imprinted PMAA. Binding affinity, that is a measure of how well the template molecule is attracted into the binding site, and binding selectivity, that is the recognition capability of MIP, were calculated from the interaction energy between the ligand and the monomers, and from docking approaches respectively. In this step, the number of hydrogen bonds formed between the functional monomer and the ligand was determined. Solvent effect on the complex formation was also considered. Our results justified experimental data of selective recognition and rebinding of the template in terms of MIP performance. Finally the diffusion coefficient of 5-FU into a PMAA matrix on the release step was determined.

In conclusions, we have provided here a proof of concept that a computational approach based on molecular mechanics, molecular dynamics and docking approaches are reliable tool for the design of MIP formulations for new templates avoiding time-consuming trial and error experimental approaches.

References

1. F. Breton, R. Rouillon, E. V. Piletska, K. Karim, A. Guerriero, I. Chianella, S. A. Piletsky, *Biosens. Bioelectron.,* 22 (2007) 1948-1954.
2. E. V. Piletska, N. W. Turner, A. P. F. Turner, S. A. Piletsky, *J. Contr. Rel.,* 108 (2005) 132-139.
3. M. Yoshida, Y. Hatate, K. Uezu, M. Goto, S. Furusaki, *Coll. and Surf. A*, 169 (2000) 259-269.
4. S. Wei, M. Jakusch, B. Mizaikoff, *Anal. Bional. Chem.*, 389 (2007) 423-431.
5. D. Pavel, J. Lagowski, *Polymer* 46 (2005) 7528-7542.
6. D. Pavel, J. Lagowski, *Polymer* 46 (2005) 7543-7556.
7. S. Monti, C. cappelli, S. Bronco, P. Giusti, G. Ciardelli, *Biosens. Bioelectron.,* 22 (2006) 153-163.
8. K. Yoneda, T. Yamamoto, E. Ueta, T. Osaki, *Cancer Lett*., 137 (1999)17-25.
9. K. R. Johnson, K.K. Young, W. Fan, *Clin. Cancer Res.,* 5 (1999) 2559-2565.
10. Discover and InsightII User Guide, Version 400p+, ACCELRYS: San Diego, CA, 1999.
11. H. Sun, S. J. Mumby, J. R. Maple, A. T. Hagler, *J. Am. Chem. Soc.*, 116 (1994) 2978-2987.
12. D. Pavel, J. Lagowski, C. Jackson Lepage, *Polymer*, 47 (2006) 8389-8399.
13. D. N. Theodorou, U. W. Suter, *Macromolecules,* 18 (1985) 1467-1478.
14. D. N. Theodorou, U. W. Suter, *Macromolecules,* , 19, (1986)139-154.
15. Polymer User Guide, Amorphous Cell Section, Version 4.0.0. Molecular Simulations Inc.: San Diego, CA, 1999.
16. *Science of materials,* W. Brostow, Ed. Wiley: New York, 1979, p. 65.
17. T. A. Andrea, W. C. Swope, H. C. Andersen, *J. Chem. Phys.,* 79 (1983) 4576-4584.
18. Y. Liu, F. Wang, T. Tan, M. Lei, *Anal. Chim.* Acta, 581 (2007) 137-146.
19. G. M. Morris, D. S. Goodsell, R. S. Halliday, R. Huey, W. E. Hart, R. K. Belew, A. J. Olson, *J. Comp. Chem.,* 19 (1998) 1639-1662.
20. L. M. Epinosa-Fonseca., J. G. Trujillo-Ferrara, *Biochem. and Biophys. Res. Comm.,* 328 (2005) 922-928.
21. S. Ci, T. Ren, Z. Su, *J. Mol. Model.,* 13 (2007) 457-464.
22. A. Mahn, G. Zapata-Torres, J. A. Asenjo, *J. Chromatogr. A,* 1066 (2005) 81-88.
23. D. Hofmann, L. Fritz, J. Ulbrich, C. Schepers, M. Boëhning, *Macromol. Theory Simul.,* 9 (2000) 293-327.
24. E. Tocci, D. Hofmann, D. Paul, N. Russo, E. Drioli, *Polymer,* 42 (2001) 521-533.
25. E. Tocci, P. Pullumbi, *Mol. Simul.*, 32 (2006) 145-154.
26. F. Puoci, F. Iemma, G. Cirillo, N. Picci, P. Matricardi, F. Alhaique, *Molecules*, 12 (2007) 805-814.

27. R. H. Gee, L. E. Fried, R. C. Cook, *Macromolecules,* 34 (2001) 3050-3059.
28. D. Hofmann, M. Heuchel, Yu. Yampolskii, V. Khotimskii, V. Shantarovich, *Macromolecules*, 35 (2002) 2129-2140.
29. H. J. C. Berendsen, J. P. M. Potsma, W. F. Gunsteren, A. Di Nola, J. R. Haak, *J. Chem. Phys.* 18 (1984) 3684-3690.
30. M. J. Whitcombe, L. Martin, E. N. Vulfson, *Chromatographia*, 47 (1998) 457-464.
31. I. A. Nicholls, K. Abdo, H. S. Andersson, P. O. Andersson, J. Ankaroo, J. Hedin-Dahlström, P. Jokela, J. G. Karlsson, L. Olofsson, J. P. Rosengren, S. Shoravi, J. Svenson, S. Wikman, *Anal. Chim. Acta*, 435 (2001) 9-18.
32. K. Karim, F. Breton, R. Rouillon, E. V. Piletska, A. Guerreiro, I. Chianella, S. A. Piletsky, *Adv. Drug Delivery Rev.*, 57 (2005) 1795-1808.
33. H. Jian-feng, Z. Quan-hong, D. Qin-ying, *Spectrochim. Acta A*, 67 (2007) 1297-1305.
34. W. Liqing, S. Baowei, L. Yuanzong, C. Wenbao, *Analyst*, 128 (2003) 944-949.
35. W. Liqing, L. Yuanzong, *J. Mol. Recogn.*, 17 (2004) 567-574.
36. S. A. Piletsky, K. Karim, E. V. Piletska , A. P. F. Turner, C. J. Day, K. W. Freebairn, C. Legge, *Analyst*, 126 (2001) 1826-1830.
37. P. J. Goodford, *J. Med. Chem.*, 28 (1985) 849-857.

SUMMARY

To design advanced dosage forms, suitable carrier materials are used to overcome the undesirable properties of drug molecules. Hence various kinds of high-performance biomaterials are being constantly developed. From the viewpoint of the optimization of pharmacotherapy, drug release should be controlled in accordance with the therapeutic purpose and pharmacological properties of active substances.

The main objective of the present thesis was to characterize the interactions between drugs and drug carriers by using combined molecular dynamics, molecular mechanics, and docking computational techniques. These simulations are likely to benefit the study of materials by increasing our understanding of their chemical and physical properties at a molecular level and by assisting us in the design of new materials and predicting their properties. Simulations are usually considerably cheaper and faster than experiments. Molecular simulations also offer a unique perspective on the molecular level processes controlling structural, physical, optical, chemical, mechanical, and transport properties.

In particular the attention was put on cyclodextrinic carriers supported on membrane and molecularly imprinted polymers.

Thus, structural information, such as the geometries of the cyclodextrinic complexes, and thermodynamic data, i.e. the variation of the enthalpy, were considered to draw a complete picture of the βCD-drug interactions. The results were in good agreement with the experimental data found in the measurement of stability constants. Finally the molecular dynamics on the polymeric system formed by adding on the surface of PEEK-WC the βCD-drug complex showed the release of the included drug in a water solution.

The docking and molecular mechanics techniques provided also informations on the geometry and the energy of complexation of a β-cyclodextrin derivative with naringin showing that the driving force for the host-guest complexation is due to the van der Waals interaction. Moreover the molecular dynamics calculations provided details on the complexation of naringin on the PEEK-WC surface containing the β-cyclodextrin derivative.

The binding affinity and selectivity of MIP towards drug template were calculated from the interaction energy between the ligand and the monomers and from docking simulations, respectively, as also the number of hydrogen bonds was determined. Our computational results shown a higher interaction energy between the drug template and monomers and justified the experimental data of selective recognition and rebinding of the template in terms of MIP performance confirming the reliability of our computational method. Moreover the diffusion coefficient of 5-FU into a PMAA matrix on the release step was determined.

Thus, atomistic modelling of material structure was a tool for understanding the mechanisms of physical processes on atomic and molecular levels, gaining insights into the molecular origins of behaviour of bulk polymers.

PARTICIPATION TO CONGRESSES

- Partecipazione al Congresso Nazionale di Chimica e Tecnologia delle Ciclodestrine – Asti (Italy) 06-08/05/07;
- Partecipazione al Congresso Gr.I.C.U. – Le Castella (Italy) 14-17/09/08
- Partecipazione al Convegno Congiunto delle Sezioni Sicilia e Calabria della Società Chimica Italiana – Rende (Italy) 01-03/12/08.

TRAINING COURSES

- Doctoral school Gr. I. C. U. - Muravera (CA) 06-11/06/09.
- Tirocinio di Ricerca: "TIME - Tirocini in operazioni integrate a membrana, di interesse anche industriale, per separazioni selettive ed a basso impatto ambientale", codice A2CNR115 in attuazione del "Programma Integrato di Voucher e Borse per l'Alta Formazione POR CALABRIA 2000-2006".

PUBBLICATIONS

- Cairo, P.; Ortuso, F.; Alcaro, S.; Fontananova, E.; Tocci, E.; Drioli, *"β-cyclodextrin interactions with three drugs used in inflammatory pathologies: an experimental and theoretical study"* – Chemical Physics Letters 2008 pag. 374-381.
- Cairo, P.; Tocci, E.; Drioli, E.; *"Modeling of drug release from polymer cyclodextrin system"* – in preparation.
- Cairo, P.; Tocci, E.; Drioli, E.; *"Computational evaluation of monomers and polymers for molecular imprinting of 5-fluorouracil for use as drug delivery systems"* – in preparation.

NATIONAL CONGRESS ACTA

- *"Molecular investigation of gas transport properties of polynorbornene models"* – Società Chimica Italiana IV Convegno Congiunto delle Sez. Calabria e Sicilia 1-3/12/08 Rende (CS);
- *"Indagine dei meccanismi di imprinting molecolare del 5-fluorouracile mediante approccio computazionale"* – Convegno Gr.I.C.U. 14-17/09/08 Le Castella (KR);
- *"Molecular recognition of naringin by polymeric membranes entrapping "β-cyclodextrins: a theoretical study"* – Congresso Nazionale di Chimica e Tecnologia delle Ciclodestrine 6-8/05/07 Asti (TO).